UNIVERSITÀ DI SIENA 1240

UNIVERSITA' DI SIENA
Dipartimento di Medicina Molecolare e dello Sviluppo

DOTTORATO DI RICERCA IN MEDICINA MOLECOLARE

Ciclo XXXVI°

Coordinatore: Prof. Vincenzo Sorrentino

Investigation on the potential of liquid biopsies in multiple myeloma and its presymptomatic stages

Settore scientifico disciplinare: BIO/18 Genetics

Candidato
Romano Liotti *Firma*

Supervisore
Prof.ssa Federica Gemignani *Firma*

Digitally signed by
Date: 2024.05.16 09:56:46 CEST
16/05/2024 09:56:4616/05/2024 09:56:46

Anno accademico 2022/2023

Index

List of Abbreviations

AID	Activation-induced deaminase
AOUP	University Hospital Company Pisana
ASO	Allele-specific oligonucleotide
aTMB	Average mutation rate per million bases
BC	Buffy-Coat
BCR	B cell receptor
BER	DNA base excision repair
BM	Bone marrow
BMI	Body mass index
BMPC	Bone marrow plasma cell
bp	Base pair
ccfDNA	Circulating cell-free DNA
CM	Circulating mutations
CNVs	Copy number variations
COSMIC	Catalogue of Somatic Mutations in Cancer
CRAB	hyperCalcemia, Renal failure, Anemia, Bone lesions
CSR	Class-Switch Recombination
CTCs	Circulating tumor cells
ctDNA	Circulating tumor DNA
DBS	Duble-stranded DNA breaks
Del	Deletions
DKFZ	Deutsches Krebsforschungszentrum
dPCR	Digital PCR
EVs	Extracellular vesicles
FLC	Free light chains
gDNA	Genomic DNA
GLOBOCAN	Global Cancer Observatory
IFI	Inframe insertion
Ig	Immunoglobulin
IgH	Immunoglobulin heavy chain
IMWG	International Myeloma Working Group
Ins	Insertions
Ins-TMB	Insertions per million of base pairs
LB	Liquid Biopsies
MC	Methyl cellulose
MDE	Myeloma-defining events
MGUS	Monoclonal gammopathy of undetermined significance
MM	Multiple myeloma
MMBP	Mutations per Mega base pairs
MMR	DNA mismatch repair
mps	Mutation per sample
MRD	Minimal residual disease
NGS	Next generation sequencing
PBMC	Peripheral blood cells
PC	Plasma cell
PCL	Plasma cell leukemia
PCR	Polimerase chain reaction
SEM	Standard error
SHM	Somatic hypermutation
SMM	Smoldering multiple myeloma
SNV	Single nucleotide variants
TCGA	The Cancer Genome Atlas Program
TMB	Mutation rate per million bases
UDI	Unique Dual Indexed
UMI	Unique Molecular Identifiers
WT	Wild type

Abstract

Multiple myeloma (MM) stands as one of the most prevalent and insidious hematological malignancies, characterized by the abnormal proliferation of malignant plasma cells within the bone marrow. This disease has a multifactorial origin, involving a complex interaction of genetic and environmental events. It evolves from an antecedent pre-malignant state termed "monoclonal gammopathy of undetermined significance" (MGUS), which can progress to MM at a rate of approximately 1% per year, sometimes through the asymptomatic stage termed "smoldering multiple myeloma" (SMM). Since MM is often diagnosed in advanced stages of the disease, there is a critical need to develop more sensitive and non-invasive diagnostic methodologies for early disease detection.

Liquid biopsies (LB), in particular, represent a promising frontier in MM diagnostics. These enable the isolation and purification of cell-free circulating tumor DNA (ccfDNA), offering a less invasive alternative to traditional bone marrow (BM) biopsies, which have long been considered the gold standard for analyzing the genetic profile of MM. Analyzing ccfDNA through LB offers significant advantages, including the possibility of monitoring the disease progression and treatment response over time. This method could also have the capability to detect genetic mutations associated with MM early on, allowing for timely and personalized therapeutic interventions. Therefore, the objective of this study was to assess the feasibility of LB in the context of MM. Specifically, LB obtained from patients at various stages of MM were compared to those from healthy control groups. The study aimed to investigate potential mutations in ccfDNA among the different cohorts.

Next generation sequencing (NGS) analysis was carried out using Unique Molecular Identifiers (UMI) and a customized panel comprising 84 recurrent genes associated with MM. This analysis was performed on a cohort consisting of patients with MGUS, SMM, and MM, including individuals exhibiting disease progression, and compared with a control group of healthy subjects. Significant mutational heterogeneity was observed in the analyzed samples, with a notable presence of mutations even in healthy subjects. Furthermore, the most frequently mutated genes within each group differed from those reported in two genomic databases for MM. Persistent mutations have also been identified in samples from patients who have had disease progression. Interestingly, no single nucleotide variants (SNVs) of *NRAS* and *KRAS*, which are commonly mutated in MM, were found in MGUS samples. Additionally, our study provided valuable insights into the types of mutations, revealing a significantly unbalanced Insertions/Deletions ratio in healthy subjects, which was subsequently rebalanced as the disease progressed. These findings underscore the dynamic nature of mutational processes in MM and highlight the potential utility of liquid biopsies in elucidating disease progression mechanisms.

We also compared different biopsy specimens from the same individual at different time points and disease stages, employing the high-depth digital PCR (dPCR) technique to detect mutations in the *NRAS* and *KRAS* genes in a cohort of 85 patients. These results revealed a correlation between the mutations found in BM and LB, with greater concordance in the LB genomic DNA (gDNA) and BM gDNA samples, highlighting the importance and potential of the use of LB.

Finally, the effects deriving from the overexpression of the *NRAS* p.Q61R mutation in multiple myeloma cell lines were explored through functional studies. Overexpression of *NRAS* appears to induce reduced metabolic activity and cell proliferation. However, functional tests revealed a greater tendency towards aggregation and adhesion, suggesting a more aggressive phenotypic behavior of MM.

Overall, this study opens new avenues for understanding MM and its presymptomatic phases, highlighting the potential and limitations of LBs in identifying key events associated with MM progression.

1. Introduction

1.1. Multiple myeloma overview

Multiple myeloma (MM) is a hematologic malignant tumor characterized by the clonal expansion of plasma cells (PCs) residing in the bone marrow (BM). Malignant plasma cells are located primarily in the bone marrow, but can also be found in other extra-medullary sites, and undergo an uncontrolled clonal proliferation which, in the majority of patients, manifests itself in an abnormal production of high quantities of a monoclonal immunoglobulin (also known as M protein or monoclonal protein) found in serum and/or urine [1]. Plasma cells are responsible for the production of antibodies to maintain humoral immunity and their rapid increase leads to the generation and accumulation of abnormal monoclonal antibody, and consequent damage to end-organs such as kidneys [2] and bone lesions that are observed in more than 90% of patients [3], with other common symptoms including anemia and hypercalcemia [4]. The first documented cases of multiple myeloma (MM) in the medical literature date back to 1840. Initially, the presence of an abnormal protein was noted in the urine of patients with MM. Subsequently, throughout the 19th century, the distinctive clinical features of the disease were identified. At the beginning of the 20th century, it was understood that the predominant cells in MM are plasma cells and that the disease is correlated with the production of immunoglobulins, which are the cellular source of antibodies [5].

1.2. Epidemiology

MM ranks as the second most prevalent hematologic malignancy following non-Hodgkin lymphoma [6]. Globally, the incidence varies with the highest rates observed in developed countries, such as the United States and Western Europe (Fig. 1). The most recent data from Globocan [7] shows that in 2022, worldwide, the incidence of new cases of MM was 2.4 cases per 100,000 person-years. In Europe the average incidence of new cases is 9.9 cases per 100,000 person-years, Italy is the second nation in Europe with the highest incidence of new cases with 10.5 cases per 100,000 person-years.

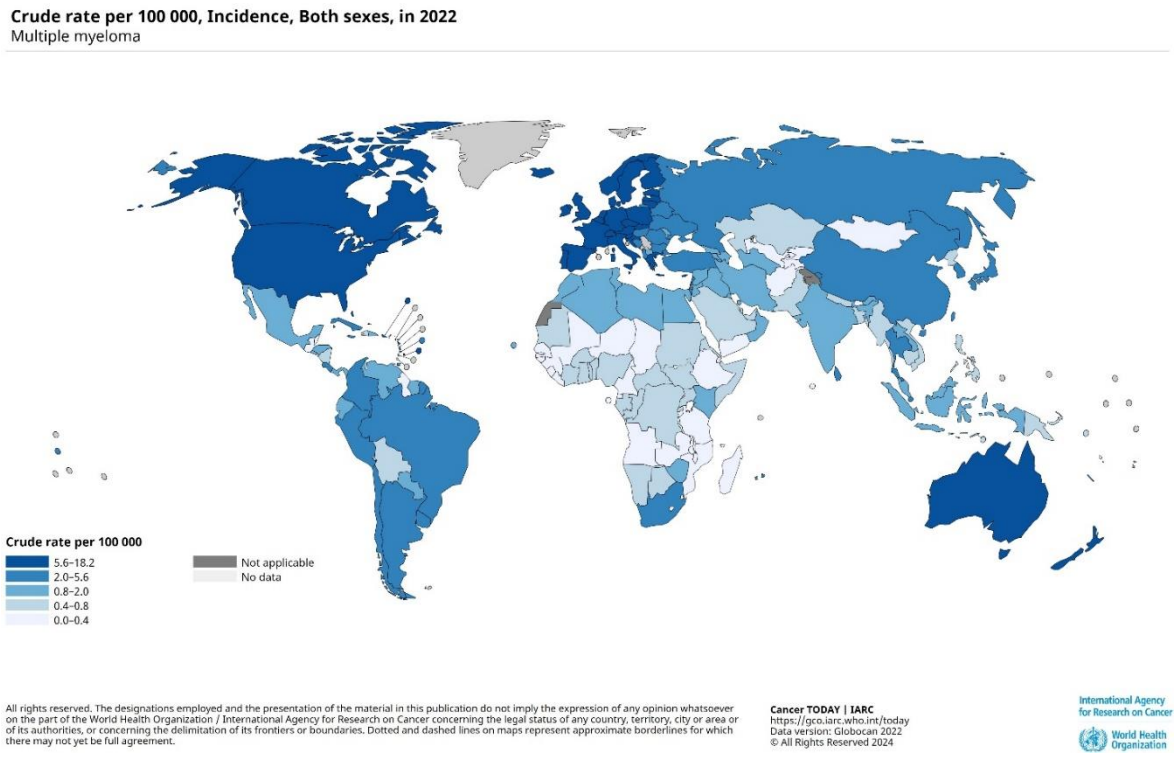

Fig. 1 Estimated incidence rate of multiple myeloma in 2022. Map obtained from GLOBOCAN 2022.

MM exhibits a slightly higher prevalence in males compared to females and is twice more common in African Americans compared to Caucasians [8]. The average age of patients at diagnosis for this condition is approximately 65 years old [9]. The global rise in incidence [10] leaded to higher observed mortality rates, although new therapies have contributed to an increase in life expectancy. Global mortality from this neoplasia rose by 94% between 1990 and 2016 [10] with a total death toll of around 120,000 worldwide in the year 2022, of which almost 32,000 in Europe (GLOBOCAN). Despite the various therapeutic treatments available, MM is still incurable, with a median survival of about 6 years [11].

1.3. Disease development mechanism

The development of mature B cells occurs through various stages of differentiation in both bone marrow and peripheral lymphoid tissues. In the bone marrow, a complex process of genetic recombination takes place in the first progenitor cells oriented towards the B line that generates a diversified set of immunoglobulins (maturation independent of the antigen). The progenitor cell of the B lymphocytes (Pro-B) originates from the stem cells, in Pro-B the rearrangement of the heavy chain begins and ends in the Pre-B cell. The expression on the cell membrane of a complete IgM molecule defines the immature B cell, while the simultaneous presence of two different isotypes, IgM and IgD, on the membrane is characteristic of the mature B cell (Fig. 2).

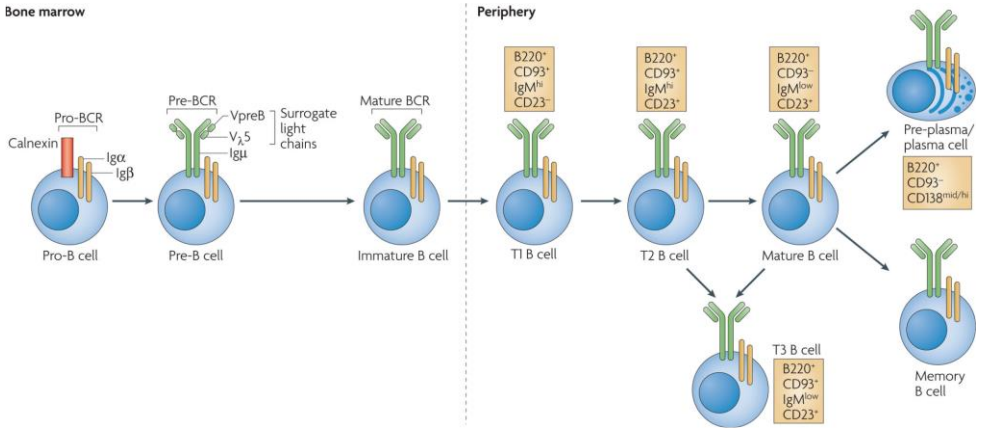

Fig. 2 Developmental stages of B lymphocytes in the bone marrow and peripheral lymphoid organs (image from J. Cambier et al.,2008) [12].

During this process of differentiation, rearrangements within the immunoglobulin (Ig) locus, comprising rearranged heavy and light chain genes, will generate the mature B cell receptor (BCR), which exhibits the capability to bind antigens present on the cell surface. B cells leave the bone marrow as naive B cells, after a meeting with their related antigens, B cells are activated and migrate to the germinal centre. Maturation of antigen affinity occurs in the germinal centre and takes place through two processes: somatic hypermutation (SHM) to produce highly specific antibodies and antigen selection. Next, class switch recombination (CSR) occurs, leading to the diversification of Ig isotypes while maintaining the same antigenic specificity (antigen-dependent maturation) (Fig. 3).

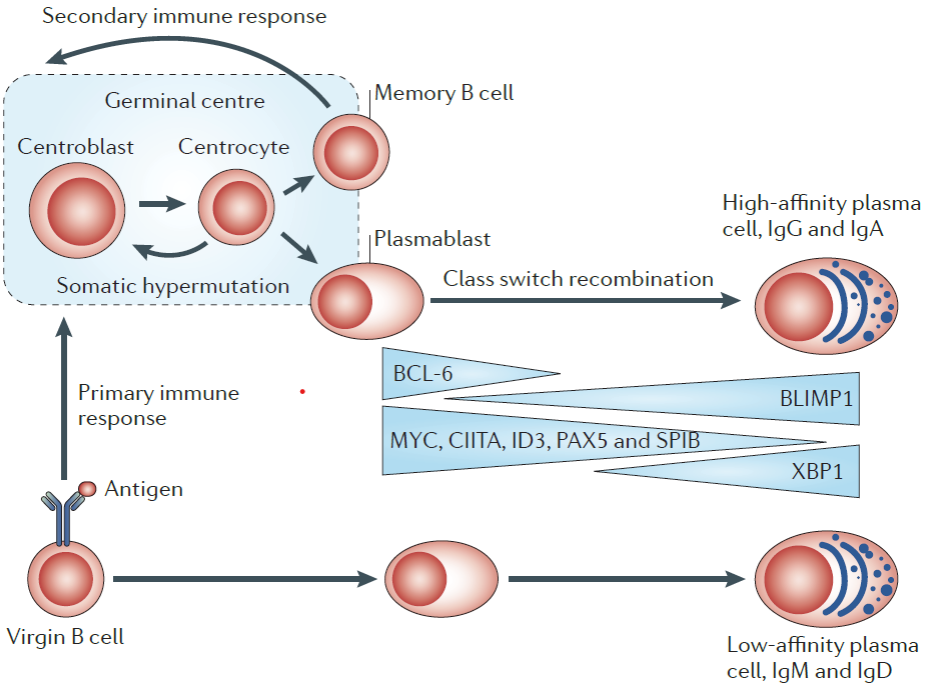

Fig. 3 Stages of B cell development, scheme of the immune response and the germinal center (image from G.Morgan et al.,2012)[13].

Once this process is completed, the plasmablast leaves the germinal center and migrates to the bone marrow where it undergoes clonal expansion resulting in differentiation into both plasma cells (secreting antibodies) and memory cells [13]. Plasma cells have the function of synthesizing and secreting large quantities of immunoglobulins. Each plasma cell secretes identical Ig with the same antigenic specificity [12]. B cells undergo continuous cycles of division and selection to generate antibodies with elevated affinity towards particular antigens and varied functional properties. This process requires the SHM and CSR to occur within the DNA sequences encoding the hypervariable regions of the immunoglobulin heavy chain (IGH) locus [13], both require activation-induced deaminase (AID) expression and are mediated by the generation of double-stranded DNA breaks (DSB) at Ig loci, these breaks can rejoin with others that coincidentally occur elsewhere in the genome. This can lead to aberrant recombinations with other genomic regions, resulting in chromosomal translocations, one of the central molecular hallmarks of myeloma [1][13]. Therefore, errors in the SHM and CSR processes imply the potential for generating alterations. If these alterations affect specific oncogenes, they may contribute to the initiation of myeloma's initial stages.

1.4. Premalignant stages and progression to MM

Multiple myeloma can be preceded by one or more precancerous conditions [14] and progress from the precursor condition defined as monoclonal gammopathy of uncertain significance (MGUS) to smoldering multiple myeloma (SMM), then to symptomatic myeloma, and ultimately to the most aggressive stage characterized by plasma cell leukemia (PCL) and extramedullary disease.

MM and its precursor conditions (MGUS and SMM) are characterized by monoclonal proliferation of plasma cells in the bone marrow. Cancerous plasma cells produce an abnormal type of monoclonal immunoglobulin called M protein, which is detectable in blood and urine [9]. The M protein, like all immunoglobulins, includes 2 identical heavy chains and 2 identical light chains (Fig. 4). Among the light chains, two serologically distinct types are recognised: k and λ [15], the rearrangement of the heavy and light chain genes during the initial development of B cells allow a different antibody-antigen affinity through the mutation of the genetic region determining complementarity [16].

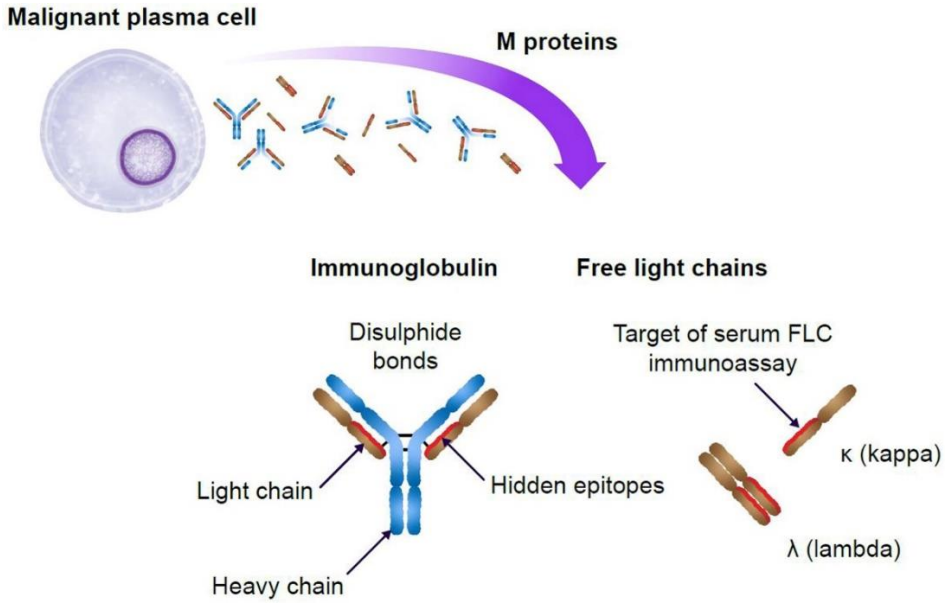

Fig. 4 M protein and free light chains (FLC) κ and λ (Image from Mikhael J, et al., 2023) [17].

During the synthesis of the M protein by aberrant plasma cells, an excess of free light chains (FLC) is produced and released together with the intact immunoglobulin molecule. These FLCs possess exposed epitopes that serve as targets for serum FLC analysis. The measurement of the ratio between FLC k and λ is an important part of the tests for the definition of the pathology, which is routinely carried out in the patient's follow-up in a non-invasive manner. An imbalanced FLC ratio indicates an accumulation of M protein, and the resulting excess FLC can cause renal failure, a characteristic symptom of MM. Early diagnosis through this analysis allows us to influence the patient's comorbidities and quality of life [16].

Patients with MGUS remain asymptomatic, and M protein is generally found at lower levels compared to MM. The annual progression risk from MGUS to MM is estimated at 1%. Furthermore, the prevalence of MGUS rises with age, with approximately 1.7% of individuals aged 50 to 59 years and 6% of those over 80 years exhibiting detectable MGUS [18][19]. SMM is a transitional more progressed precancerous phase and it is characterized by a greater disease burden, with a yearly progression risk of 10% during the initial five years, followed by 3% annually for the subsequent five years, and eventually 1% per year thereafter [20].

Based on the type of immunoglobulin that is produced by myeloma cells, different subtypes of myeloma can be distinguished. The antibody classes are called IgG, IgA, and can be further divided into subclasses, IgD, IgE and IgM. Approximately, 65% of MM patients have IgG myeloma, the second most common type being IgA. Immunoglobulins are composed of two heavy chains and two light chains. Light chains can exist in two types: kappa light chains, found in 60% of antibodies, and lambda light chains, found in 40%.

However, in patients affected by MM, variations in this ratio can occur due to neoplastic cells originating from a single B lymphocyte clone producing only one type of immunoglobulin with the same light chain. [21]. In the pre-malignant stage of MGUS the IgM class is the second most common after IgG; however, cases of IgM myeloma are relatively few because the condition of IgM MGUS is associated with a predisposition to develop other types of B-cell lymphoproliferative disorders [21]. Despite serial follow-up and laboratory testing of patients at MGUS stage, most MM cases are still diagnosed after the clinical presence of MM-related symptoms [22].

1.5. Diagnosis

The diagnosis of MM necessitates the occurrence of one or more myeloma-defining events (MDE) along with the evidence of a minimum of 10% clonal plasma cells in biopsy-proven bone marrow analysis. The conclusive diagnosis necessitates a bone marrow biopsy, which determines the percentage of infiltration of clonal plasma cells, along with additional tests to detect serum levels of monoclonal protein, biochemical screening including liver and renal function assessments, and radiographic imaging in order to identify osteolytic lesions as early as possible. In contrast to malignancies that commonly metastasize to bone, bone lesions in MM exhibit an absence of neoplastic formations within the bone. [11].

Specific MDE include CRAB features: hyperCalcemia, Renal failure, Anemia, Bone lesions. CRAB manifestations aid in identifying potential MM patients, as they represent the predominant symptoms typically caused by MM. Additionally, MDE incorporate three distinct biomarkers: clonal bone marrow plasma cell (BMPC) percentage ≥ 60%, an involved-to-uninvolved serum free light-chain ratio ≥100, and the identification of more than one focal lesion on magnetic resonance imaging. In the absence of end-organ damage, the presence of one or more biomarker is sufficient for diagnosis [1]. The term "involved" refers to the light chains bound to the myeloma-producing antibody, while "uninvolved" refers to those not bound.

Importantly, the MGUS and SMM stages are completely asymptomatic with no evidence of the characteristic MM-specific organ damage or CRAB features [23] so these conditions are usually detected incidentally within the definition diagnosis of unrelated conditions.

The diagnostic characteristics for MGUS, SMM, and MM can be defined and summarized in the Table 1 below:

STAGE	CRITERIA FOR DEFINITION
MGUS	• Serum M protein present but usually < 3 g/dl • Clonal PCs in bone marrow < 10% • Absence of CRAB features or amyloidosis attributable to plasma cell proliferative disorder
SMM	• Serum M protein ≥ 3 g/dl • Clonal PCs in bone marrow between 10% and 60% • Absence of MDE or amyloidosis attributable to PC proliferative disorder
MM	• Clonal PCs in bone marrow ≥ 10% • Presence of a bone or extramedullary plasmacytoma confirmed by biopsy • Presence of CRAB features and MDE

Table 1 Updated diagnostic criteria of the IMWG (International Myeloma Working Group) for the definition of MGUS, SMM and MM

These parameters and models utilized for risk stratification in myeloma precursor disease rely on indirect metrics of the condition, including M protein levels, percentage of PCs in BM, and free light chain ratios. Consequently, this approach presents limitations in accurately assessing risk [24][25]. Furthermore, there is a lack of dependable biomarkers for personalized prognostication distinguishing patients prone to progressing to MM from those who will not [26]. Current care and clinical management guidelines for patients with myeloma precursor conditions recommend continuous monitoring of patients without treatment until progression to full-blown malignancy [23][27][28].

For patients diagnosed with MGUS and SMM, to date a reliable marker has not yet been identified to predict the risk of progression towards MM, furthermore the risk of evolution is extremely variable between different individuals. To allow an early diagnosis, clinical practice involves long-term follow-up of MGUS and SMM adapted based on the risk of progression to symptomatic disease and life expectancy, including specific laboratory tests [14].

The progression risk stratification model in patients with MGUS and SMM is based on that provided by the Mayo Clinic. In particular, for SMM, reference is made to the 20-20-20 risk stratification model updated with the revised diagnostic criteria of the IMWG (International Myeloma Working Group) [29]. The prognostic scoring system provides an estimate of the risk of progression and is based on independent risk factors such as cut-off values for serum M protein, the ratio of involved to uninvolved serum FLC, and for SMM on plasma cell infiltration of the bone marrow, as independent risk factors (Table 2).

Mayo Clinic risk stratification model					
MGUS			SMM		
Number of risk factors: • Serum M-protein ≥15 g/L • Non-IgG subtype • Abnormal FLC ratio	Risk of progression at 20 years	N° Patients	**Number of risk factors:** • Serum M-protein >20 g/L • FLC ratio >20 • BMPC >20%	Risk of progression at 2 years	N° Patients
0: low risk	5%	449 (38%)	0: low risk	5%	424 (37%)
1: low to intermediate risk	21%	420 (37%)	1: intermediate risk	17%	312 (27%)
2: intermediate to high risk	37%	226 (20%)	2-3: high risk	46%	415 (36%)
3: high risk	58%	53 (5%)			

Table 2 Mayo Clinic models for risk stratification of progression of MGUS and SMM [14].

1.6. Genetic factors and *RAS* genes

The exact cause of multiple myeloma remains unclear, with theories pointing to a combination of genetic and environmental factors as potential contributors to the risk of developing the disease. Several occupational categories and chemicals exposure have been suggested as possible factors. A recent meta-analysis has shown a significant association between MM risk and the firefighters and hairdresser categories as well as employees exposed to engine exhaust [30]. The conventional cancer-related risk factors, such as smoking, obesity, and alcohol consumption, have yielded conflicting results in relation to MM [31]. While several observational studies have linked a high body mass index (BMI) with an elevated risk of MM, its significance remains uncertain [32].

Inspired by epidemiological research revealing a tendency for MGUS and MM within families, there has been a substantial focus on uncovering specific DNA sequence variations linked to MM susceptibility [33][34]. Up to date, 24 independent loci associated with MM risk have been identified in Western European populations (Table 3), these risk variants representing approximately 16% of the SNP MM heritability [35].

Locus	Lead variant	Ref	Alt	RAF	Genes	OR	*P* value
2p23.3	rs6746082	A	C	0.76	*DNMT3A, DTNB*	1.29	1.22 × 10−7
	rs7577599	T	C	0.77		1.24	1.24 × 10−16
2q31.1	rs4325816	T	C	0.77	*SP3*	1.12	7.37 × 10−9
3p22.1	rs1052501	C	T	0.2	*ULK4*	1.32	7.47 × 10−9
	rs6599192	G	A	0.25		1.26	8.75 × 10−18
3q26.2	rs10936599	C	T	0.75	*MYNN, TERC, LRRC34*	1.26	8.70 × 10−14
	rs10936600	A	T	0.75		1.2	5.94 × 10−15
5q15	rs56219066	T	C	0.71	*ELL2*	1.25	9.6 × 10−10
	rs1423269	A	G	0.71		1.17	1.57 × 10−11
5q23.2	rs6595443	A	T	0.48	*CEP120*	1.11	1.20 × 10−8
6p21.3	rs2285803	T	C	0.27	*HLA region*	1.19	9.67 × 10−11
	rs3132535	A	G	0.27	*HLA region*	1.2	2.97 × 10−17
6p22.3	rs34229995	C	G	0.03	*JARID2*	1.37	1.31 × 10−8
6q21	rs9372120	T	G	0.19	*ATG5*	1.18	9.09 × 10−15
7p15.3	rs4487645	C	A,T	0.65	*CDCA7L, DNAH11*	1.38	3.33 × 10−15
7q22.3	rs17507636	C	T	0.74	*CCDC71L*	1.12	9.20 × 10−9
7q31.33	rs58618031	T	C	0.75	*POT1*	1.12	2.73 × 10−8
7q36.1	rs7781265	G	A	0.09	*SMARCD3, ABCF2, CHPF2*	1.19	9.71 × 10−9
8q24.21	rs1948915	T	C	0.35	*CCAT1*	1.13	4.20 × 10−11
9p21.3	rs2811710	C	T	0.63	*CDKN2A*	1.15	1.72 × 10−13
10p12.1	rs2790457	G	A	0.73	*WAC*	1.12	1.77 × 10−8
11q13.3	rs603965 (rs9344)	G	A	0.51	*CCND1*	1.82	7.95 × 10−11
16p11.2	rs13338946	T	C	0.27	*Several genes including FBRS SRCAP, PRR14, RNF40*	1.15	1.02 × 10−13
16q23.1	rs7193541	T	C	0.61	*RFWD3*	1.13	5.00 × 10−12
17p11.2	rs4273077	A	G	0,11	*TNFRSF13B*	1.26	7.67 × 10−9
	rs34562254	G	A	0.1		1.3	3.63 × 10−17
19p13.11	rs11086029	T	A	0.25	*KLF2*	1.14	6.79 × 10−11
20q13.13	rs6066835	T	C	0.09	*PREX1*	1.26	1.36 × 10−13
22q13	rs138740	C	T	0.37	*TOM1*	1.18	5.7 × 10−8
	rs138747	A	T	0.36		1.21	2.58 × 10−8
22q13.1	rs877529	G	A	0.44	*CBX7, APOBEC3 cluster*	1.23	7.63 × 10−16
	rs139402	T	C	0.44		1.23	4.98 × 10−26

Table 3 The table lists the risk variant associated with MM at each locus. Risk Allele Frequency (RAF) from HaploReg v4.1 (data obtained from Pertesi, M., et al.,2020) [35].

Candidate genes at each locus were identified based on DNA coding sequence variants with strong effects and relevance in the mechanisms of development of the pathology. Furthermore, studies on MM and MGUS family members highlight genes such as *DIS3* and *CDKN2A*, with highly interesting variants in their association with MM [35].

MM manifests as a profoundly heterogeneous cancer, propelled by numerous factors, encompassing cytogenetic anomalies, alterations within the bone marrow microenvironment, and dysregulated immune responses. [1]. A healthy plasma cell transforms into a malignant myeloma cell through a more branched heterogeneous multiphase process in which sub-clones diverge upon acquisition of new events. The intricate molecular mechanisms and the causative agents responsible for this progression are not yet fully characterized [23]. In the early stages of the pathology, dysfunctional cells belonging to the MGUS clone, following the development of sufficient genetic anomalies, acquire a clonal advantage and expand and evolve. These processes lead to the development of the proliferative clone, no longer confined to the bone marrow and capable of rapid expansion. Cells at this stage exhibit substantial genetic alterations, and precursor subclones are present at low frequencies owing to competitive interactions for stromal niche occupancy in the bone marrow. This

phase of the disease could be considered initiated by a founder and migratory phenomenon, whereby a cell capable of surviving and growing in the peripheral blood faces no competition. Many genetic alterations have been proposed as driving events in the genesis of myeloma [13][36] (Fig. 5).

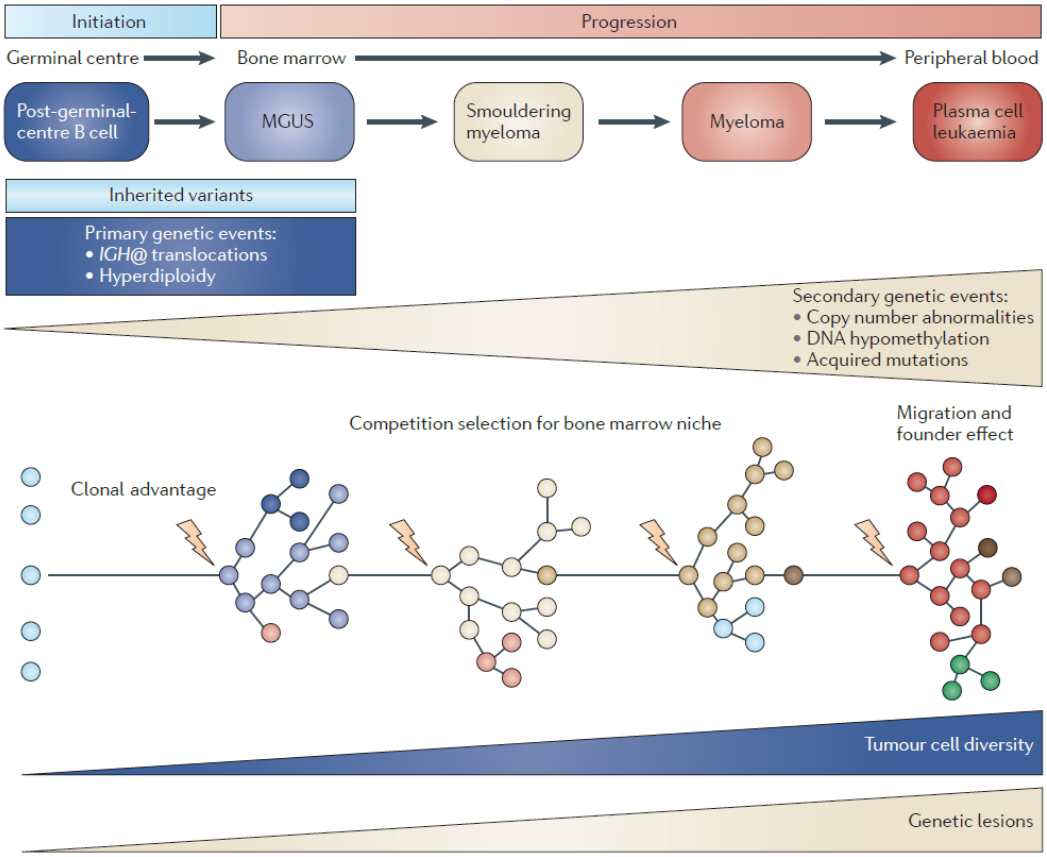

Fig. 5 Initiation and progression of myeloma. IGH@, immunoglobulin heavy chain locus (image from G. J. Morgan, et al., 2012)[13].

The primary genetic anomalies implicated in precursor states' progression, potentially culminating in multiple myeloma, include chromosomal translocations implicating the immunoglobulin heavy chain (IgH) genes and aneuploidy occur, with hyperdiploidy being the predominant event. For example, it has been observed that the rapidity of pathological evolution is influenced by the specific cytogenetic abnormalities underlying the disease; individuals with t(4;14) translocation, del(17p), and gain(1q) demonstrate an elevated risk of progression from MGUS or SMM to MM [11], and the SNP rs603965 on gene *CCND1*, selectively predisposes for MM with somatic t(11;14)(q13;q32) [35].

However, it is believed that these alterations although present in the early stages of myeloma precursor conditions at lower frequencies, are insufficient to initiate the development of MM. This is evidenced by the fact that many patients with MGUS and SMM harbor these alterations for decades without exhibiting any signs of progression. Therefore, it is hypothesized that secondary alterations are required to trigger progression to MM [23]. Within a pre-malignant plasma cell clone, secondary genetic events such as CNVs, secondary translocations and point mutations in oncogenic

pathways drive clonal evolution and characterize tumor progression [37]. The frequency of secondary genetic alterations escalates from MGUS to SMM, and subsequently to MM. Secondary cytogenetic abnormalities, such as gain(1q), del(1p), del(17p), del(13), and *RAS* mutations, manifest as the disease progresses. Both primary and secondary cytogenetic abnormalities exert an influence on the disease progression, response to treatment, and prognosis. The interpretation and impact of cytogenetic abnormalities in MM vary based on the disease stage at which they are identified. [11].

With the progression of the disease, myeloma PCs lose confinement to the bone marrow and disseminate to extramedullary sites. The transition across these disease states is believed to require the acquisition of genetic mutations that contribute to the emergence of myeloma's biological hallmarks. Although no singular genetic event delineates the transition from MGUS and SMM to MM, patients with certain genetic and epigenetic anomalies, including DNA methylation, exhibit a higher propensity for progression to MM [1]. However, the precise mechanisms driving the transformation to MM are not yet fully characterized [24][23]. MM is therefore characterized by pronounced genetic heterogeneity both between patients, each presenting a distinct amalgamation of chromosomal rearrangements and genetic mutations, and at the intraclonal level, with a majority of patients displaying a complex subclonal architecture [38].

The RAS/MAPK (Rat Sarcoma/Mitogen-Activated Protein Kinase) pathway has been identified as the most commonly mutated in MM, with the *NRAS*, *KRAS* genes exhibiting the highest number of mutations; these genes are pivotal in the control of cell proliferation, differentiation, and survival. Their aberrant activation in an oncogenic milieu is generally associated with malignant transformation, invasiveness, aggressiveness of the disease and drug resistance [39]. Activating mutations within the RAS signalling pathway are reported in about half of newly diagnosed myelomas and even more frequently in relapsed/refractory cases [40][41] *KRAS*, *NRAS* and *BRAF* mutations have been frequently observed in high tumor cell fractions [41] and are considered driver mutations in MM. The most common hotspot mutations occur at codons 12, 13 and 61 in the *KRAS* and *NRAS* genes, with *NRAS* p.Q61R being the most frequent mutation [42].

KRAS mutations have been rarely detected in cases of MGUS [37]; however, it is the most frequently mutated gene in SMM, suggesting its involvement in the progression from SMM to MM [43]. *NRAS* mutations seem to play a crucial role in promoting drug resistance. Indeed, a prevalence of *NRAS* mutations has been observed in relapsed MM [44], consequently, *NRAS* mutations have been associated with reduced sensitivity to treatments in relapsed MM [45].

1.7. Liquid Biopsies and ccfDNA

In clinical practice, BM biopsies remain the gold standard to access the genetic profile of MM, enabling its diagnosis and the assessment of therapeutic treatment. However, due to their highly invasive nature, BM biopsies are not ideal for ongoing patient monitoring. Additionally, they may not provide a comprehensive representation of the diverse intratumoral mutational profile seen in MM [46].

A valid surrogate for tumor tissue biopsies are LBs which can allow to obtain useful information for diagnostic and prognostic purposes [47][48]. LBs also hold the potential for suggesting responses to various therapies. The term "LBs" refers to the sampling and analysis of various biological fluids, especially plasma or serum, to detect a range of tumor components, such as circulating cell-free DNA (ccfDNA), circulating tumor cells (CTCs), miRNAs and extracellular vesicles (EVs). LBs have obvious advantages, for example sampling can be repeated frequently over time to monitor the evolution of the disease as the procedure is minimally invasive.

The main approach of LB involves the isolation of ccfDNA from peripheral blood (plasma or serum), which consists of short fragments of extracellular fragmented DNA freely circulating in the biofluid. ccfDNA is usually released from cells through apoptosis and necrosis processes in the form of short, highly fragmented nucleic acid sequences [49]. ccfDNA levels are higher in cancer patients than in healthy ones: physiologically, the concentration of ccfDNA in the blood is low (0 – 0.1 ng/µl), but can reach 5 ng /µl approximately in patients with tumor and metastases [50].

When a tumor is present, circulating tumor DNA (ctDNA), which represents the fraction of ccfDNA released by tumor cells, can be detected in plasma or serum. Circulating ctDNA consists of fragments of 160–180 base pairs, corresponding approximately to the size of a mononucleosomal unit [51]. Because the majority of ccfDNA arises from cell death associated with physiological events [52], ctDNA represents only a minor fraction (0.1–10%) of total circulating cell-free DNA [53]. In early-stage cancer patients, the ctDNA fraction may also be very low [51], but in the case of an advanced pathological condition the quantity of ctDNA, and ccfDNA in general increases [50].

The study of ccfDNA has proven to be increasingly important and interesting with regards to applications in the clinical field for MM. The molecular analysis of ccfDNA circulating in the plasma represents a very important source of biomarkers that can provide specific information regarding tumor genetic heterogeneity and the mechanisms of pathological progression [46]. Exploring ccfDNA opens up the opportunity for recurrent patient screening, enabling early detection and prognosis through the identification of tumor-related abnormalities [54]. It also facilitates personalized treatment approaches, ongoing therapy monitoring, and the assessment of potential resistance, while helping determine the risk of recurrence [55][56].

1.8. Liquid biopsies in the MM

The number of studies on ccfDNA in MM is quite limited, but the results obtained to date are promising and indicate a potential role of ccfDNA especially in monitoring minimal residual disease (MRD) in patients with MM.

Sata et al. [57], is among the first to compare peripheral blood with BM biopsies. Using quantitative PCR with allele-specific oligonucleotide (ASO) primers for the detection of rearrangements in the loci for the Ig chains, peripheral blood cells (PBMC) were compared with those of the bone marrow (BMPC) and with $CD20^{+}$ $CD38^{-}$ B cells of the BM and serum ccfDNA. The study, although carried out on a small population, demonstrated a strong correlation between BMPC and PBMC, highlighting that the ccfDNA reflects the presence of MM clones in the patients, in fact the DNA sequences found in the peripheral blood were identical to those found in the bone marrow for most cases. Therefore, it was hypothesized, the presence of clonal plasma cells circulating in peripheral blood and the possibility of using PBMC instead of BMPC for MRD monitoring.

A different study [58] instead, it uses Next Generation Sequencing (NGS) to define the rearrangements in the loci for the MM-specific Ig chains in the circulating cells and in the ccfDNA of patients with MM, and also using peripheral blood for tracing after the start of treatment. The results associate positivity for circulating cells with ccfDNA positivity in MM although discordant in 30% of cases, and also show a correlation between ccfDNA positivity and the patients' remission status. This study suggests that circulating cells in MM are not the only source of ccfDNA and that ccfDNA may reflect tumor burden more completely. This theory is supported by further tissue comparison studies.

Kis et al. [59], compared the analysis of ccfDNA and BM by sequencing the exons of *KRAS*, *NRAS*, *BRAF*, *EGFR* and *PIK3CA* genes, managing to detect even very low frequencies of the mutant allele in ccfDNA. The analysis detected in the cfDNA almost all the mutations also found in the BM, moreover, additional mutations not detected in the BM were found in the ccfDNA. In conclusion, the study proposes the analysis of ccfDNA not only for the molecular profiling of the disease but also for the detection of unidentified subclones in the BM.

Similarly, another study [60] analyzes the presence of activating mutations of four oncogenes *KRAS*, *NRAS*, *BRAF* and *TP53* by NGS of paired samples of ccfDNA from plasma and gDNA from BM cells. Some mutations were detected only in ccfDNA and others in common with BM, furthermore a higher mutational frequency was observed in patients with relapsed myeloma. These findings demonstrate the existence of spatial and genetic heterogeneity in advanced disease, and that ccfDNA molecules can arise from multiple tumor sites within a patient.

All these studies demonstrate that the genetic composition of MM is complex and evolves during the progression of the disease, furthermore they promote the use of LBs as an addition or replacement to BM biopsy for monitoring the disease or evaluating the effectiveness of treatments. However, further studies are needed to confirm these findings and to define the role of ccfDNA in the management of MM.

1.9. Biological analysis applied on ctDNA: dPCR and NGS

Various approaches have been developed to detect mutations in the circulating tumor DNA (ctDNA) fraction with high specificity and sensitivity. These include digital PCR (dPCR) and next-generation sequencing (NGS) with molecular indexing. [47][61].

dPCR mutation assays are well-suited for rapidly and precise identification of individual sequence-specific mutations in DNA derived from different types of samples. dPCR mutation tests are hydrolysis probe-based duplex tests that identify the presence of specific mutation sequences. These assays use primers and probes, which enhance the specificity and sensitivity of the assay, enabling the detection of mutations present at 0.1% in a wild-type genomic DNA background within a single well of the nanoplate. One probe detects the mutant allele, while the other probe detects the wild-type allele, with each probe conjugated with a specific fluorophore (e.g. FAM/HEX) for mutant + wild-type detection. Each reaction is analyzed in one or more wells of a nanoplate, with the reaction mixture distributed and separated into approximately 26,000 partitions. Partitioning allows for an increase in target-specific concentration. The assay outcome reveals the fractional abundance of the mutant target, and the result in copies per microliter is also acquired.

Next-generation sequencing technologies have emerged as a robust platform for analyzing ccfDNA, enabling the detection of cancer-associated genetic and epigenetic aberrations, including mutations, CNVs, and DNA methylation changes across larger genomic regions in a diverse range of tumor types [62][63]. At present, NGS based on highly sensitive unique molecular identifiers (UMI) for liquid biopsy testing is a method that opens up new perspectives compared to single gene testing. However, the biggest problem is sufficient yields of ccfDNA, which are essentially necessary to obtain meaningful test results [64].

The UMI are a type of molecular barcoding that provides error correction and enhances sequencing accuracy. These markers consist of short sequences used to uniquely tag each DNA molecule within a sample library prior to the library amplification phase for each sample. By incorporating unique sequences on each original DNA fragment, it becomes possible to distinguish variant alleles present in the sample (true variants) from errors introduced during library preparation, target enrichment, or sequencing (Fig. 6). Hence, the true variants will be consistently present in all the reads sharing the same UMI, whereas errors (false variants) will only be detected in a subset of the reads with the same UMI.

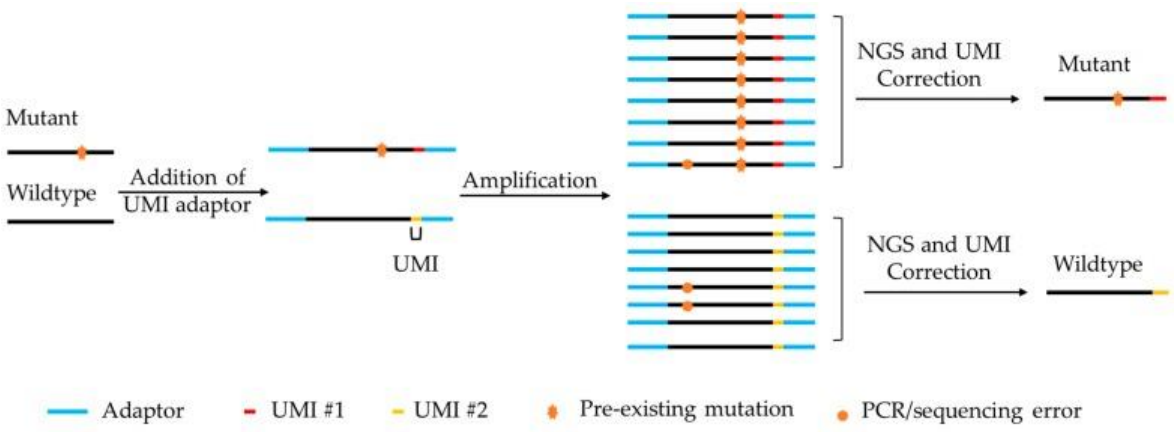

Fig. 6 Unique Molecular Identifier (UMI) technology and its application in somatic mutation detection (image from C.C. Huang, et al.,2019) [51].

Using UMIs during sequencing can significantly reduce the occurrence of false-positive variant calls and significantly enhance the sensitivity of verified true variant detection [65]. These UMIs uniquely tag each nucleic acid in the initial sample, allowing bioinformatics software to accurately eliminate duplicate reads and PCR errors, consequently reporting unique reads and removing identified errors prior to the final data analysis. The sequencing workflow with UMI generates amplified and indexed libraries both with UMI tags and with the classic Unique Dual Indexed (UDI) primers. Utilizing UDI, each index is unique to each library derived from the respective sample, ensuring that all nucleic acids within a sample are labelled with the same sequence tag. Consequently, the resulting library can be pooled with others and sequenced simultaneously in a single run.

2. Aims of the study

Given the current absence of an effective cure for MM, there is a critical need to identify potential biomarkers associated with presymptomatic stages that indicate an elevated risk of disease development, thereby enhancing prognostic outcomes. Early detection is imperative, requiring the use of minimally invasive diagnostic approaches, distinct from conventional bone marrow biopsies. Liquid biopsy emerges as a promising alternative, offering the advantage of periodic monitoring with minimal discomfort and adverse effects particularly beneficial for individuals within the typical age range of MM onset.

Consequently, this study primarily focuses on the analysis of ccfDNA extracted from plasma of patients at various stages of MGUS, SMM, and MM disease. Its investigation presents an opportunity to explore potential similarities and differences among biological samples obtained from different conditions, despite the inherent complexity and heterogeneity of the pathology posing a considerable challenge in identifying significant targets.

The objective of this study was to evaluate the utility of LBs in getting information on patients affected by MM or its presymptomatic stages, detecting mutations in early stages, examining the differences through sensitive methods such as NGS and dPCR and investigating their potential effects. This study could open new views for understanding MM and its presymptomatic phases, highlighting the potential and limitations of LBs.

In summary, the goals of the present study were: (1) to verify the presence of mutations in ccfDNA (in short “circulating mutations”, CM) within the genes associated with MM in patients affected by MGUS; (2) to characterize the CM in relation to the evolution of the disease (using the same patients in their clinical follow up); (3) to characterize the CM in a cohort of MM patients; (4) to study any eventual presence of CM in a cohort of unaffected people.

3. Materials and methods

3.1. Population

This study involved a retrospective collection of biobank-stored samples. From October 2020, peripheral blood samples of over 4,000 individuals have been collected, of which 350 individuals have MM, 60 have SMM, and 900 have monoclonal gammopathy of undetermined significance MGUS. In addition, BM samples of approximately 100 individuals have been collected, of which approximately 70% have MM, 20% have SMM, and 10% have MGUS. In addition to the patient's diagnosis, the criteria for selecting samples of interest to investigate were the absence of other tumors, the fewest possible comorbidities, and the presence of at least two samples at different times in our biobank. In addition, attention was paid to selecting patients with MGUS who have been diagnosed for at least 2 years, and to prioritizing patients with MM at diagnosis who have at least one sample prior to the start of therapy. Among the samples that meet these criteria, the oldest samples were selected with priority.

3.2. Biobank

The construction of the biobank of biological samples was approved by the Regional Ethics Committee for Clinical Trials, in the monocentric study program in collaboration with the Laboratory of Clinical Pathology of the Azienda Ospedaliera Universitaria Pisana (AOUP). All peripheral blood samples have encrypted code, the clinical information of patients is linked to the acquisition of specific informed consent by patients and the treatment of this information has been carried out in accordance with the provisions of national laws and administrative provisions in force.

An aliquot of 500 µL was taken from each peripheral blood sample to be stored at -20°C. Subsequently, the remaining volume was centrifuged at 400 xg for 15 min at room temperature (RT) to separate it into the plasma fractions, nucleated cells, and red blood cells. The plasma is further centrifuged at 1400 xg for 10 min at RT, the supernatant is stored at -80°C. The nucleated cell part taken is diluted in a 1:1 ratio with Phosphate Buffered Saline 1X (PBS – Life Technologies, Carlsbad, CA), this solution is added slowly to a double volume of Histopaque-1077® (Sigma-Aldrich, St. Louis, MO), centrifuged at 400 xg for 30 min at RT. The cell ring or Buffy-Coat (BC) well separated from the other components, is resuspended in PBS 1X and centrifuged at 400 xg for 10 min at RT. The cell pellet obtained is resuspended in 1 mL of freezing medium consisting of 70% bovine fetal serum (FBS - Life Technologies, Carlsbad, CA) and 30% dimethyl sulfoxide (DMSO - Life Technologies, Carlsbad, CA), to be stored at -80°C.

From each peripheral blood sample, an aliquot of peripheral blood, a plasma aliquot, and a BC aliquot were obtained, each suitably processed and stored at an appropriate temperature. The BM was processed according to the same protocol adopted for the samples of peripheral blood, with the only difference being that the cellular pellet was resuspended in 1 mL of freezing medium consisting of 90% FBS and 10% DMSO.

3.3. ccfDNA extraction and QC

The ccfDNA extraction was performed using a QIAamp® MinElute® ccfDNA kit (Qiagen, Hilden, DE), following manufacturer specifications, specially formulated for efficient purification of free circulating DNA (ccfDNA) from human plasma. The method of this solid phase extraction kit includes a first step that efficiently processes liquid samples using paramagnetic particles capable of binding DNA and a second step consisting of columns equipped with a silica membrane at the base, which binds and retains DNA. The extracted DNA was measured with Qubit™ DNA HS Assay Kit (Life Technologies, Carlsbad, CA) and the DNA quality was evaluated by Agilent 2100 Bio-Aanalyzer (Agilent Technologies, Santa Clara, CA) with the Agilent High Sensitivity DNA Kit (Agilent Technologies, Santa Clara, CA).

3.4. gDNA extraction and QC

The genomic DNA (gDNA) extraction was performed using a PureLink® Genomic DNA Mini Kit (Life Technologies, Carlsbad, CA), following the manufacturer's specifications, used for efficient purification of gDNA from peripheral blood, Buffy-Coat, the cellular component of the BM, and human cell lines. The method of this solid phase extraction kit consists of columns equipped with a silica membrane at the base and is based on the selective binding of gDNA to the membrane in the presence of chaotropic salts. The quantity and quality of the extracted DNA were measured with NanoDrop™ Lite Spectrophotometer (Life Technologies, Carlsbad, CA).

3.5. NGS sample

52 samples of ccfDNA extracted from plasma from 40 individuals were analyzed by next-generation sequencing (NGS). In this retrospective study, patients with an evolution of the pathology were chosen and compared with patients affected by MGUS and a group of healthy patients as controls. Table 4 summarizes the analyzed cohort characteristics.

Patient and sample caratteristics	n
Patient	35
Median Age (Range) In Years	(57 e 89)
Gender	
Male	19
Female	16
Patient evolved	
MGUS-SMM	5
MGUS-MM	3
MGUS-SMM-MM	1
Heavy-chain subtype	
IgG	23
IgA	2
IgM	0
Light Chain subtype	
Kappa	13
Lambda	12
Sample	52
Clinical status at plasma collection (n)	
No tumor (healthy)	10
MM	7
SMM	8
MGUS	27
Average volume plasma (ml)	2
Average ccfDNA extracted from plasma (ng)	10
Relative concentration ctDNA (100-400bp)/total ccfDNA	>20%
Time interval of sampling from diagnosis (Months)	
MGUS	> 24
SMM	< 3
MM	< 3

Table 4 Characteristics of patients and samples analyzed by NGS.

3.6. Targeted Panel Design

The custom myeloma-targeted sequencing gene panel was designed using the DesignStudio software tool (Illumina, San Diego, CA, USA) and included a capture-based approach of coding exons or hotspot positions of 84 genes typically involved in MM (*ACTG1; ANK2; ARID1A; ATM; ATR; BIRC2; BIRC3; BRAF; CCND1; CD79B; CDKN2A; CDKN2C; FAF1; CSMD3; CXCR4; CYLD; DIS3; DNAH5; DNAH9; DST; DTX1; EGR1; FAM46C; FAT1; FAT3; FAT4; FBN2; FGFR3; HIST1H1E; HMCN1; IGLL5; IRF1; IRF4; KALRN; KDM6A; KLHL6; KMT2C; KMT2D; KRAS; LAMA1; LRP1B; LTB; MAX; MCL1; MYBBP1A; MYC; MYD88; MYO10; NFKB2; NFKBIA; NOTCH1; NOTCH2; NRAS; NRXN1; OBSCN; PCDHA1; PCLO; PIM1; PKHD1; PRDM1; PRKD2; PTPN11; PTPRD; RASA2; RB1; ROBO1; RYR1; RYR2; RYR3; SLAMF7; SP140; SYNE1; TACC2; TCL1A; TNFAIP3; TNFRSF17; TP53; TRAF2; TRAF3; UBR5; USH2A; UVSSA; ZFHX4; ZNF292*). We designed an exonic coverage panel for 84 MM-related genes considering the regions of coding sequences (CDS) ± 50 bp UTR regions, the final covered size corresponds to approximately 785,843 bp (panel size 785 Kb) (Twist Bioscience HQ, South San Francisco, CA).

3.7. Library preparation and UMI

The panel exome library preparation has been performed using the Library Preparation with the Twist UMI Adapter System (Twist Bioscience HQ, South San Francisco, CA), this kit allows you to prepare libraries with random duplex UMIs. UMI adapters are important for high depth sequencing to detect low frequency mutations.

The library preparation has been optimized and modified than the manufacturer's instructions. In particular, the fragmentation step was not performed; it was loaded for input on average 10 ng of double-stranded ccfDNA. The Concentration of the UMI was modified based on the profile and quantity of the input sample, trying to maintain a UMI concentration of 0.15x. UMI Adapter Ligation Step at 20° C for 15 min, according to the manufacturer's instructions, was extended to 3 hours. For the amplification step of the library, 11 PCR cycles have been set for each sample.

Libraries were quantified using Qubit™4 dsDNA Broad Range Quantitation Assay (Invitrogen, Carlsbad, CA) and qualified both on Bio-Analyzer with the Agilent High Sensitivity DNA Kit (Agilent Technologies, Santa Clara, CA, USA) and on TapeStation 2200 with the kit Agilent DNA 1000 (Agilent Technologies, Santa Clara, CA, USA), to evaluate success and amplification.

This library preparation protocol is optimized for enrichment with Twist Target Enrichment Kit (Twist Bioscience HQ, South San Francisco, CA). Samples with similar ccfDNA electropherogram profiles were grouped together, from 5 to 8 pre-enriched libraries were pooled up to a maximum concentration of 2500 ng for capture-bead-based hybridization. In the final purification of the post-

capture libraries, the concentration of the beads was increased from 1x to 1.5x. The pooled and captured libraries were then pooled on Novaseq 6000 S4 flowcell (Illumina, San Diego, CA). Sequencing was set to 150 PE until a theoretical depth of 10,000x was reached. Deeper sequencing enhances the limit of detection, enabling the identification of any potentially missed variants Generally, the sequencing depth of our NGS assay was intended to be sufficiently high to detect low burden variants.

3.8. Bioinformatics NGS analysis

The raw data generated from Novaseq 6000 ™ were demultiplexed and converted using the DRAGEN BCL conversion tool provided by Illumina®. Raw sequencing reads were quality-checked using FastQC software (v0.11.4, http://www.bioinformatics.babraham.ac.uk/projects/fastqc/). For each individual sample, the nucleotide sequences with their base quality scores in text format file (Fastq), the binary alignment map file (Bam), and the variant calling file (Vcf) were generated. Illumina DRAGEN Somatic app is based on the DRAGEN v4.2.4 pipeline and was used to process the trimmed reads and aligned with the human reference genome, GRCh38/hg38 available at UCSC Genome Browser.

Duplicate fragments having the same UMI are collapsed in a consensus sequence. The reads that appear to have come from the same original molecule are grouped together by template, and then templates are compared considering 5' and 3' ends of both reads. Fragments that match in both ends and have the same UMI are collapsed. Reads derived from the same unique molecule are initially classified based on their source strand and then merged into single-strand consensus sequences. To apply stringency to the duplex, collapse a minimum number of 2 input reads to form a consensus read to ensure that duplex consensus reads consist of at least 1 read from both the top and bottom strand. For visualization of the read-alignment status, the Bam files were loaded in Integrative Genomics Viewer (IGV_2.9.4; The Broad Institute, Cambridge, MA, USA).

The bam files obtained from Illumina Dragen somatic pipeline were used for variant calling using Map/Align + Somatic Small Variant Caller. Was Enabled Common Germline Variant Tagging, enabling this option uses population databases to tag potential germline variants in the INFO field with Germline Status. Current databases include both exome and genome sequencing data from GnomAD. The Nirvana variant annotation was enabled to generate an output file with RefSeq annotations for variants in all output Dragen VCFs.

All filtered variants with high depth were assessed. High depth enables variant calling with presets optimized for liquid biopsy analysis with post-collapsed coverage rates of roughly 2000-2500 X and target allele frequencies of 0.4% and higher by checking if and in which frequencies the variants were present, it was verified that these variants were not due to duplicates, artifacts, or background noise.

Only the PASS somatic variants were considered at the quality check on which custom selection and visualization filters were applied in all samples to identify the most interesting variants and a possible pattern of mutations among patients with evolution of the disease.

Flags for frequency <5% of the population, a flag for predicted damaging and excluding intronic variations were inserted. They were also explored using the PolyPhen tools for variant pathogenicity assignment. The mutations predicted as probably damaging and possibly damaging were counted together in the analysis. The custom filters were applied and compared in different groups of data, first, the variants obtained in all the samples were considered, then the variants present only in the samples from MGUS patients, then the variants present only in the healthy samples, and finally only the variants present in the subjects who had an evolution of the disease in pre- and post- evolution samples. These validated variants were further annotated using BaseSpace Variant Interpreter (https://variantinterpreter.informatics.illumina.com/home) and were manually verified in IGV. Variants identified were compared with MMRF CoMMPass Study database (https://portal.gdc.cancer.gov/) and on publicly available resources listed at cBioPortal (https://www.cbioportal.org) and the COSMIC data (https://cancer.sanger.ac.uk/cosmic).

3.9. Digital PCR

The digital PCR (dPCR) test was used to sensitively and accurately identify individual mutations of specific sequences present in DNA. A large group of patients at different stages of the disease were analyzed. In this experiment, DNA extracted from plasma, BC and BM was investigated, also comparing samples taken at different times for the same patient. In particular, plasma and BC samples collected at least 30 days before the BM collection were selected. This assay was optimized for the detection of mutant sequences in wild-type background DNA using the dPCR LNA Mutation Assays Kit (Qiagen, Hilden, DE) using the QIAcuity digital PCR (dPCR) instrument (Qiagen, Hilden, DE). Samples were analyzed using the ddPCR Mutation Assay (Bio-Rad Laboratories, Hercules, CA) in a duplex reaction with FAM fluorophore mutant probes and HEX fluorophore wild-type probes. For *KRAS* and *NRAS* dPCR Mutation Assays were used:

KRAS p.Q61H c.183A>C (Bio-Rad, Assay ID: dHsaMDS675847171);
NRAS p.Q61R c.182A>G (Bio-Rad, Assay ID: dHsaMDV2010071);
NRAS p.Q61K c.181C>A (Bio-Rad, Assay ID: dHsaMDV2010067).

PCR reactions were assembled into individual tubes according to the following protocol: 10 µl of 4x Probe PCR Master Mix (Qiagen); 2 µl of 20x dPCR Mutation Assay (FAM/HEX); the amount of DNA was variable based on the concentration (for ccfDNA at least 20 ng/reaction was used; for gDNA 400 ng/reaction was used); nuclease-free water free until the total volume of 40 µl is reached.

The contents of each tube were aliquoted into the wells of a 26,000-partition, 24-well nanoplate (Qiagen), with each reaction mix being distributed across 4 wells. Two non-template controls, 1 positive control, and 1 negative control were inserted into each nanoplate. DNA extracted from PSN-1 cell lines was used as a negative control for all dPCR mutational assays, while DNA from the following cell lines was used as a positive control for each dPCR mutational assay: Hs766T (*KRAS* p.Q61H c.183A >C); ARK (*NRAS* p.Q61R c.182A>G); JJN-3 (*NRAS* p.Q61K c.181C>A). The Nanoplate were sealed using the accompanying QIAcuity Nanoplate Seal from the QIAcuity Nanoplate Kit (Qiagen). PCR reactions were conducted under the following conditions: 95°C for 2 min, followed by 40 cycles at 95°C for 15 s, 55°C for 1 min. Subsequently, the target was acquired by measuring the fluorescence of all positive partitions, the total amount of target DNA in all partitions of a well is determined by multiplying the average amount of target DNA per partition by the number of valid partitions. The QIAcuity Software Suite was employed to analyze mutation frequencies in target samples by quantifying the absolute number of copies of each wild-type and mutant target present in samples, and by determining the mutation frequency in each sample.

3.10. Cell Cultures

One type of Multiple myeloma cell lines is used for the experiments. U266-B1 (ATCC® TIB-196™ - ATCC, Rockville, MD) is a B lymphocyte isolated from the peripheral blood of patient with multiple myeloma. Were grown in RPMI 1640 Medium (Gibco BRL, Grand Island, NY, USA) with 15% fetal bovine serum (FBS) (Life Technologies, Carlsbad, CA) previously inactivated at 55°C for 1 hour, 1% penicillin/streptomycin 100X (Euroclone S.P.A., Milan, IT). Cell lines were incubated at 37°C in a humidified atmosphere incubator containing 5% CO_2.

3.11. Plasmid transfection

Multiple myeloma cell lines U266-B1 were stably transformed with two plasmids for the overexpression of the *NRAS* p.Q61R c.182A>G mutation and for the overexpression of the wild type (wt) *NRAS* gene and a third plasmid with empty vector used as a control. The resulting cell lines were then named:

O.E. NRAS WT for cells containing the plasmid for over-expression of *NRAS* WT.

O.E. NRAS Q61R for cells containing the plasmid for over-expression of the *NRAS* mutated.

O.E. Ctrl for cells containing the plasmid with the empty vector.

Were grown in RPMI 1640 Medium (Gibco BRL, Grand Island, NY, USA) with 15% fetal bovine serum (FBS) (Life Technologies, Carlsbad, CA) previously inactivated at 55°C for 1 hour, 1% penicillin/streptomycin 100X (Euroclone S.P.A., Milan, IT), 1 µg/mL Puromycin Dihydrochloride (Gibco BRL, Grand Island, NY, USA). Cell lines were incubated at 37°C in a humidified atmosphere incubator containing 5% CO_2.

The process of plasmid synthesis and transfection was performed as part of a collaboration by the Genomics and Proteomics Core Facilities, Deutsches Krebsforschungszentrum, Heidelberg (DKFZ). The map of these plasmids is shown in Fig. 7.

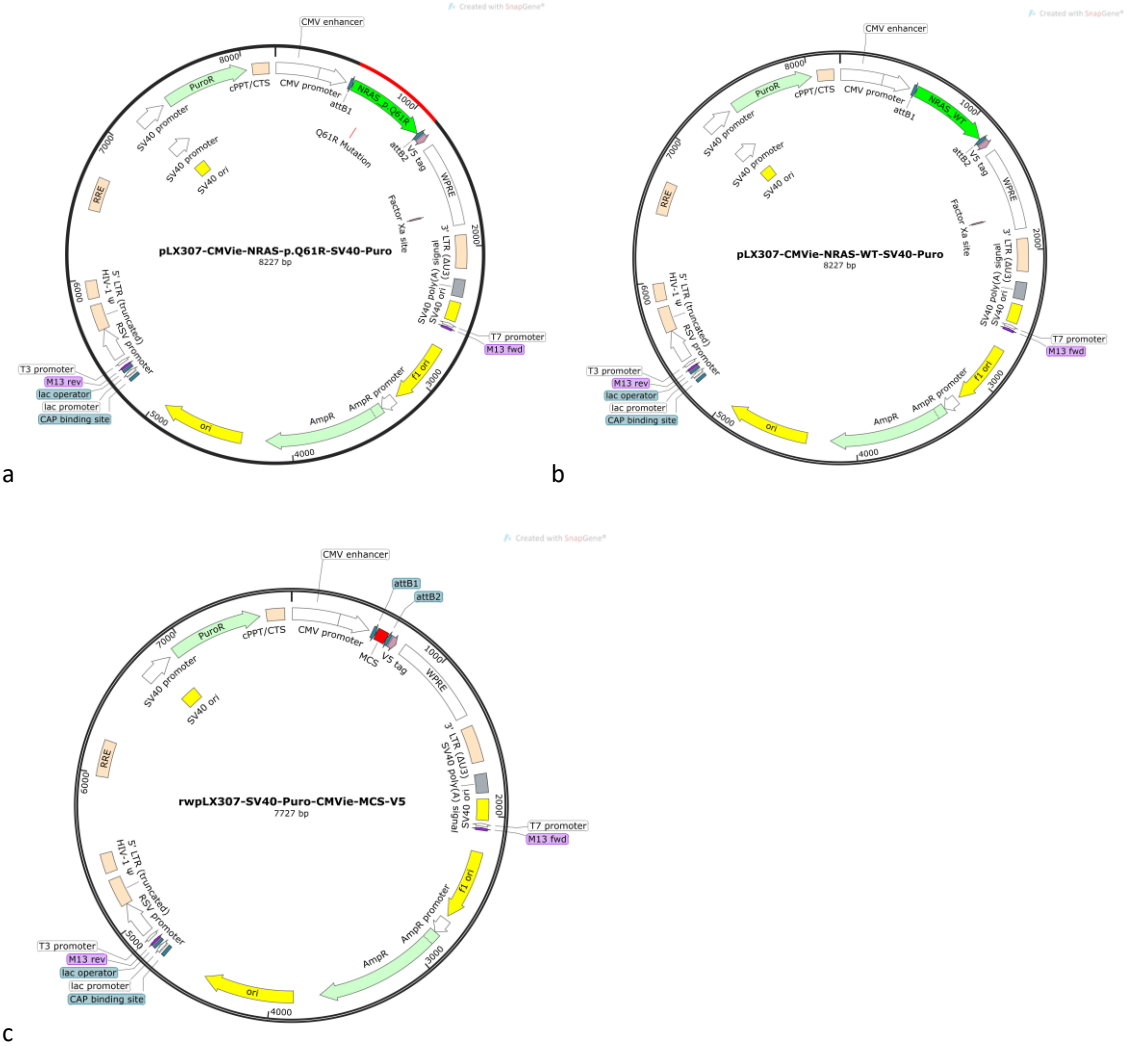

Fig. 7 Map of plasmids for cell transformation a) plasmid for overexpression of the NRAS p.Q61R mutation b) plasmid for overexpression of the wild type NRAS gene c) plasmid with empty control vector.

3.12. RNA extraction and cDNA synthesis

Total RNA was extracted from human MM cell lines using the PureLink™ RNA Mini Kit (Life Technologies, Carlsbad, CA). The pellet was resuspended in PBS and subjected to purification, according to the protocol provided by the manufacturer. The RNA was eluted in 40 µL of RNase free water. Extracted RNA was measured with Qubit™ RNA BR Assay Kit (Life Technologies, Carlsbad, CA) and total RNA was reverse transcribed into cDNA using the QuantiTect® Reverse Transcription Kit (QIAGEN, Hilden, DE) according to the manufacturer's instructions.

3.13. Real time PCR

Real Time qPCR is a technique that allows the simultaneous amplification and quantification of target mRNA. Quantitative real-time PCR was performed using HOTFIREPol® EvaGreen® qPCR Mix Plus (no ROX), 5X (Solis Biodyne, Tartu, EE) according to the manufacturer protocol. The analysis was carried out in parallel for the U266-B1; O.E. NRAS WT; O.E. NRAS Q61R; O.E. Ctrl. PCR was performed at 95°C for 12min followed by 40 cycles at 95°C for 15s, 65°C for 20s, and the dissociation step at 72°C for 20s and plate read. Final step for the melting curve 65°C to 95°C, increment of 0.5°C x 0:05 (Meltcurve) + plate read. Data were analyzed using CFX ManagerTM software (Bio-Rad Laboratories, Hercules, CA). The relative expression of mRNA in cells were calculated using ΔΔCt; and being a relative quantification analysis, we used the *GAPDH* housekeeping genes as a comparative reference gene. To analyze the expression of *NRAS* and *GAPDH*, we used the primers:

NRAS Forward: 5' – CAAACTGGTGGTTGGAG – 3'
NRAS Reverse: 5' – TTGGTCTCTCATGGCACTGTAC – 3'
GAPDH Forward: 5' – CGCTCTCTGCTCCTCCTGTT – 3'
GAPDH Reverse: 5' – CCATGGTGTCTGAGCGATGT – 3'

3.14. Protein extraction

Proteins were extracted from cells by a lysis buffer consisting of 50 mM Tris-HCl pH8, 1% TritonX 100x, 0.25% Sodium Deoxycholate, 10% proteinase inhibitor (PI), 1mM phenyl methyl sulfonyl fluoride (PMSF). This lysis buffer was added for $1x10^6$ cells pelleted previously at 300 xg for 5 min. The samples were left on ice for 30 min and subsequently centrifuged at 4°C at 12000 xg for 30 min, then the supernatant was recovered and stored at 80°C for subsequent applications. Protein quantification was carried out using the PierceTM BCA Protein Assay Kit (Life Technologies, Carlsbad, CA) according to the specifications reported by the manufacturer. Bovine serum albumin (BSA -

Sigma-Aldrich, St. Louis, MO) was used to create the standard curve, from which the concentrations of the samples were then obtained. The protein quantification was determined measuring the absorbance at 562nm from each well by FLUOstar OPTIMA microplate reader (BMG LABTECH, Ortenberg, Germany).

3.15. Western Blot

The analysis was performed on U266-B1; O.E. NRAS WT; O.E. NRAS Q61R; O.E. Ctrl. Approximately 40 µg of proteins were used for each cell line analyzed. The protein samples were diluted with Loading Buffer 4x (Tris-HCl 125mM pH 6.8, SDS 2%, glycerol 10%, bromophenol blue 0.02% and ß-mercaptoethanol 5%) and denatured for 5 minutes at 95°C. The samples were then loaded and separated on a specific 12% polyacrylamide gel. At the end of the separation, the proteins were transferred to a Trans-Blot® Turbo ™ Mini Nitrocellulose membrane (Bio-Rad Laboratories, Hercules, CA) using the Trans-Blot Turbo Transfer system (Bio-Rad Laboratories, Hercules, CA). After an initial staining with Ponceau red, the membranes were blocked in solution with 3% powdered milk in TBS-T 1X for 60 min and subsequently incubated overnight at 4° C with the primary monoclonal antibody towards the protein to be investigated. After overnight incubation, three washes were performed in TBS-T 1X before incubating the membranes with anti-Rabbit or anti-Mouse secondary antibody depending on the primary antibody tested, in TBS-T 1X for 60 min at room temperature. Finally, the membranes were incubated 5 minutes in the dark in ECL Western Clarity™ Substrate detection solution (Bio-Rad Laboratories, Hercules, CA). Hybridization signals were detected by the ChemiDoc XRS system (Bio-Rad Laboratories, Hercules, CA), and images were quantitatively analyzed using ImageJ image analysis software. Each antibody used was diluted as described in Table 5. In the case of the characterization of the mutational status of the *NRAS* gene, monoclonal antibodies against both the NRas protein and the mutated NRas protein (p.Q61R) were used in the cell lines on which the experiments were carried out. To compare protein levels the GAPDH gene was used as housekeeping.

Gene	Host species	Diluition	Company
NRas mut (p.Q61R)	Rabbit	1:1000 in milk 3%	Abcam, Cambridge, UK
NRas	Mouse	1:500 in milk 3%	Santa Cruz Biotechnology, Inc., Dallas, TX
GAPDH	Mouse	1:10000 in BSA 5%	ProteinTech Europe, Manchester, UK
HRP Anti-Mouse	Goat	1:2000 in milk 3%	ProteinTech Europe, Manchester, UK
HRP Anti-Rabbit	Goat	1:2000 in milk 3%	ProteinTech Europe, Manchester, UK

Table 5 Antibody details

3.16. Colony Assay

For the clonal cell expansion experiment, a solution of Methyl cellulose (MC) final concentration 20g/L (Sigma-Aldrich, St. Louis, MO) in serum-free RPMI 1640 Medium (Gibco BRL, Grand Island, NY, USA) was prepared. The solution was placed on a magnetic stirrer, gradually adding the necessary volume of medium, until the solution was homogeneous. The experiment was carried out in parallel for the U266-B1; O.E. NRAS WT; O.E. NRAS Q61R; O.E. Ctrl. For U266-B1, $5x10^4$ cells/mL were resuspended in RPMI 1640 Medium (Gibco BRL, Grand Island, NY, USA) with 45% fetal bovine serum (FBS) (Life Technologies, Carlsbad, CA), 3% penicillin/streptomycin 100X (Euroclone S.P.A., Milan, IT). Cell cultures transfected with the plasmid were resuspended $5x10^4$ cells/mL in RPMI 1640 Medium (Gibco BRL, Grand Island, NY, USA) with 45% fetal bovine serum (FBS) (Life Technologies, Carlsbad, CA), 3% penicillin/streptomycin 100X (Euroclone S.P.A., Milan, IT), 3µg/mL Puromycin Dihydrochloride (Gibco BRL, Grand Island, NY, USA). In a 2 mL volume of MC, prepared as described above, 1 mL of cell suspension for each line tested was resuspended. The MC+cells suspension was vortexed and incubated at 4°C for 15 min. Subsequently, 3 mL of MC+cells solution were distributed per well of the 6-well plate (Euroclone S.P.A., Milan, IT) for each line and in technical triplicate. The cell lines were incubated at 37°C and 5% CO_2 in the Incucyte® S3 Live-Cell Analysis System (Sartorius, Göttingen, DE) acquiring a photo of the entire well every 24h for 10 days. Images were analyzed by calculating the number and confluence of colonies with the Incucyte® Classic Confluence Analysis program on Incucyte® Base Analysis Software and also using ImageJ image analysis software.

3.17. Cell cycle

For cell cycle analysis, $1x10^5$ cells were seeded per cell line tested; analysis was performed on U266-B1; O.E. NRAS WT; O.E. NRAS Q61R; O.E. Ctrl. the cells were collected after 24h, 48h, 72h, for fixation in ethanol. After a short washing in PBS 1x (Life Technologies, Carlsbad, CA), the cell suspension was centrifuged 5 min to 300 xg, the pellet was resuspended first in 500 mL of PBS and then was added 1.5 mL of ethanol 95% cold drop by drop on the cells stirring on vortex. After incubation of 5 min at room temperature, 6 mL of PBS was added. Subsequently, the cells fixed in ethanol were stained with a solution of propidium iodide (Sigma-Aldrich, St. Louis, MO) 200 µg/ml, sodium citrate 0.1% (Sigma-Aldrich, St. Louis, MO), RNase A (Life Technologies, Carlsbad, CA) final concentration 12.5 µg/mL, Nonidet P40 (Biosigma S.P.A., Verona, IT) 0.1%. Propidium iodide (PI) binds nucleic acids by intercalation in the bases when bound to nucleic acid has a maximum excitation of ~535 nm and a maximum emission of ~615 nm. In a flow cytometer, CytoFLEX™ Platform (Beckman Coulter s.r.l., Brea, CA) positive PI staining cells were detected using a 610/20 band step, and data was analyzed to interpret cell cycle phases using CytExpert Software.

3.18. Transwell

To study a possible involvement of the role of *NRAS* in the behavior of the cell lines under analysis, a cell migration test was carried out using the Transwell insertion device. For migration studies, the transwell inserts with 3 µm pores in a 12-well format (Corning Costar, Cambridge, UK) were used. A total of 1×10^5 cells in 300 µL of serum-free medium were seeded into the upper chamber and 500 µL of complete medium with 100 ng/mL SDF-1 in the lower chamber. The experiment was carried out in parallel for the U266-B1; O.E. NRAS WT; O.E. NRAS Q61R; O.E. Ctrl. The assay was performed for each cell line tested in triplicate. After 24 h incubation at 37°C, the cells inside the membrane were fixed with fluorescent dye DAPI (Abcam, Cambridge, UK). Cell density in the upper chamber, inside the membrane, and in the lower chamber was assessed and the confluence of the migration area was calculated with ImageJ software.

3.19. CellTiter-Glo® 2.0

The CellTiter-Glo® 2.0 cell viability assay (Promega, Madison, WI) was used to measure ATP of U266-B1; O.E. NRAS WT; O.E. NRAS Q61R; O.E. Ctrl. The assay was performed for each cell line tested in triplicate following the manufacturer's specifications. The assay is an indicator of cell health, ascertaining the quantity of viable cells within the culture through ATP quantification, indicative of metabolically active cellular populations. The luminescence measurement correlates linearly with the viable cell count in the culture. The luminescence signal was determined from each well using the FLUOstar OPTIMA microplate reader (BMG LABTECH, Ortenberg, DE).

3.20. RealTime-Glo™ MT

The RealTime-Glo™ MT Cell Viability Assay (Promega, Madison, WI) was used to evaluate the metabolic activity of U266-B1; O.E. NRAS WT; O.E. NRAS Q61R; O.E. Ctrl. The assay was performed for each cell line tested in triplicate. With this Cell Viability Assay, it was possible to monitor cell viability in the same sampling well for up to 48 hours, following the manufacturer's specifications. The assay measures the reduction potential of viable cells and is ATP independent, providing a method for determining viability. Only metabolically active cells will shed the substrate, and luminescence production is directly proportional to the number of live cells. Dead cells cannot reduce the substrate. The luminescence signal was determined from each well by the FLUOstar OPTIMA microplate reader (BMG LABTECH, Ortenberg, DE).

3.21. Statistical analysis

The number of mutations in many cases was normalized to the mutational rate per million bases (TMB). Experiments were independently repeated a minimum of three times and values were presented as mean ± standard error (SEM). Data following a normal distribution were analyzed using the ANOVA test; Tukey's comparison was used for multiple comparisons. When the data were not normally distributed, we used the Kruskal-Wallys test and the Dunn's multiple comparisons test. The Wilcoxon test was used as a nonparametric test for comparing the means of two groups. No data points were excluded from the analyses. Values of $p<0.05$ were considered statistically significant (*$p<0.05$, **$p<0.01$, ***$p<0.001$, ****$p<0.0001$). All statistical analyses were performed using GraphPad Prism software 8.0. Individual data points are graphed or can be found in the source data.

4. Results

4.1. NGS

The NGS analysis was performed mainly in subjects affected by MGUS and in patients for whom we were able to detect an evolution of the pathology, with the aim of characterizing a mutational profile (detectable in the plasma) in these phases. First of all, filters have been applied: (i) positive pass quality, (ii) exclusion of synonymous mutations; (iii) exclusion of intronic regions. We found significant mutational heterogeneity among the samples analyzed for a total of 4537 CM in 394 Gbp sequenced, i.e. a mutation burden of, on the average, 0.0152 mutations per Mega base pairs (MMBP) within the 84 selected genes. There were 760 CM detected in at least one of the healthy people also present in at least one of the patients under study. These CM were considered not relevant for the disease; therefore, they were excluded from any further analysis.

Finally custom filters were applied to eliminate germline mutations ending with 3176 CMs (average TMB = 0.00806 MMBP). Overall, we found 1448 mutations in MGUS samples (53.63 mutation per sample, mps; average TMB= 0.0077; range TMB= 0,0018-0,0188), 372 mutations in SMM (46.5 mps; average TMB=0.0070; range TMB= 0.0020 -0.0133), 617 mutations in MM (88.14 mps; average TMB=0.0101; range TMB= 0.0074-0.0184) and 739 mutations in healthy patients (73.9 mps; average TMB=0.0105; range TMB= 0.0041-0.0214). We did not find any statistically significant difference among these groups of people (Fig. 8).

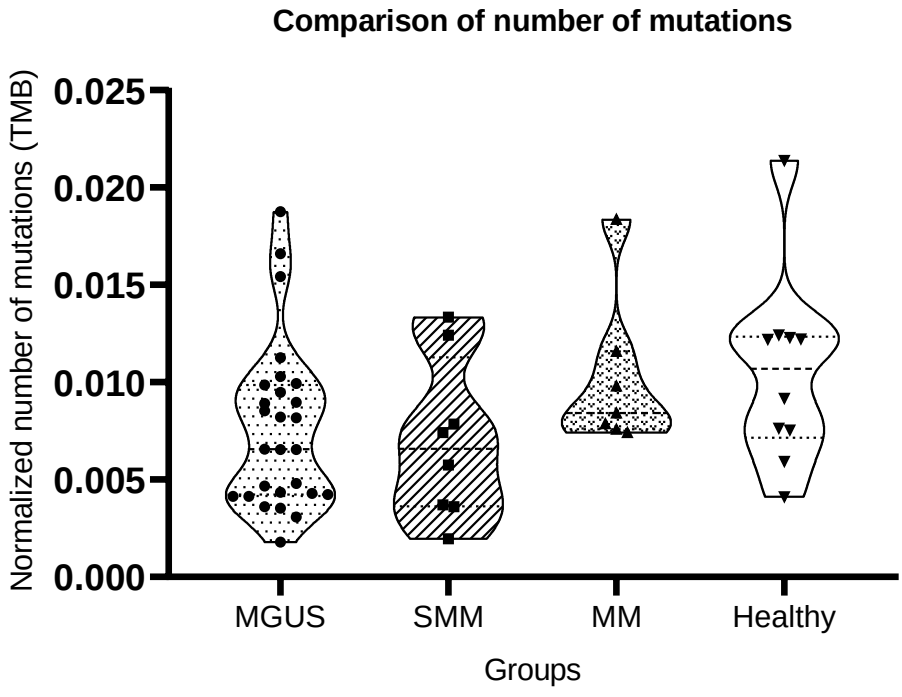

Fig. 8 Number of mutations were normalized by mutation rate per million bases (TMB), found in each patient divided into MGUS, SMM, MM and Healthy groups. Statistical significance was examined using Kruskal-Wallis H-test; the dotted pattern indicates the quartiles while the dashed pattern indicates the median.

We analysed the pattern of CM per sample and per gene. In Fig. 9 we simply show the presence/absence of CM per gene per sample, where a filled dark square represents the presence of at least one CM in the gene in that sample. However, several samples showed multiple mutations within the same gene and the mutation load could depend on the size of the gene, therefore in Fig. 10 we compared the distribution of the number of mutations first normalized by the mutation rate per million bases per sample (TMB), then we compared the TMB taking into account the size of the coding sequence of each gene for each individual sample.

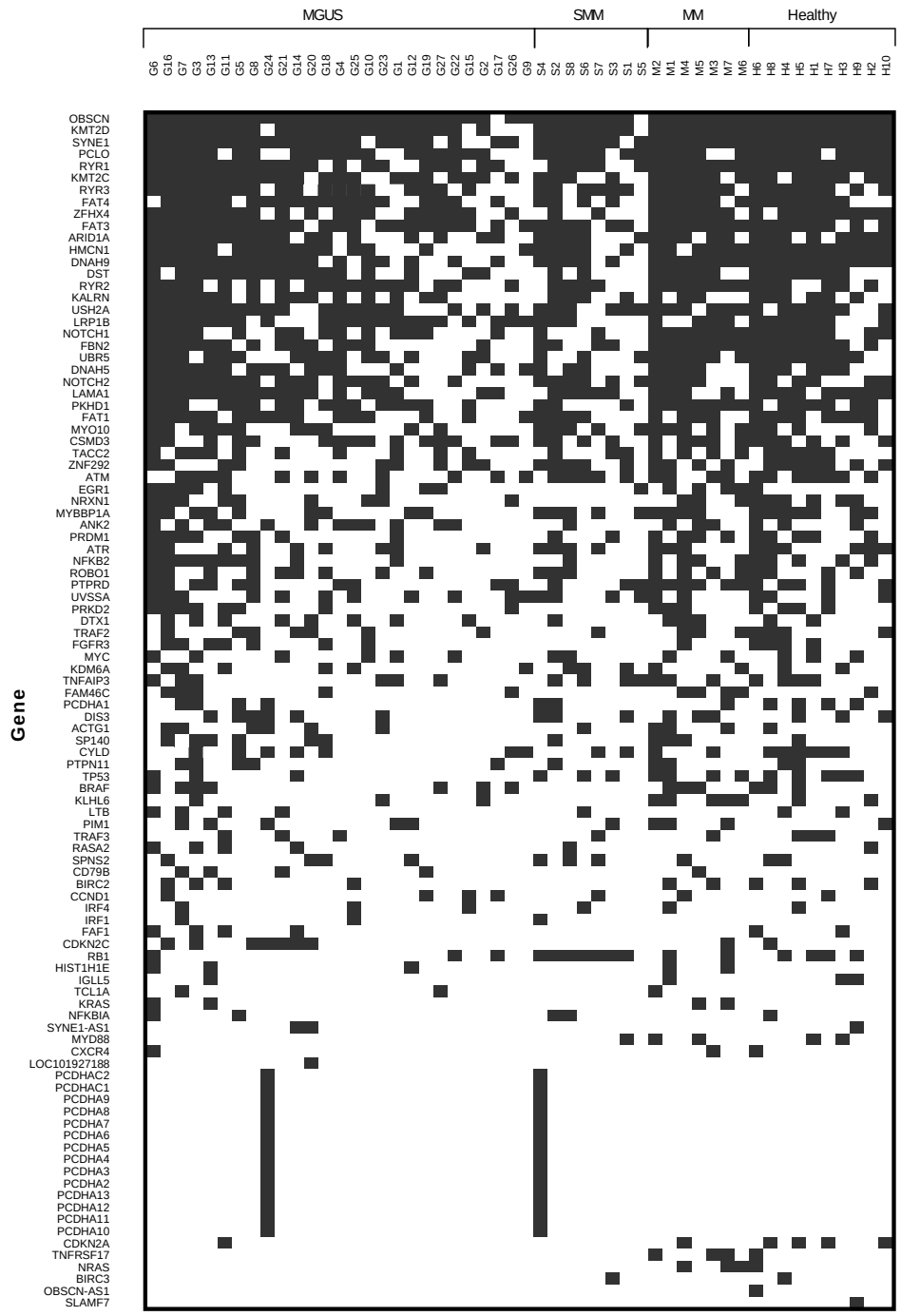

Fig. 9 Graphic distribution of the number of mutations in genes in each individual patient, each dark field indicates that that gene in that sample has at least one mutation.

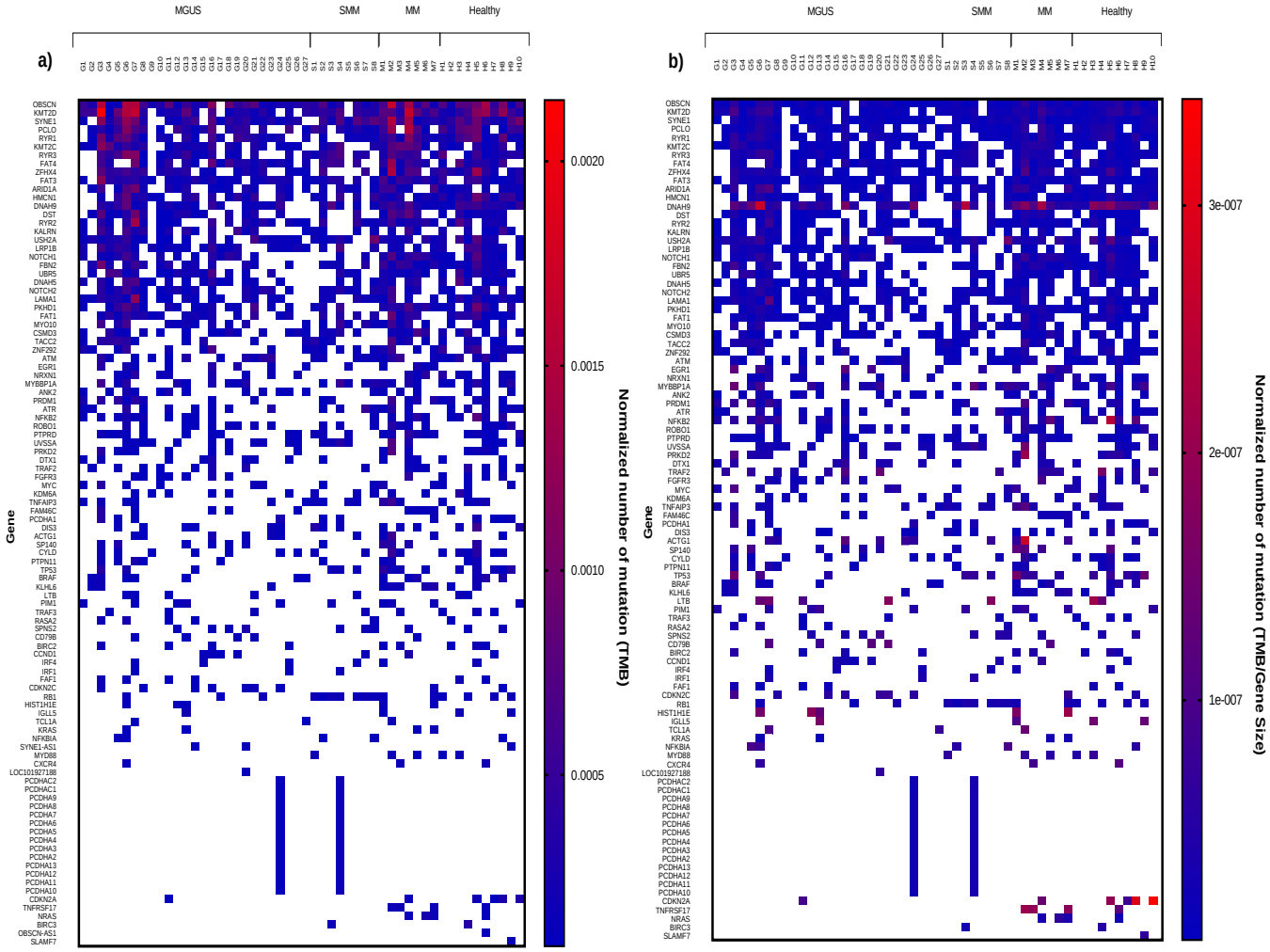

Fig. 10 a) Graphic distribution of the number of mutations normalized by mutation rate per million bases (TMB) in genes in each individual sample. b) Graphical distribution of the number of mutations normalized based on the mutation rate per million bases (TMB) and compared to the size of the coding sequence of the genes for each individual sample

In Fig. 10a) we can observe how some genes have a high number of mutations in different samples, but if we relate the data to the size of the coding sequence of the gene (Fig. 10 b), the TMB per gene results quite similar. We can interpret the graph in Fig. 10b) as the possibility that a gene shows mutations mostly based on its size suggesting that the occurrence of mutations is randomly distributed across the selected genes.

Then, we analyzed the distribution of patients carrying mutations within a given gene shared by health state (i.e. for each category: number of patients with a mutation in a given gene / total patients). Fig. 11 shows that, despite slight variations, the only statistically significant difference was between the MGUS and the MM group with a higher frequency of MM patients carrying mutations within genes such as *FBN2*; *NOTCH1*; *PKHD1*; *RYR2*; *DNAH9*; etc., than patients with MGUS.

The frequency of patients within groups was also compared with that reported in two genomic databases, The Cancer Genome Atlas (TCGA) and cBioPortal, for MM, and here we found a statistically significant difference with all groups analyzed (Fig. 11).

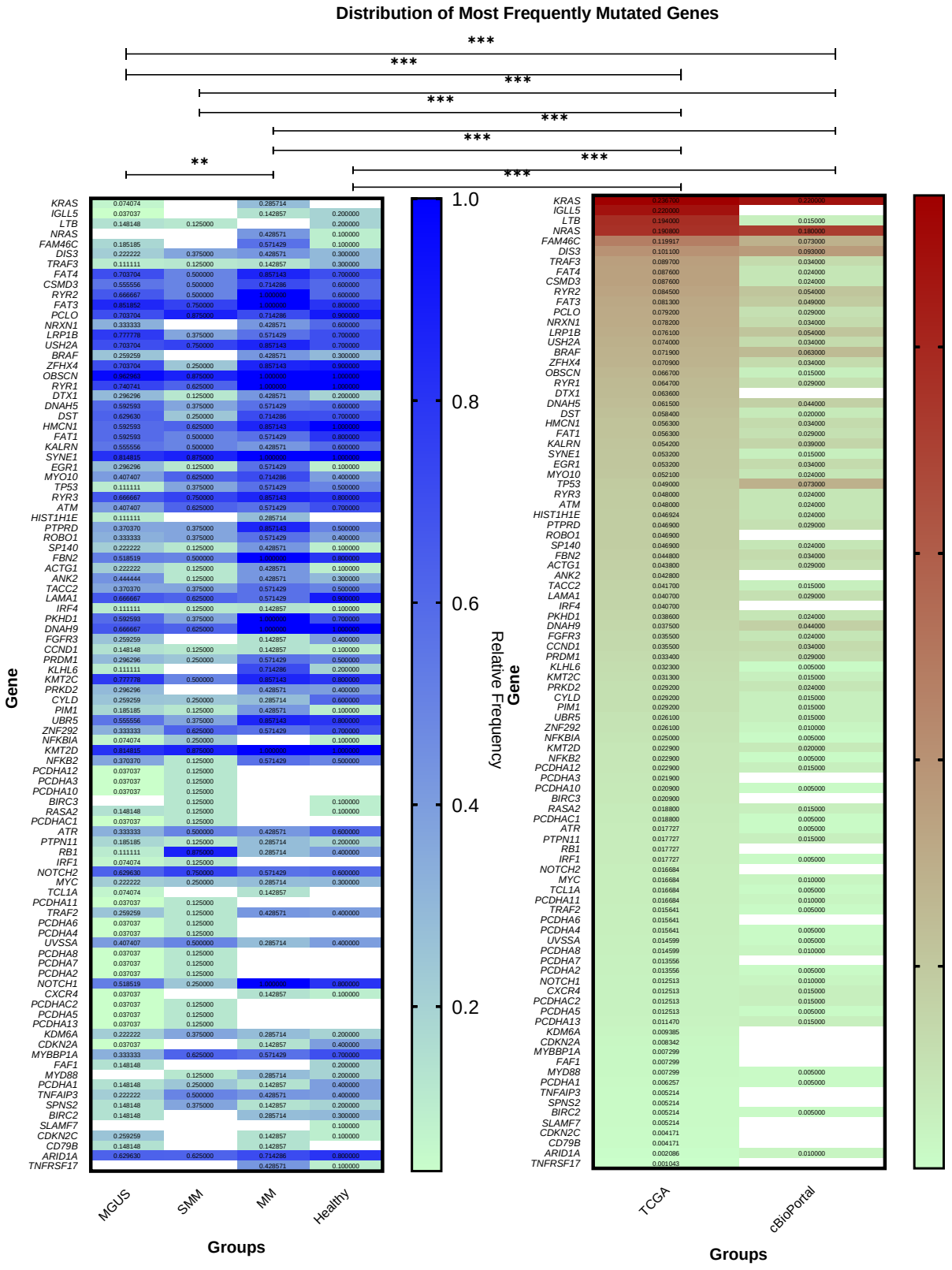

*Fig. 11 Frequency distribution of patients carrying mutations within specific genes, categorized by health state (i.e. for each health group: number of patients with a mutation in a given gene / total patients). Comparison among different health state groups (left) and these groups with TCGA or cBioPortal (right). Statistical significance was examined using Kruskal-Wallis H-test; (**p<0.005, ***p<0.0005)*

The high frequency of alterations identified in all groups and also among healthy subjects, suggests a high background probably of hematopoietic origin [66]. To allow a distinguishable profile to be defined, the frequency for each gene in the healthy groups was compared to that of the healthy controls (Fig. 12).

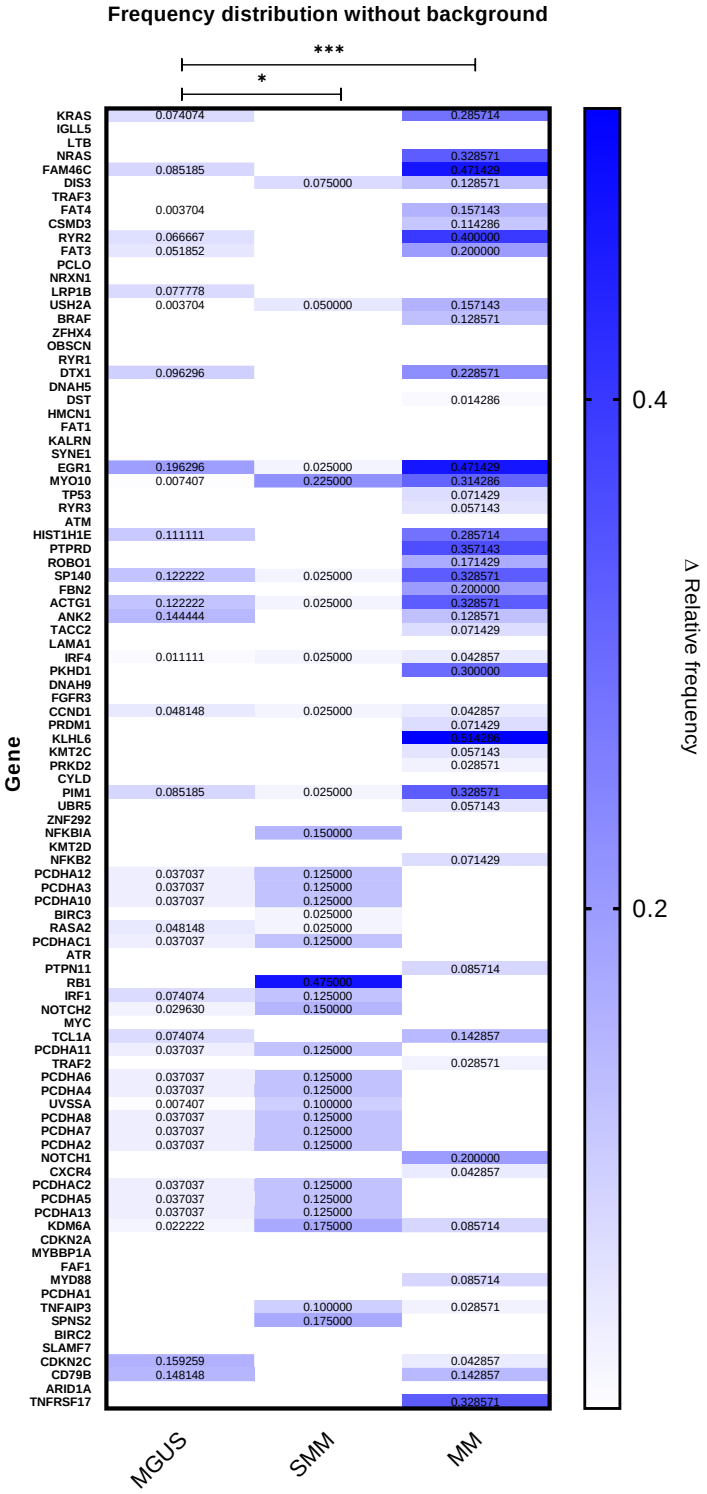

*Fig. 12 Backround-subtracted relative mutational frequency distribution in each gene and divided into health status groups. Only positive differences in frequency for that gene are reported for that group compared to healthy people. Statistical significance was examined using the Kruskal-Wallis H test; (*p<0.05; ***p<0.0005)*

The data obtained taking this background into consideration presents the most relevant genes for health status. Compared to the healthy group, in the MM group we found an increase in the frequency of the genes *ACTG1, BRAF, DTX1, FAM46C, FAT3, FBN2, HIST1H1E, IGR1, KLHL6, KRAS, MYO10, NOTCH1, NRAS, PIM1, PKHD1, PTPRD, ROBO1, RYR2, SP140, TNFRSF17, USH2A*, which partially recapitulate the profile described in TCGA.

Interestingly, no point mutations (SNVs) in *NRAS* and *KRAS* were found in almost any MGUS patient samples, deletions were detected in only 2 of the 27 MGUS samples analyzed, *KRAS* c.426del (1 bp del, frameshift) and *KRAS* c.226del (1 bp del, frameshift). While 4 out of 7 total MM samples analysed present some mutations in the *NRAS* and *KRAS* genes. The *NRAS* c.164_182del mutation is present in 3 MM samples while the *KRAS* c.*101_*106del; *KRAS* c.*90del and *NRAS* c.336_338del, each appear individually in a sample of MM. Moreover, we analysed the TMB found in 9 patients who experienced the progression of the disease. In fact, for each of them, blood samples were available at the time of MGUS and at the time of their evolution into SMM or MM. The data overall suggested a slight tendency to increase the MMBP as the disease progresses even thought this data is not statistically significant and each patient shows its own peculiar shaping of the mutational profile (Fig. 13) In fact, passing from MGUS into SMM/MM, patients # 1, 4, 5, 9 showed a steady TMB, patients # 2, 8 showed an increase while patients #3, 6 showed a reduction. Patient #7 further suggested that this measure can vary through the time, and it is not a marker of the progression of MGUS into MM.

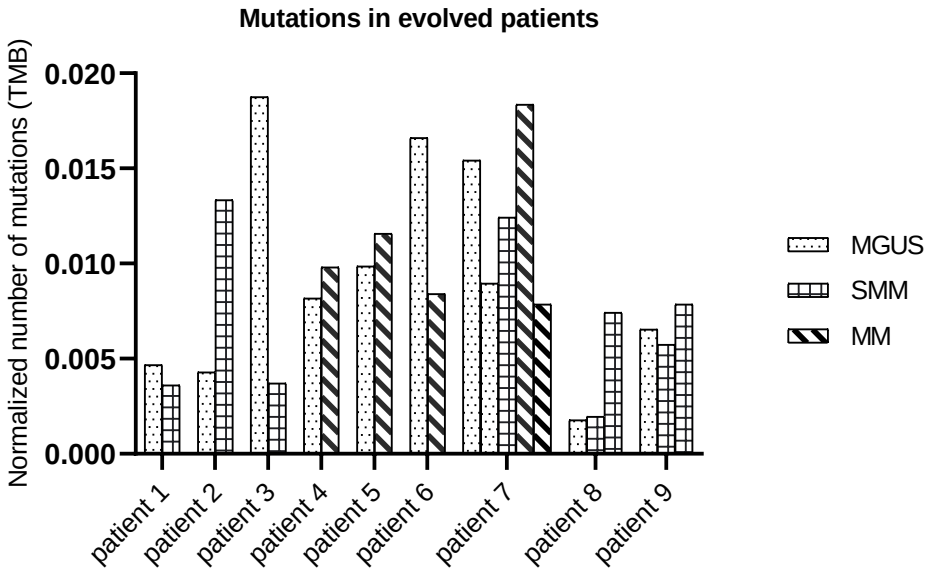

Fig. 13 TMB detected at the diagnosis of MGUS, SMM, and MM of each patient with the evolution of the disease. Statistical significance was examined using the Wilcoxon matched-pairs signed-rank test (p>0.05).

Among the 9 patients considered before, there were 38 persistent mutations, i.e. mutations detected in the same individual at different health states. All of them were unique and distributed in 27 genes namely, *ANK2; ATM; FAT1; FAT3; FBN2; KALRN* (2 different mutations)*; KDM6A; KMT2C* (2 different mutations)*; KMT2D* (5 different mutations)*; LRP1B; MYD88; OBSCN; PKHD1; PTPRD; RYR1* (3 different mutations)*; RYR2* (2 different mutations)*; RYR3; SYNE1; ZFHX4* (2 different mutations). In these patients, 1078 new mutations were also identified, having the characteristic of being present only in the sample diagnosed with SMM or MM but absent in the sample diagnosed with MGUS (Fig. 14). Present data prevented to assign a mutational profile that could allow to distinguish MGUS patients at high risk of evolution.

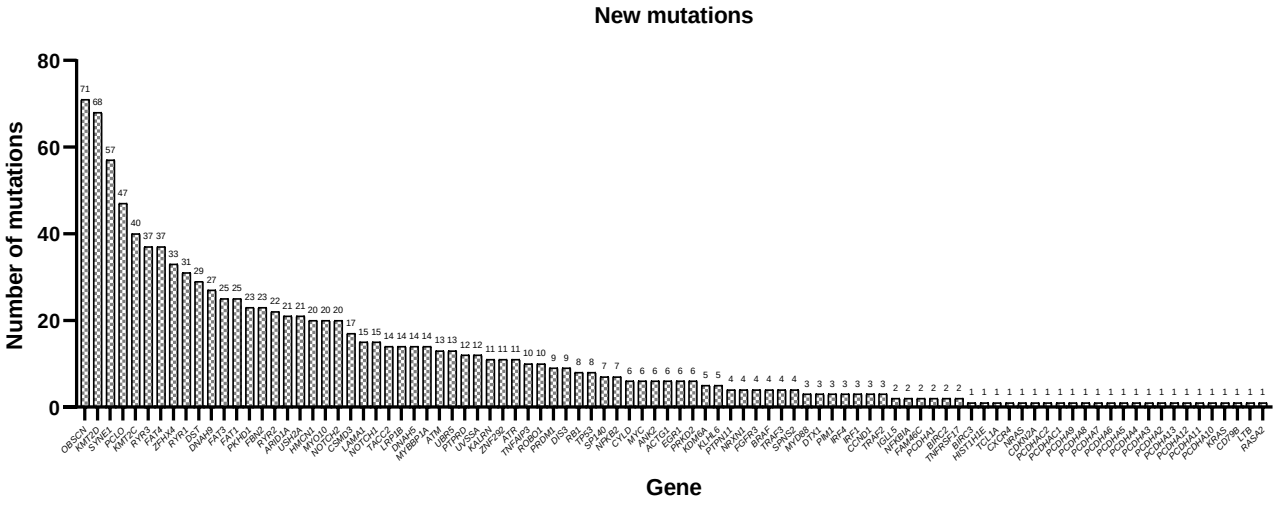

Fig. 14 Number of new gene mutations identified in patients with evolution of the disease. Above bar the number of mutations.

The mutated genes observed in patients with evolution were investigated for a possible correlation in specific pathways but having started from the NGS investigation of a panel of 84 selected genes, it was not possible to detect a predominant pathway.

Only for 72 mutations (2% of the total mutations), a prediction carried out by Polyphen was available, thus we evaluated the possible functional impact of these mutations within each health group. Although we do not observe a statistically significant difference, we can detect an increasing trend of predicting a damaging effect of mutations as the disease progresses; of the 11 predicted mutations in Healthy 5 are probably damaging and 6 benign, of the 38 mutations in MGUS 17 are probably damaging and 21 benign, we detect only 1 probably damaging mutation in SMM and of the 22 mutations in MM 18 are probably damaging and 4 are benign.

When the distribution of the different types of CM detected in the different groups was analysed, we found that the predominant type of mutation (in all groups) was the frameshift variations, while inframe insertions (IFI) were significantly reduced in the healthy group (Fig. 15).

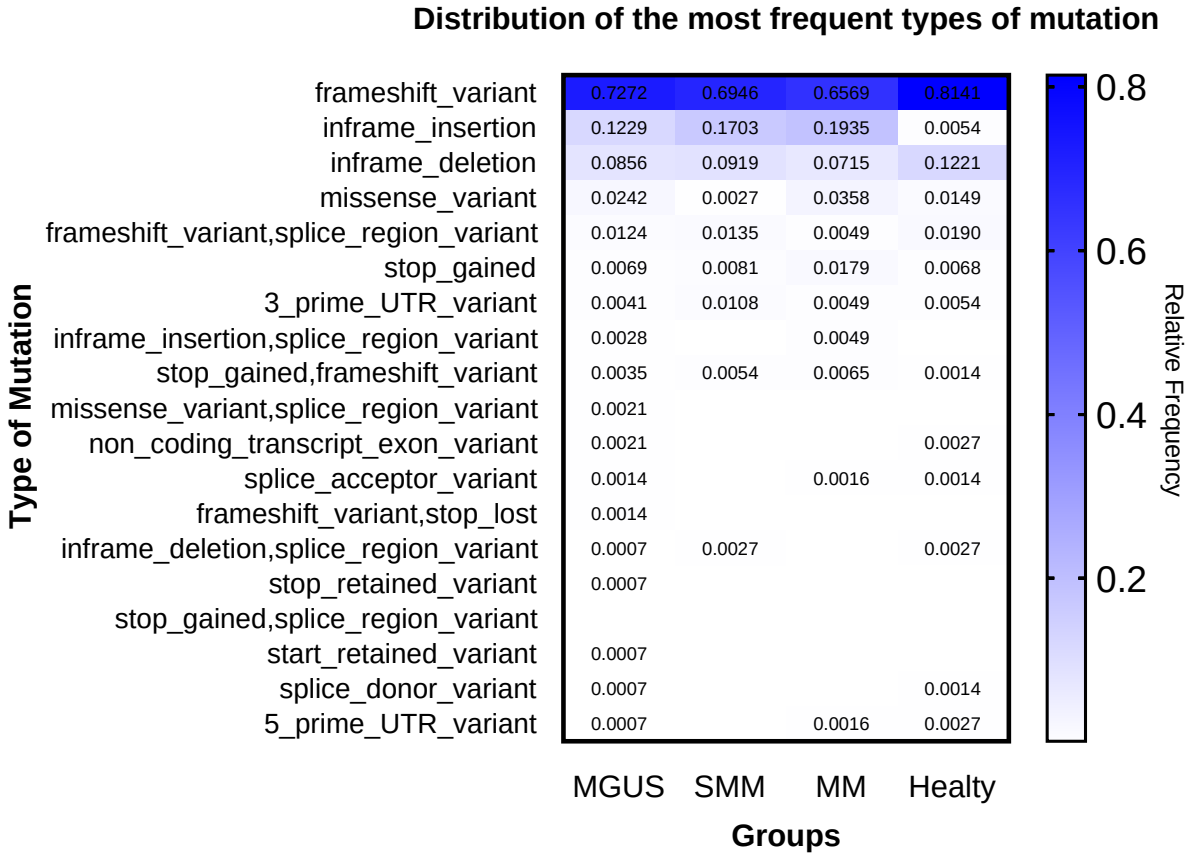

Fig. 15 Distribution of the most frequent types of mutation divided for health state. The relative frequency of each type of mutation detected within each health group is reported in each cell. Statistical significance was examined using Kruskal-Wallis H-test; (p>0.05)

We analyzed in detail all insertions (Ins) and deletions (Del) included in the groups of inframe and framshift variations, divided for the number of inserted/deleted nucleotides, as reported in Table 6.

	Healthy				MGUS				SMM				MM			
	INS		DEL		INS		DEL		INS		DEL		INS		DEL	
Variation of 1nt	33	(4,6%)	439	(61,7%)	137	(9,9%)	595	(43,0%)	48	(13,3%)	120	(33,1%)	103	(17,9%)	161	(27,9%)
Variation of 2nt	6	(0,8%)	108	(15,2%)	57	(4,1%)	127	(9,2%)	17	(4,7%)	25	(6,9%)	44	(7,6%)	24	(4,2%)
Variation of 3nt	4	(0,6%)	50	(7,0%)	105	(7,6%)	52	(3,8%)	21	(5,8%)	10	(2,8%)	56	(9,7%)	24	(4,2%)
Variation of 4nt	0	(0,0%)	5	(0,7%)	18	(1,3%)	12	(0,9%)	14	(3,9%)	2	(0,6%)	14	(2,4%)	2	(0,3%)
Variation of 5+nt	3	(0,4%)	63	(8,9%)	144	(10,4%)	136	(9,8%)	59	(16,3%)	46	(12,7%)	116	(20,1%)	33	(5,7%)
Total	46	(6,5%)	665	(93,5%)	461	(33,3%)	922	(66,7%)	159	(43,9%)	203	(56,1%)	333	(57,7%)	244	(42,3%)
Ins/Del	0,07				0,50				0,78				1,36			

Table 6 Distribution, percentage, and ratio of the Insertions and Deletions divided by number of nucleotides and health state.

From the data in Table 6, puzzlingly, we noticed a very low presence of Ins in the group of healthy subjects, compared to the other groups. Overall, we observed: in healthy patients 46 ins and 665 del, in MGUS 461 ins and 922 del, in SMMs 159 ins and 203 del, in MMs 333 ins and 244 del; the counted mutations are unique. Furthermore, the ins/del ratio was low (0.07) in healthy people, and it was strongly increased with the health state in the order MGUS (0.5) < SMM (0.78) < MM (1.36).

The inframe insertions (IFI) have been analyzed in detail and the duplications appear predominant (Table 7). The group of healthy subjects is the only one that differs from the others in the number of IFI detected, the other groups do not seem to show substantial differences in the number and type of variation

	MGUS	SMM	MM	Healthy
Total IFI	182	63	122	4
IFI > 3 bp	77	42	66	0
IFI = 3 bp	105	21	56	4
Nucleotide duplication	169	62	121	1
Nucleotide insertion	13	1	1	3
Change aminoacid	85	41	66	3

Table 7 Distribution of the number of inframe insertions counted and divided by group of patients and by the type of variation.

Analyzing the number of Ins and Del divided by health state and normalized by the average mutation rate per million bases (aTMB) (Fig. 16), we can observe how the presence of insertions increases as the disease progresses.

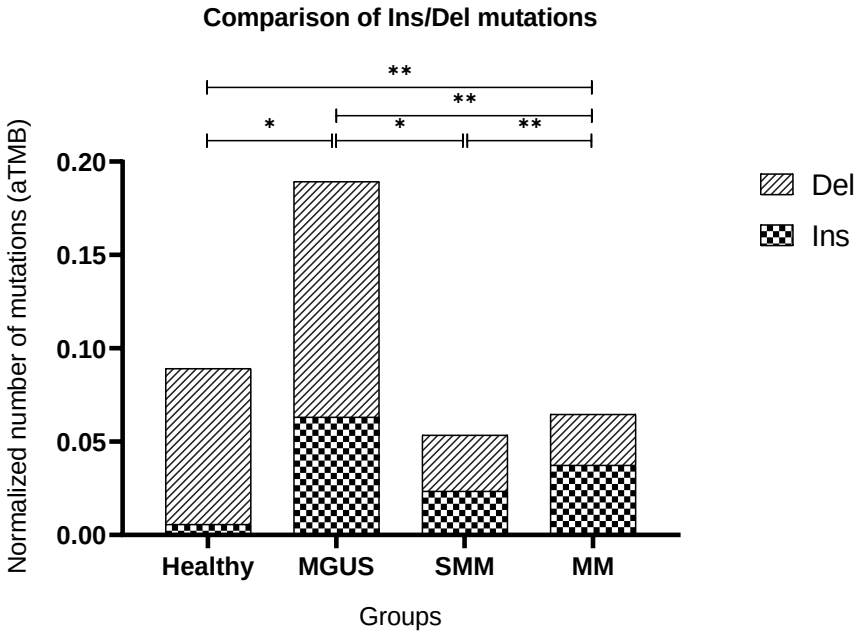

*Fig. 16 Comparison of the ratio of the number of Ins/Del mutations for each health group and normalized by the average mutation rate per million bases (aTMB) Statistical significance was examined using Kruskal-Wallis H-test; (*p<0.05, **p<0.005).*

The data show how in healthy individuals the Ins/Del ratio is strongly unbalanced with Ins almost absent, while in the MM stage we can observe how Ins are even slightly higher than Dels. The Healthy group, with the lowest frequency of Ins, is significantly different from the groups with more advanced clinical conditions. For each group a different distribution of the number of Ins in the samples was observed (Fig. 17), the data have been normalized on TMB and show that the overall number of Ins found in the healthy group differs, in a statistically significant way, compared to the other groups.

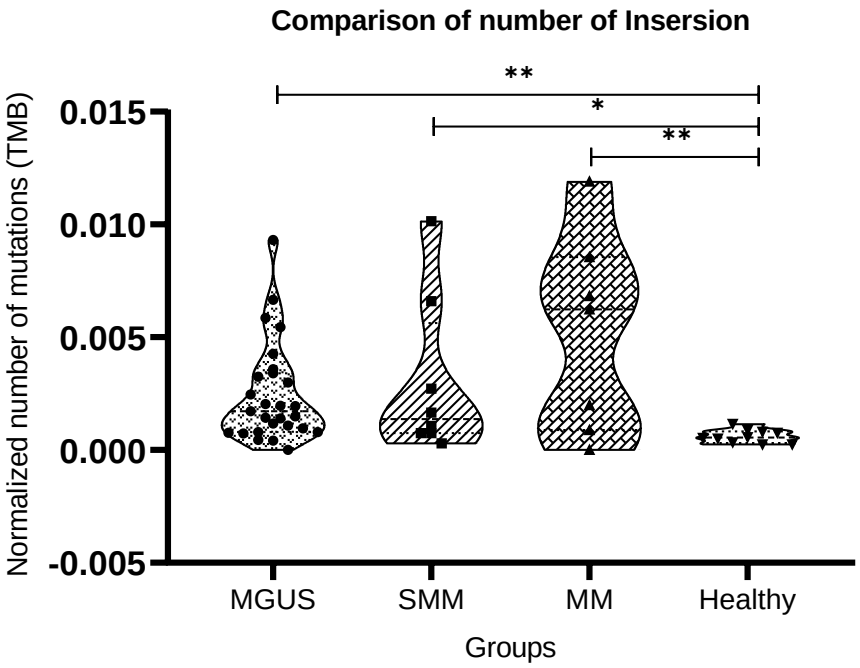

*Fig. 17 Comparison of the number of insertions normalized based on the mutation rate per million bases (TMB), found in each patient divided into health status groups. Statistical significance was examined using the Kruskal-Wallis H test (*p<0.05, **p<0.005). The dotted pattern indicates the quartiles while the dashed pattern indicates the median.*

We calculated the frequency of Ins for each gene divided by health state (Fig. 18). Data shows that the frequency of insertions found in healthy patients is low and differs in a statistically significant manner compared to the other groups. The graph shows a relative frequency profile of Ins for each group similar to the one calculated previously for all mutation types, suggesting that these insertions occur more frequently in *OBSCN*, *KMT2D*, *SYNE1, RYR1*, *PCLO* etc., but their occurrence is dependent on the size of the gene rather than depending by other mechanisms.

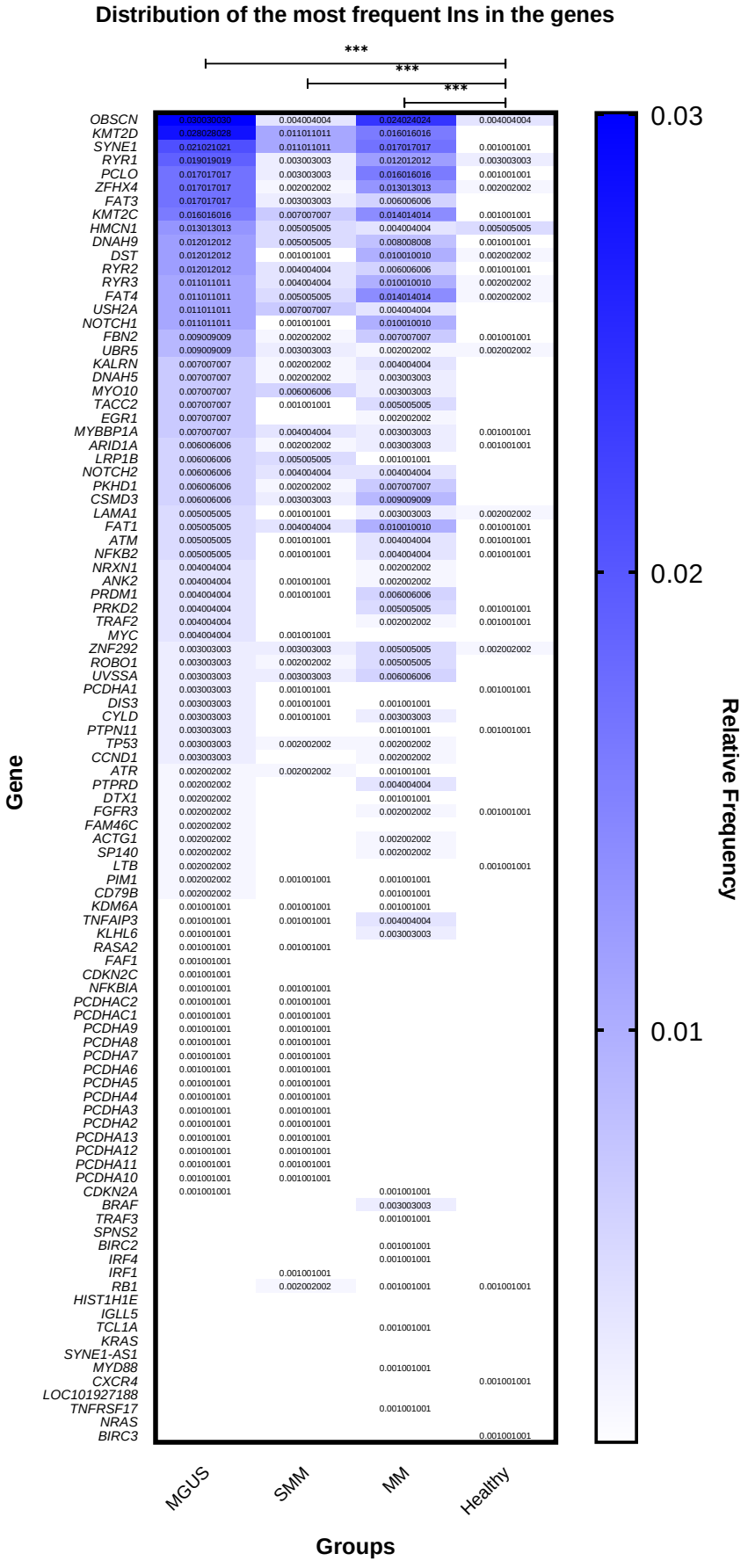

*Fig. 18 Distribution of the relative frequency of insertions detected in each gene and divided into health status groups. Each cell shows as frequency the number of insertions observed in that gene compared to the total number of insertions counted (in all groups). Statistical significance was examined using Kruskal-Wallis H-test; (***p<0.0005).*

Finally, we compared the number of Ins counted per sample and gene. In Fig. 19 we show the samples first in order of pathological evolution for patients with evolution, and then the remaining individual samples are divided into the health state groups, the data are normalized by the TMB.

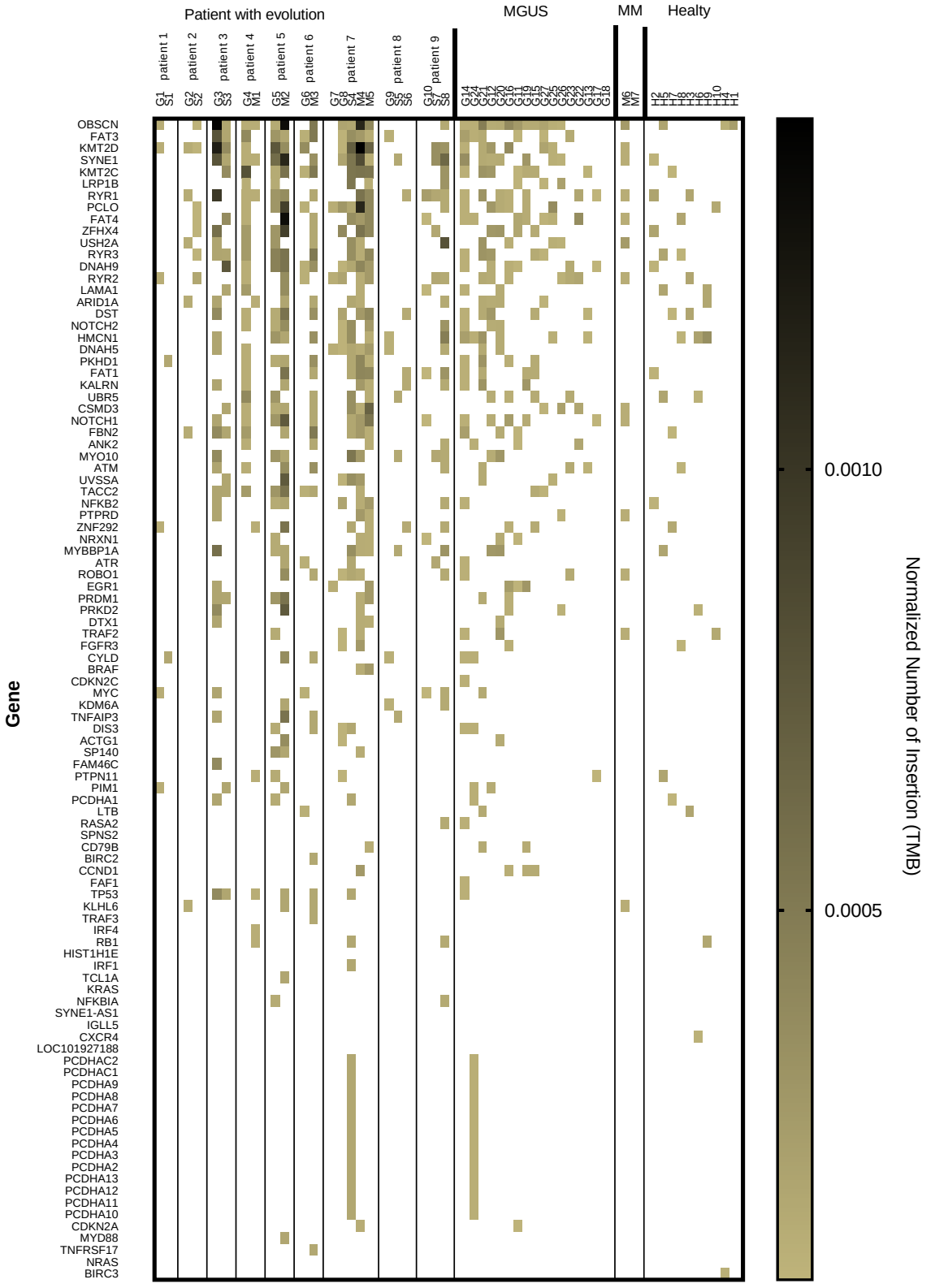

Fig. 19 Comparison of the number of insertions detected in each gene and subdividing the samples by order of pathological evolution in each patient. Each cell shows the number of insertions observed in that gene and in that sample, normalized by mutation rate per million bases (TMB).

The counted mutations are unique, but the same mutation can be found in multiple samples from the same group, in particular, 28 Ins distributed in 21 genes were counted namely, *MYBBP1A* (2 Ins); *MYC*(1 Ins); *NOTCH1*(2 Ins); *KMT2D*(2 Ins); *DTX1*(1 Ins); *DNAH9*(2 Ins); *ARID1A*(1 Ins); *FAT3*(3 Ins); *TP53*(1 Ins); *OBSCN*(1 Ins); *PRDM1*(1 Ins); *RYR3*(2 Ins); *TACC2*(1 Ins); *KMT2C*(1 Ins); *PKHD1*(1 Ins); *TRAF2*(1 Ins); *DIS3*(1 Arm); *PIM1*(1 Ins); *ZFHX4*(1 Ins); *FAT1*(1 Ins); *RYR1*(1 Ins). These mutations are distributed 17 in the MGUS group, 1 in SMM and 10 in MM.

The burden of Ins that we could observe, although varied, overall suggests a slight tendency to acquire insertions and lose deletions as the disease progresses even though this data is not homogeneous (Table 8). We observe that in each sample for each gene there can be several different Ins and Dels, and patients with pathological progression each show their own mutational profile.

Group	patient 1		patient 2		patient 3		patient 4		patient 5		patient 6		patient 7					patient 8			patient 9		
Sample	G1	S1	G2	S2	G3	S3	G4	M1	G5	M2	G6	M3	G7	G8	S4	M4	M5	G9	S5	S6	G10	S7	S8
Ins	6	2	6	8	61	22	43	9	54	105	12	47	4	30	67	94	73	5	5	5	9	9	42
Del	27	22	16	89	60	8	16	80	23	30	157	10	140	43	12	46	13	7	8	44	32	20	7
Ins/Del	0,22	0,09	0,38	0,09	1,02	2,75	2,69	0,11	2,35	3,50	0,08	4,70	0,03	0,70	5,58	2,04	5,62	0,71	0,63	0,11	0,28	0,45	6,00
Ins-TMB	8,02 E-04	3,54 E-04	8,66 E-04	7,15 E-04	1,19 E-02	4,18 E-03	5,74 E-03	1,20 E-03	8,24 E-03	1,95 E-02	1,48 E-03	8,10 E-03	5,44 E-04	2,97 E-03	1,19 E-02	1,31 E-02	9,91 E-03	6,16 E-04	8,20E-04	7,75 E-04	7,34 E-04	1,58 E-03	6,70 E-03

Group	MGUS																
Sample	G14	G24	G21	G12	G20	G16	G11	G19	G15	G27	G25	G26	G23	G22	G13b	G17	G18
Ins	34	23	31	24	21	22	16	15	11	11	10	10	6	6	4	4	0
Del	12	24	22	6	25	100	62	19	9	20	28	11	24	17	83	15	46
Ins/Del	2,83	0,96	1,41	4,00	0,84	0,22	0,26	0,79	1,22	0,55	0,36	0,91	0,25	0,35	0,05	0,27	0,00
Ins-TMB	4,06 E-03	2,93 E-03	4,94 E-03	3,48 E-03	3,18 E-03	2,79 E-03	1,44 E-03	2,25 E-03	1,67 E-03	1,10 E-03	1,25 E-03	1,10 E-03	9,42 E-04	1,11 E-03	4,12 E-04	3,42 E-04	0,00 E+00

Group	MM		Healthy									
Sample	M6	M7	H2	H5	H7	H8	H3	H6	H9	H10	H4	H1
Ins	15	0	8	6	6	6	4	5	5	2	2	2
Del	34	42	29	105	61	116	59	104	35	40	97	70
Ins/Del	0,44	0,00	0,28	0,06	0,10	0,05	0,07	0,05	0,14	0,05	0,02	0,03
Ins-TMB	2,00 E-03	0,00 E+00	8,05 E-04	1,16 E-03	5,01 E-04	5,72 E-04	7,64 E-04	5,45 E-04	8,89 E-04	3,36 E-04	2,46 E-04	2,48 E-04

Table 8 Comparison of the number of insertions and deletions, in each sample divided by patients or health groups; with the Ins/del ratio and frequency of insertions per million of base pairs (Ins-TMB).

In fact, with the exception of patients 4 and 8, all the others presents either an increase in the Ins or decrease in the Del, patient 6, 7 and 9 showed a simultaneous increase in the Ins burden and decrease in the Del burden. Comparing the healthy subjects with all the others, we observed that the number of insertions detected, both in-frame and frameshift, was significantly reduced, with a highly unbalanced ratio Ins/Del of 0.07, this ratio raised to 0.5 in MGUS, 0.78 in SMM and 1.36 in MM.

Moreover, the frequency of insertions per million of base pairs (Ins-TMB) definitively increases from healthy (average= 6.06E-04), MGUS (average= 2.48E-03), SMM (average= 3.38E-03), and MM (average= 7.69E-03). The Ins/Del ratio combined with the TMB of the insertions (Ins-TMB) seem to be highly indicative of disease progression however, it should be noted that some MGUS and even some MM patients were in the range of the healthy donors for both parameters. However, these factors represent an interesting endpoint deserving further studies.

4.2. dPCR

dPCR analyses were performed on a large cohort of patients and several biopsy tissues. The *KRAS* Q61H, *NRAS* Q61R, *NRAS* Q61K mutations were investigated, as the literature says they are the most frequent mutations in MM [42].

In particular, we compared the DNA extracted from different biopsy samples for the same individual at different times and, when possible, also at different stages of disease progression, taking care to select plasma and BC samples taken at least 30 days before the BM collection. Overall, DNA from different biopsy tissues of 85 individuals was investigated for a total of 288 samples analyzed. Initially, we only analyzed ccfDNA samples extracted from the plasma of 35 individuals, including 31 patients with MGUS, 1 with SMM and 3 with MM, for the investigation of the *KRAS* Q61H mutation, and no positivity was found.

We subsequently analyzed and compared the DNA from the tissues of 50 individuals including 22 MGUS, 9 SMM, 13 MM; some individuals presented pathology evolutions and in particular 3 with evolution from MGUS to SMM, 1 with evolution from SMM to MM, 1 with evolution from MGUS to MM and 1 with evolution from MGUS to SMM to MM. For the comparison of the tissues, all 3 mutations under examination were investigated as schematized in Table 9. In particular, the ratio calculated between copies of mutated DNA per µL and copies of wt DNA per µL was reported.

A)		*KRAS* Q61H			*NRAS* Q61R			*NRAS* Q61K		
Patient	**Diagnosis**	**BM**	**BC**	**Plasm**	**BM**	**BC**	**Plasm**	**BM**	**BC**	**Plasm**
1	MGUS		0	0,00053		0			0	
2	MGUS			0		0,00012	0		0	
3	MGUS		0	0		2,50E-05			2,60E-05	
4	MGUS		8,60E-05	0		0			0	
5	MGUS		0	0		0			2,50E-05	
6	MGUS		0	0		1,90E-05			0	
7	MGUS	0		0	0	0		2,90E-05	0	
8	SMM	0		0	3,10E-05	0		0	9,90E-05	
9	SMM	0,0004	0,000021	0	0,000021	0		0	0	
10	SMM	**2,73341**	0,00012	0,000046	1,70E-05	0		0,000029	0	
11	SMM	0,000055	0		0	0		0	0	
12	SMM	0	0					0,01532	0	
13	MM	0	0	0	0	0		5,40E-05	0,000021	
14	MM	0	0	0	2,30E-05	0,000021		0	0	
15	MM	0		0	0,00009	0		0,00011	0	
16	MM	0		0	0,000036	0	0,00032	0,000038	0	
17	MM	0	0		0	0		0,00013	0,000046	
18	MM	0	0		0	0,000028		0	0	
19	MM	8,80E-05	0		0,00015	0,000025		0	0	
20	MM	0,000069	0,000042		0	0		0,000026	0,000021	
21	MM	0	0		0	0		**1,52383**	0	
22	MM				3,40E-05	1,60E-05		0,00014	0	
23	MM	5,00E-05	4,90E-05		0	0		4,40E-05	0	
24	MM	0	2,10E-05		0,00926			2,30E-05		

B)		*KRAS* Q61H			*NRAS* Q61R			*NRAS* Q61K		
Patient	**Sample Diagnosis**	**BM**	**BC**	**Plasma**	**BM**	**BC**	**Plasma**	**BM**	**BC**	**Plasma**
25	MGUS		0			0			0	
	SMM	0			2,7E-05			0		
26	MGUS		0			0			1,8E-05	
	SMM	0			0			0		
27	MGUS		7,6E-05			0			0	
	SMM	9,6E-05	0		0			0	0	
	MM	0	4,4E-05					2,8E-05	0	
28	MGUS		0			2,1E-05			0	
	SMM	0			**0,59432**			0		
29	SMM		0			0			0	
	MM	0			0			4,1E-05		
30	MGUS					0			6E-05	0
	MM			0	0			**8,71748**		

C)		*KRAS* Q61H			*NRAS* Q61R			*NRAS* Q61K		
Patient	**Diagnosis**	**BM**	**BC**	**Plasm**	**BM**	**BC**	**Plasm**	**BM**	**BC**	**Plasm**
31	MGUS			0		0	0		0	
32	MGUS		0	0		0			0	
33	MGUS			0		0	0			
34	MGUS		0	0		0			0	
35	MGUS		0	0		0			0	
36	MGUS		0	0					0	
37	MGUS			0		0	0		0	
38	MGUS		0	0		0				
39	MGUS		0	0		0			0	
40	MGUS			0		0	0		0	
41	MGUS			0		0	0			
42	MGUS			0		0	0		0	
43	MGUS		0	0					0	
44	MGUS		0	0		0				
45	MGUS		0	0						
46	SMM		0	0		0			0	
47	SMM	0	0		0	0		0	0	
48	SMM	0	0		0	0		0	0	
49	SMM	0	0		0	0		0	0	
50	MM	0	0	0	0			0	0	

Table 9 A) subdivision of patients by diagnosis and mutation investigated, the values in the cells indicate the ratio between copies of mutated DNA per µL and copies of wt DNA per µL; empty cell indicates that DNA from that tissue has not been analyzed. B) subdivision of patients with evolution, the samples are separated based on the diagnosis, the mutations investigated are shown in the column, the values in the cells indicate the ratio between copies of mutated DNA per µL and copies of wt DNA per µL; empty cell indicates that DNA from that tissue has not been analyzed. C) subdivision by diagnosis of patients with absence of the mutation investigated; the empty cell indicates that the DNA of that tissue has not been analyzed

In Table 9A) the results show 30 individuals on which at least one partition with mutated DNA was found in a sample analyzed for one of the 3 mutations under examination. Among these individuals we can distinguish 7 MGUS, 5 SMM, 12 MM, 3 with MGUS-SMM evolution, 1 with SMM-MM evolution, 1 with MGUS-MM evolution and 1 with MGUS-SMM-MM evolution. We can observe that 12 patients exhibited multiple mutations at the same time:

10 individuals with *KRAS* Q61H mutations of which 2 MGUS 3 SMM 4 MM and 1 with MGUS-SMM-MM evolution; this mutation was found in 7 BM, 8 BC and 2 Plasma;

15 individuals with *NRAS* Q61R mutations of which 3 MGUS 3 SMM 7 MM and 2 with MGUS-SMM evolution; this mutation was found in 11 BM, 8 BC and 1 Plasma;

19 individuals with *NRAS* Q61K mutations of which 3 MGUS 3 SMM 9 MM and 1 with MGUS-SMM evolution, 1 with SMM-MM evolution, 1 with MGUS-MM evolution and 1 with MGUS-SMM-MM evolution; this mutation was found in 15 BM and 8 BC.

Overall, we observed that in 28 patients having BM, 23 had at least one of the mutations investigated, in 50 patients having BC 21 had at least one of the mutations investigated, and in 32 patients having Plasma 3 had at least one of the mutations investigated. Furthermore, we can report that 33 BM out of 83 analyzed, 24 BC out of 129 analyzed and 3 plasma out of 41 analyzed presented at least one of the mutations under examination.

Among patients positive for any of these mutations, we observed that 13 individuals had a certain degree of tissue-dependent correspondence in the number of copies of the mutated DNA comparing the BM with LBs, in particular the following ratios BM/BC, BM/Plasma and BC/Plasma were considered as indicated in Table 10.

A) Patient	Diagnosis	*KRAS* Q61H BC/BM	*KRAS* Q61H Plasma/BM	*KRAS* Q61H Plasma/BC	*NRAS* Q61R BC/BM	*NRAS* Q61R Plasma/BM	*NRAS* Q61R Plasma/BC	*NRAS* Q61K BC/BM	*NRAS* Q61K Plasma/BM	*NRAS* Q61K Plasma/BC
1	MGUS			0						
2	MGUS						0			
3	MGUS			0						
4	MGUS			0						
5	MGUS			0						
6	MGUS			0						
7	MGUS		0		0			0		
8	SMM		0		0			0		
9	SMM	5,25E-02	0	0	0			0		
10	SMM	4,39E-05	1,68E-05	3,83E-01	0			0		
11	SMM	0			0			0		
12	SMM	0						0		
13	MM	0	0	0	0			3,89E-01		
14	MM	0	0	0	9,13E-01			0		
15	MM		0		0			0		
16	MM		0		0	8,89E+00	0	0		
17	MM	0			0			3,54E-01		
18	MM	0			0			0		
19	MM	0			1,67E-01			0		
20	MM	6,09E-01			0			8,08E-01		
21	MM	0			0			0		
22	MM				4,71E-01			0		
23	MM	9,80E-01			0			0		
24	MM	0								

B) Patient EVO	Sample Diagnosis	*KRAS* Q61H BM/BC	*KRAS* Q61H BM/Plasma	*KRAS* Q61H BC/Plasma	*NRAS* Q61R BM/BC	*NRAS* Q61R BM/Plasma	*NRAS* Q61R BC/Plasma	*NRAS* Q61K BM/BC	*NRAS* Q61K BM/Plasma	*NRAS* Q61K BC/Plasma
25	MGUS-SMM	0			0			0		
26	MGUS-SMM	0			0			0		
27	MGUS-SMM-MM	7,92E-01 4,58E-01			0			0 0		
28	MGUS-SMM	0			3,53E-05			0		
29	SMM-MM	0			0			0		
30	MGUS-MM				0			6,88E-06	0	0

Table 10 A) tissue-dependent proportionality obtained from the ratio of the number of copies of the mutated DNA for each tissue compared with the other tissues having the same mutation and divided by patient and diagnosis B) tissue-dependent proportionality obtained from the ratio of the number of copies of the mutated DNA for each tissue compared with other tissues having the same mutation and divided by patient and by evolution of the diagnosis in the sample collection times

By analyzing patients positive for these mutations in different tissues we observed that:

5 patients (2 SMM, 2 MM, and 1 with MGUS-SMM-MM evolution) were positive for *KRAS* Q61H mutation;

5 patients (4 MM and 1 with SMM-MM evolution) were positive for *NRAS* Q61R mutation;

4 patients (3 MM and 1 with MGUS-MM evolution) were positive for *NRAS* Q61K mutation.

If we compare for the same individual the different biopsy tissues analyzed with each other to evaluate the mutational correspondence between BM and LB we can observe 13 matches and 21 non-matches comparing BM and BC; 2 matches and 1 mismatch comparing BM and Plasma; 1 match and 6 mismatches comparing BC and Plasma. On average, DNA extracted from BC compared to DNA extracted from BM seems more sensitive and suitable for LB than ccfDNA extracted from plasma.

4.3. Cells

In this study, the possible role, and effects of the *NRAS* p.Q61R mutation, as the most frequent mutation in MM [67], were analyzed using different types of cellular tests on a commercial U266-B1 cell line of multiple myeloma and transfected for the overexpression of the mutation under analysis. Overexpression was obtained by transfecting the U266-B1 cell line with a plasmid for the overexpression of *NRAS* in its mutated form p.Q61R and in the WT form as well as a third control plasmid. The cell lines are called respectively: O.E. NRAS Q61R, O.E. NRAS WT and O.E. Ctrl. To verify and confirm the correct overexpression in the cell lines, the expression levels of *NRAS* mRNA were evaluated through Real-Time qPCR analysis and confirmed with protein expression analysis through the Western Blot technique.

4.3.1. Realtime PCR

The expression level of the *NRAS* mRNA in the cell lines under examination was tested using the Real Time qPCR technique and we were able to see that the expression of *NRAS* mRNA in the O.E. NRAS Q61R and O.E. NRAS WT cell lines is significantly greater than in U266-B1 and O.E. Ctrl cell lines. To verify the correctness of the analysis in the cell lines under examination, a control analysis of the expression level was also carried out for the housekeeping gene *GAPDH* which was expressed in all the samples. The difference in gene expression between the tested cell lines is statistically significant and confirms the correct overexpression of the transfected cells (Fig. 20).

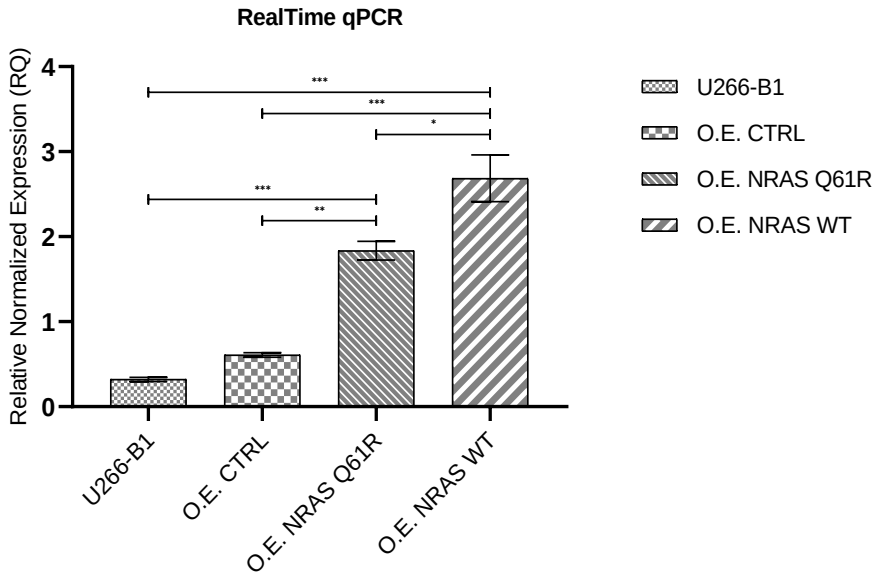

*Fig. 20 Real Time PCR Plot, expression of NRAS on U266-B1, O.E. NRAS Q61R, O.E. NRAS WT and O.E. Ctrl. Statistical significance was examined using ANOVA, Tukey's multiple comparisons test. Each bar represents the mean ± SEM (*p<0.05, **p<0.005, ***p<0.0005)*

4.3.2. Western blot

The levels of NRas protein in the cell lines under examination were tested using the Western Blot technique and the high levels of NRas protein were confirmed in O.E. NRAS WT and O.E. NRAS Q61R cell lines compared to U266-B1 and O.E. Ctrl control cell lines. To verify the correctness of the analysis in the cell lines under examination, an analysis of the expression level was also carried out for the housekeeping gene GAPDH which was expressed in all samples.

The results of the characterization of the mutational status of the NRas protein highlight how, in the O.E. NRAS WT cell line the NRAS protein is present at higher levels than the other cell lines, while in the O.E. NRAS Q61R cell line, is the only one to present the mutated protein detected by specific monoclonal antibodies against the mutated NRas p.Q61R protein (Fig. 21).

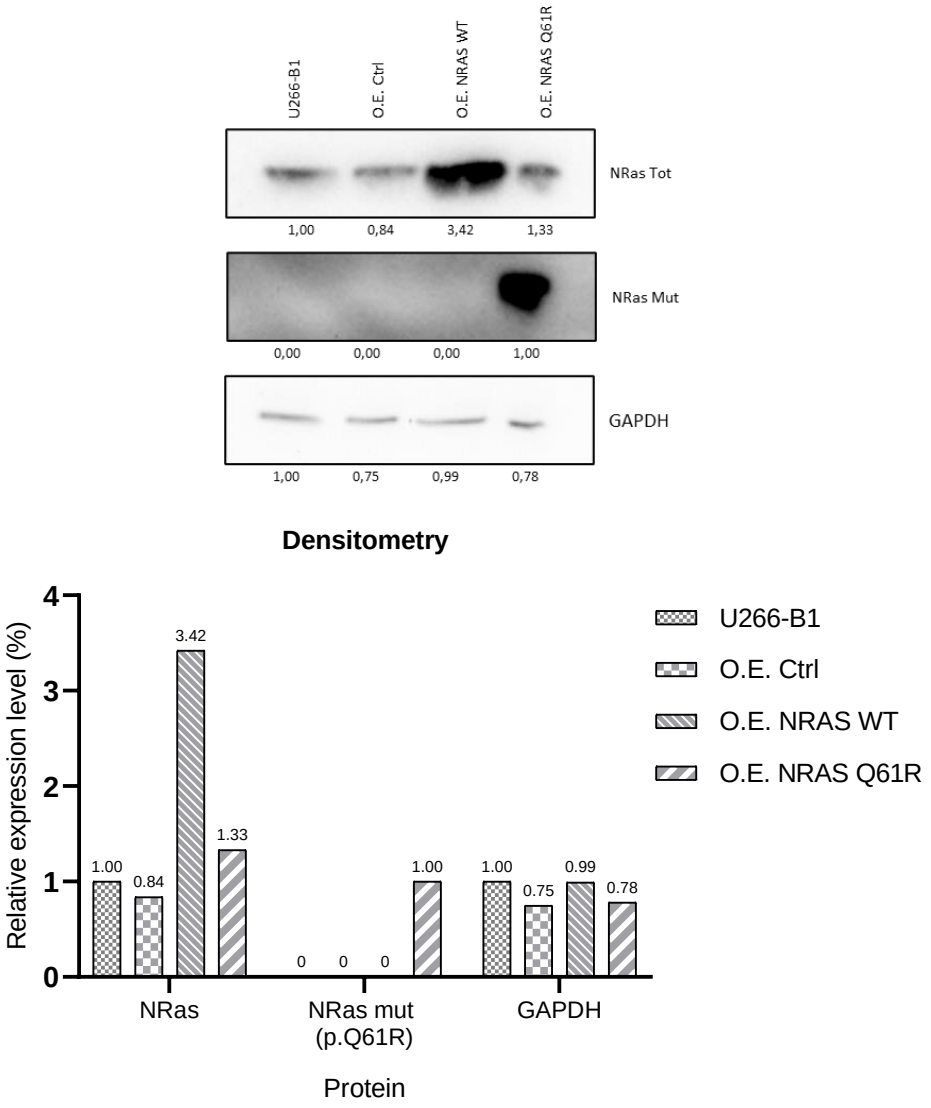

Fig. 21 Western blot analysis on U266-B1, O.E. NRAS Q61R, O.E. NRAS WT and O.E. Ctrl, and densitometry graph of Western Blot analysis on U266-B1, O.E. NRAS Q61R, O.E. NRAS WT and O.E. Ctrl. Numerical values indicate relative density.

4.3.3. Transwell

Following the confirmation of overexpression obtained in the transfected cell lines, we investigated a possible involvement of *NRAS* in the behavior of O.E. NRAS WT and O.E. NRAS Q61R cell lines compared to the U266-B1 and O.E. Ctrl cell lines. Therefore, a cell migration test was carried out using the transwell insertion device in the presence of an SDF-1 chemoattractant inside the well in which the transwell will be inserted, to guide the migration of the cells through the cell membrane device.

The experiment was carried out in parallel for U266-B1; O.E. NRAS WT; O.E. NRAS Q61R; O.E. Ctrl and was performed for each cell line in triplicate. After 24 hours of incubation at 37°C, cells did not migrate into the lower chamber, however cells were found within the membrane which were fixed with fluorescent dye DAPI. The cell density within the membrane was then assessed. Analyzing the confluence of the migration area it would appear that the overexpression of the *NRAS* gene, regardless of its mutational status, would induce a greater tendency towards aggregation and/or adhesion. In particular O.E. NRAS WT and O.E. NRAS Q61R cell lines covered the migration area approximately seven times more than U266-B1 and O.E. Ctrl cell lines (Fig. 22).

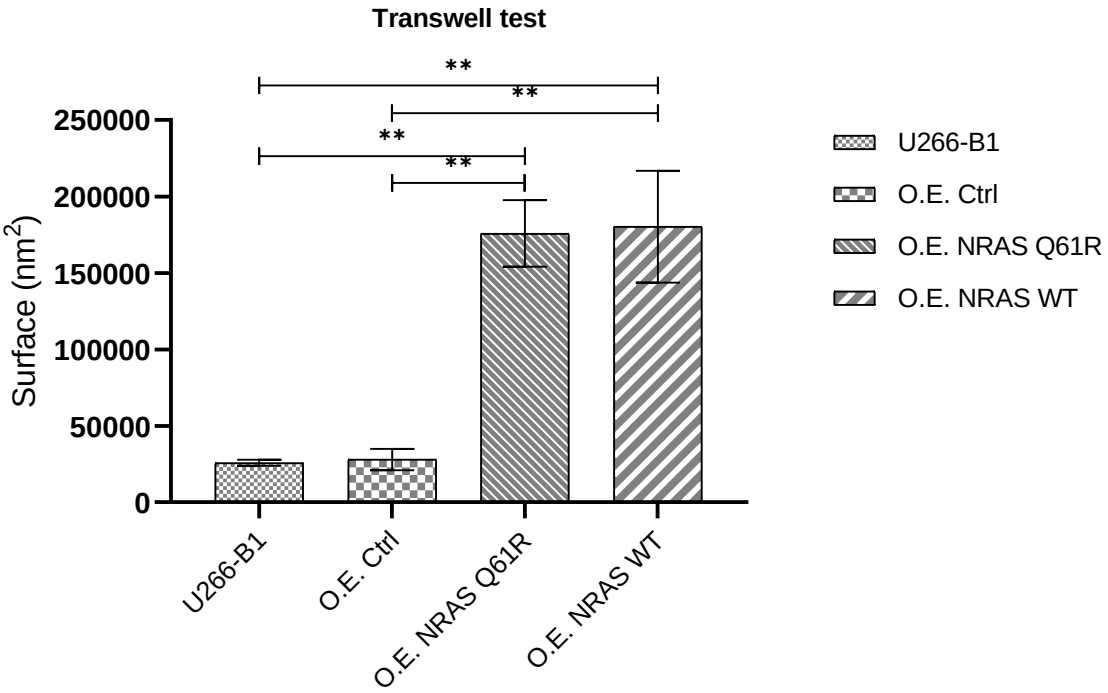

*Fig. 22 Transwell migration test on U266-B1, O.E. NRAS Q61R, O.E. NRAS WT and O.E. Ctrl. Statistical significance was examined using ANOVA, Tukey's multiple comparisons test. Each bar represents the mean ± SEM (**p<0.005)*

4.3.4. Colony assay

Transwell migration tests revealed cellular phenotypic behavior tending towards the formation of aggregates in the *NRAS* overexpressing lines; therefore, we wanted to confirm what we observed with a specific experiment for the cellular ability to form colonies.

The experiment was carried out in parallel for U266-B1; O.E. NRAS WT; O.E. NRAS Q61R; O.E. Ctrl. The test was performed for each cell line tested in triplicate by acquiring a photo of the whole well every 24 hours for 10 days.

The increase in cell density inside was then evaluated by analyzing the confluence of the entire well. The results show how cells overexpressing *NRAS*, have a greater tendency to form colonies than U266-B1 and O.E. Ctrl cell lines. The results of the 3way ANOVA test indicate that this is a statistically significant difference (P<0.0001) (Fig. 23).

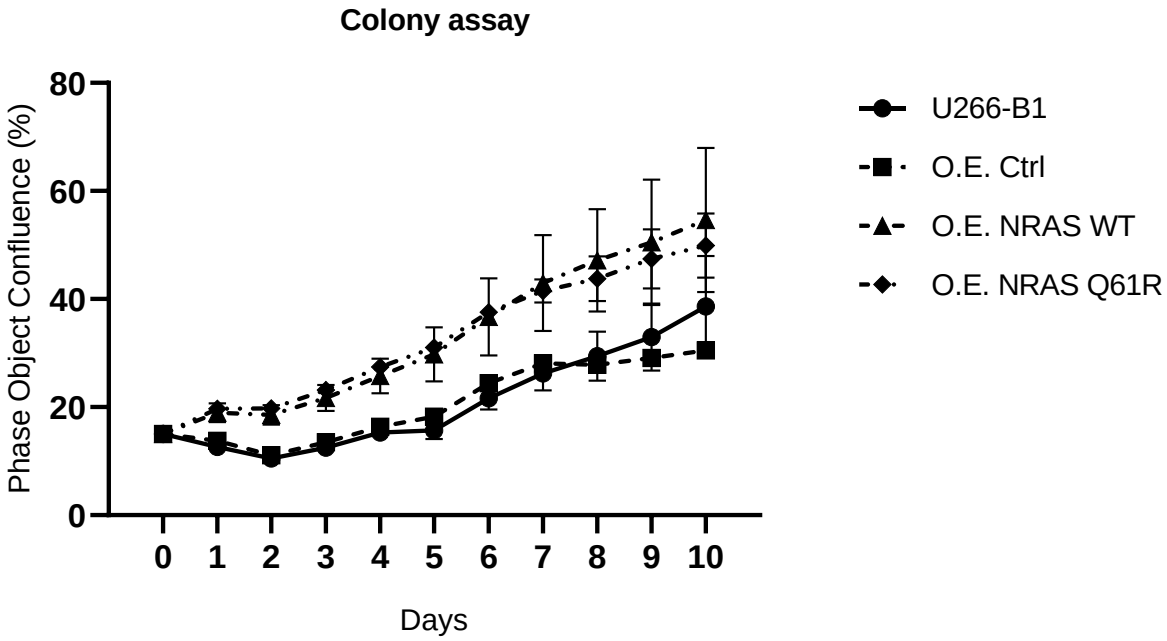

Fig. 23 The graphs represent data obtained from the colony assay during the 10 days of observation. Each bar represents the mean ± SEM.

4.3.5. Cell cycle

To verify whether the over expression of the *NRAS* gene could affect cellular replicative characteristics and therefore confer greater aggressiveness on the cells, cell viability tests were performed. The study of the cell cycle on the U266-B1; O.E. NRAS WT; O.E. NRAS Q61R; O.E. Ctrl cell lines was performed by analyzing the amount of DNA by intercalating propidium iodide in the cells by fixing them 48 hours after cell seeding. The results highlight that there is no difference between the cells analyzed and the majority of cells appear to be in the G1 phase of the cell cycle (Fig. 24).

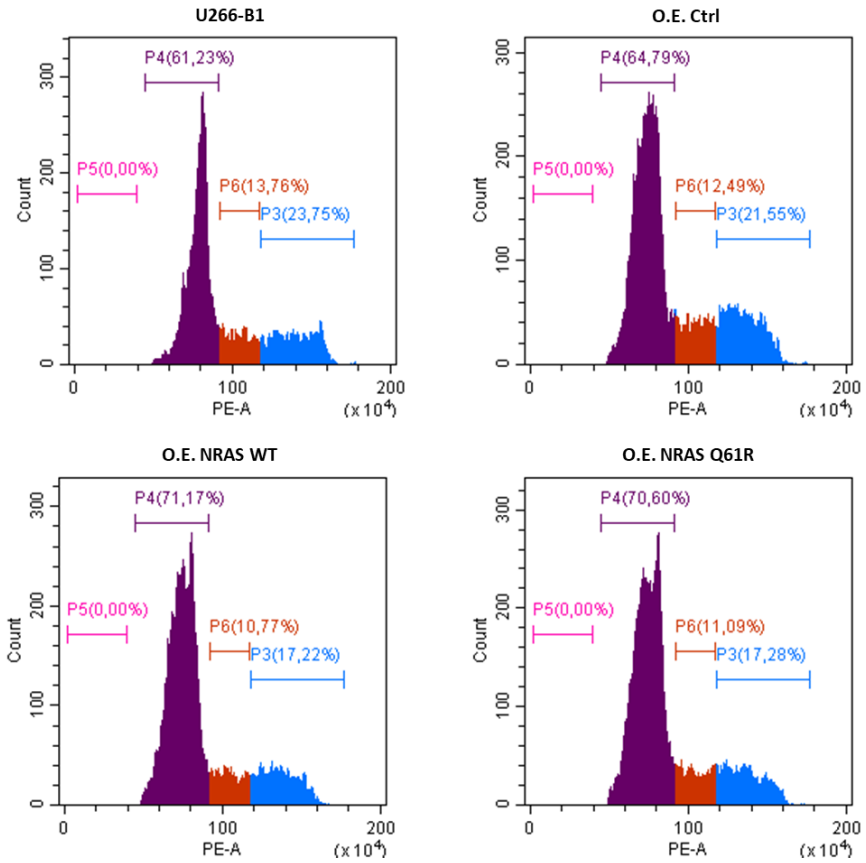

	G1	S	G2
U266-B1	62%	14%	24%
O.E. Ctrl	66%	13%	22%
O.E. NRAS WT	72%	11%	17%
O.E. NRAS Q61R	71%	11%	18%

Fig. 24 The results reported in the graphs show the DNA content on the abscissa axis, while the number of cells on the ordinate axis. If the cell is in G1, its DNA content will be diploid and represented graphically by the P4 area, while if the cell is in G2 phase the content will be tetraploid and graphically represented by the P3 area, in the S phase each cell will have a content of DNA different from the others, but still included between the G1 and G2 phases represented graphically by the P6 area.

4.3.6. RealTime-Glo

The test measures the reduction potential of viable cells and is independent of ATP, this test made it possible to monitor cell viability in the same sampling well for up to 48 hours, the luminescence produced is proportional to the number of live cells in culture.

The assay was performed in triplicate on U266-B1; O.E. NRAS WT; O.E. NRAS Q61R; O.E. Ctrl cell lines, the data were normalized by dividing them by the average of the value at time 0. From this test we observe that at 24 and 48 hours the O.E. NRAS WT and O.E. NRAS Q61R cell lines have reduced viability compared to U266-B1 and O.E. Ctrl cell lines. The results of the 3way ANOVA test indicate that this is a statistically significant difference($P<0.001$) (Fig. 25).

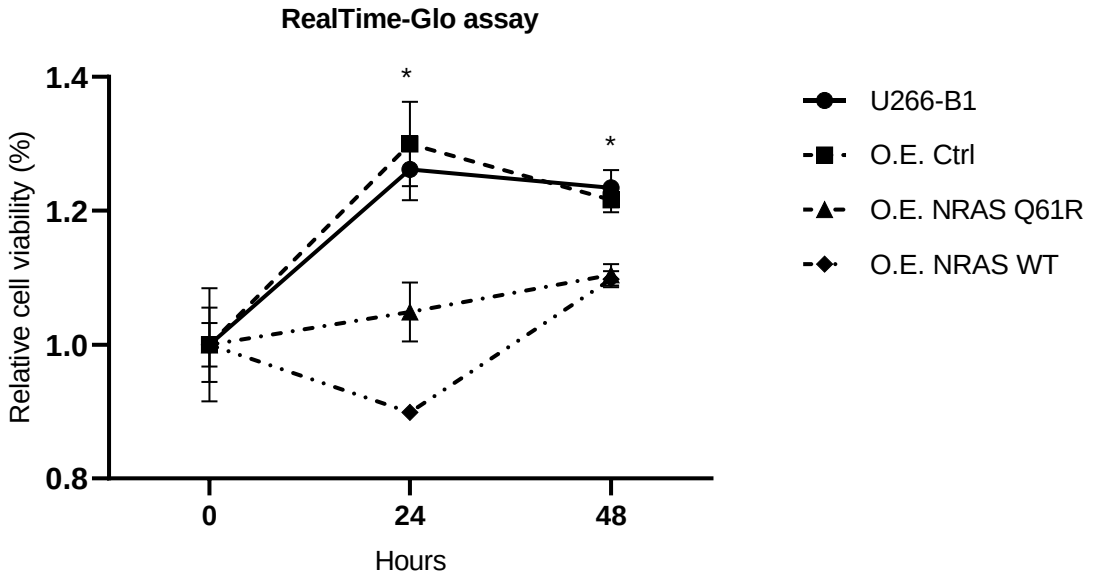

Fig. 25 Graphs represent data acquired via the RealTime-Glo™ MT Cell Viability Assay at 0, 24, and 48 hours. Each bar represents the mean ± SEM. Significant differences highlighted (*) were tested using a 2-way ANOVA test. The following multiple comparisons are significant p<0.05: U266-B1 vs. O.E. NRAS Q61R; U266-B1 vs. O.E. NRAS WT; O.E. Ctrl vs. O.E. NRAS Q61R; O.E. Ctrl vs. O.E. NRAS WT; Following multiple comparisons are not significant p>0.05: U266-B1 vs. O.E. Ctrl; O.E. NRAS Q61R vs. O.E. NRAS WT

4.3.7. CellTiter-Glo

The assay is an indicator of cell health, determining the number of viable cells in the culture by quantifying ATP, which indicates the presence of metabolically active cells. The assay was performed in triplicate on U266-B1; O.E. NRAS WT; O.E. NRAS Q61R; O.E. Ctrl cell lines and luminescence was measured after 48 hours. The results show a statistically significant reduction of metabolism, associated with ATP production, for the *NRAS* overexpressing cell lines. Specifically, a reduction of proliferation was observed in O.E. NRAS WT and O.E. NRAS Q61R cell lines; compared to U266-B1 and O.E. Ctrl cell lines (Fig. 26).

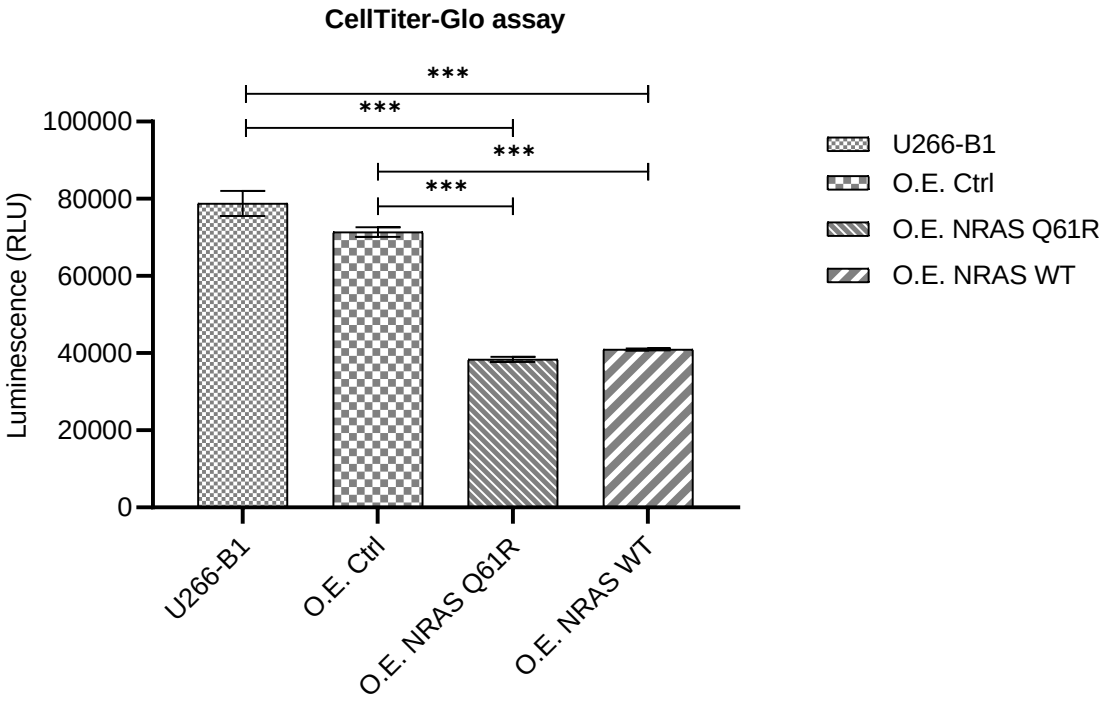

*Fig. 26 CellTiter-Glo viability assay on U266-B1, O.E. NRAS Q61R, O.E. NRAS WT e O.E. Ctrl. Statistical significance was examined using ANOVA, Tukey's multiple comparisons test. Each bar represents the mean ± SEM (***p<0.005)*

5. Discussion

The investigation of ccfDNA to evaluate the dynamic mutational landscape of myeloma and identify early predictors of disease progression is considered a tool with great potential, that makes it a minimally invasive alternative to tissue biopsies. In clinical practice, bone marrow biopsies are still the golden standard to access the genetic profile of MM. In the presymptomatic stages of myeloma, in which bone marrow biopsies are not planned, LBs could offer the possibility of frequent monitoring to detect early mutations and better identify patients with an unfavorable risk profile[19]. It has already been observed that some of the mutations typically involved in MM are also present in the bone marrow biopsy of patients with MGUS [23] and that some of which are predictive of the evolution of the pathology [68]. Therefore, LBs used as a method for monitoring the pathology, in addition to providing information on the evolutionary risk of patients, could provide useful information for the real-time clinical management of patients with MM in their clinical and therapeutic follow-up.

However, screening for cancerous markers especially in presymptomatic individuals is hampered by several factors, one of the most challenging issues is the availability of a sufficient ccfDNA concentration in pre-symptomatic patients, which at this stage is generally very low [64]. In other words, the number of mutant ctDNA molecules present in plasma is mostly proportional to the tumor burden [69], making the early detection particularly problematic.

In this study, based on high-depth sequencing with UMI, a highly sensitive analysis of ccfDNA was performed to screen for frequently mutated genes in MM, confirming the possibility of detecting CM in LB. The use of a targeted panel of genes allowed to obtain a high sequencing coverage but at the same time had the disadvantage of investigating only a specific selection of regions which is based on current knowledge and therefore may not reflect the entire biological basis of the disease. The high number of overall alterations identified in our samples does not allow us to define a distinguishable profile between different health groups and at an individual level, however we can observe in MGUS a slightly lower average mutation number compared to the MM group. According to what we have observed, it seems that the distribution of the most frequently mutated genes within each health group differs from that reported in two genomic databases (TCGA and cBioPortal) for MM, in other words it seems that the ccfDNA extracted from plasma does not recapitulate the mutational profile observed in DNA extracted from the BMs of MMs reported in genomic databases. The difference we observe is probably attributable to the different nature of the samples analyzed.

The NGS analysis carried out in the genes typically associated with MM revealed the presence of CM in healthy subjects used as a control group, adding a level of difficulty in interpreting the role of the mutational landscape. J. Liu et al. have highlighted how in the ccfDNA of healthy subjects there is a

high presence of mutations derived from clonal haematopoiesis, which in addition to being a potential source of false positives, do not allow an effective distinction from tumor-derived mutations in LBs [66]. According to our results, at a first glance, this phenomenon constitutes a sort of "background" that hampers the possibility to define a distinguishable and classifiable mutation profile among the different health groups, in particular at individual level. Therefore, on individual bases, it seems that the clonal haematopoiesis constitutes a barrier for the use of ccfDNA in the diagnosis or study of MGUS and its evolution. However, it should be also noticed that on group bases, once the background's mutation profile has been subtracted, the most interesting genes show up, in patients with MGUS, we found an increase in the number of mutations within *EGR1*, *CDKN2C*, *CD79B*, *ANK2*, *ACTG1*, and *SP140 genes.* A previous work [70] on the mutational landscape of MGUS patients was performed by purifying selected malignant PCs by flow cytometry and cell sorting ($CD138^{+}$, $CD19^{-}$, $CD56^{+/-}$). In this study, the total number of mutations of MGUS patients was slightly lower than that of MM patients. In MGUS patients the authors described few MM-associated mutations in the *KRAS*, *HIST1H1E*, *NRAS*, *DIS3*, *EGR1*, and *LTB* genes. Despite the different biological material analyzed (ccfDNA in our study), the results, overall, do not differ from our analysis.

Among the multiple somatic mutations detected, no SNVs were recorded in the *KRAS* and *NRAS* genes, which are the most frequently mutated genes in MM (TCGA). However, in our setting, patients with MM showed deletions in these genes. Despite these mutations were unlikely to be activating (i.e. gain of function) but rather loss of function, it is interesting to note that, overall, in MM patients there was a much higher prevalence of mutations within *RAS* genes than in healthy donors (+28% *KRAS*; +33% *NRAS*; +12% *BRAF*). Moreover, we found an increased frequency of MM patients (vs healthy donors) carrying mutations within *ACTG1, BRAF, DTX1, FAM46C, FAT3, FBN2, HIST1H1E, IGR1, KLHL6, KRAS, MYO10, NOTCH1, NRAS, PIM1, PKHD1, PTPRD, ROBO1, RYR2, SP140, TNFRSF17, USH2A*, that partially recapitulate the profile described in TCGA. Of note, previous works [70] found recurrent mutations within *KLHL6* and *HIST1H1E* in purified PCs from MGUS patients. In summary, overall, we conclude that the analysis of ccfDNA can still return the footprint of the disease, once the background constituted by the clonal haematopoiesis, is taken into account and removed.

We have identified numerous mutations in the *ARID1A* gene already identified in other studies as a prognostic indicator for poor clinical outcomes in MM since it contains a DNA-binding domain and functionally implicated in transcriptional regulation [71][72]. Mutations in genes with epigenetic function and enzyme-related (e.g. *ARID1A*, *HIST1H1E, SETD2*) occur frequently in myeloma precursor conditions. However, we have recorded other mutations implicated in signalling pathways such as mutations in chromatin regulatory genes, *KMT2C*/*KMT2D.* These mutations are prevalent in patients affected by MGUS, and this result follows what is already known in the literature for patients with newly diagnosed MM, suggesting that these genes may also have a role in the precancerous phases

of the disease [71]. Dysregulation of these epigenetic pathways in malignant PC [24][73], contributes to forming part of the genetic landscape of MGUS and SMM myeloma precursor conditions [27][13]. Tessoulin et al. [74] had also observed that high mutation rates in epigenetic modifier genes were also present in human myeloma cell lines.

We obtained extra-information from the study of the mutation types. The distribution of missense, insertion and deletions allowed us to identify some very interesting characteristics. Comparing the healthy subjects with all the others, we observed that the number of insertions detected, both in-frame and frameshift, was significantly reduced, with a highly unbalanced ratio Ins/Del of 0.07 (range = 0.02 - 0.27). Intriguingly, this ratio raised to 0.5 (range= 0 - 4.00) in MGUS, 0.78 (range= 0.09 - 6.00) in SMM and 1.36 (range= 0 - 5.61) in MM. Moreover, the frequency of insertions per Million of base pairs definitively increases from healthy (average = 6.06E-04; range= 2.46E-04 - 1.16E-03), MGUS (average = 2.48E-03 ; range= 0.00E+00 - 1.19E-02), SMM (average = 3.38E-03; range= 3.54E-04 - 1.19E-02), and MM (average = 7.69E-03; range= 0.00E+00 - 1.95E-02).

Both parameters can be altered when considering the healthy donors as having the “normal” ranges, and we found that among MGUS patients only 19% of patients had normal levels of both parameters, in SMM 37% and in MM 14%. The Ins burden in the 9 patients with pathological progression suggests a tendency to acquire insertions as the disease progresses. The TMB and the frequency of Ins unique to each gene in healthy patients was low (with a total number of insertions as much as 8) and differs significantly compared to other groups. The ins/del ratio combined with the TMB of the insertions seem to be highly indicative of disease progression. However, it should be noted that some MGUS and even some MM patients were in the range of the healthy donors for both parameters. Therefore, the burden of insertions is unlikely to be used as marker of diagnosis or prognosis on individual bases. However, it is an interesting endpoint that deserves further studies. In our small series, we could notice that, among the MGUS patients who evolved, 89% showed an increase of at least one of the two parameters. Actually, previous genomic studies reported an ins/del ratio close to 1 in BM of MM patients [75]. Indels, although less common than single nucleotide variants, represent an important factor in studies of cancer mutational signatures, as they are associated with notable functional consequences [76]. In particular, the inframe indels occur at a higher frequency than frameshift indels among protooncogenes, while among tumor suppressor genes frameshift indels are more common [77]. The indels are often found in the cancer genomes and tumours with deficiencies of specific DNA repair pathways (e.g. mismatch repair, or DSB repair) are associated with increased frequencies of specific indels [78]. A pancancer analysis within TCGA showed that In-frame indels are associated with a more adverse outcome. In-frame indels were mostly associated with elevated *APOBEC1* expression, frameshift indels were mostly associated with DNA mismatch repair (MMR) mutational status [77].

The activation of APOBEC/AID proteins (activation-induced cytidine deaminase) has been associated with mechanisms that generate indels during the process of antibody diversification. The aberrant activity of these mechanisms is known to be a mutator phenotype with a high impact for the progression of carcinogenesis in leukemia and B-cell lymphoma [78] [79]. Moreover, aberrant AID activity is one of the major mutational processes known in MM, pushing the mutational landscape of aberrant clone towards a malignant fate, giving rise to myeloma in its early stages [80] [81]. Therefore, theoretically, the increase of in/del ratio could be ascribed to an aberrant activity of AID/APOBEC. Specific experiments [78] showed that, when APOBEC is active, insertions are introduced with a slightly higher frequency than deletions in the maturating Ig chain and this corresponds to the in/del ratio observed in BM. In summary, our observation that in ccfDNA from MM patients the in/del ratio is close to 1 could be the result of the AID/APOBEC constitutive activation [78].

Another possible mechanism that could explain the increasing insertion burden among patients could be the progressive increased expression of HUWE1 observed to occur during the progression from MGUS to SMM, and finally to MM. This E3 ubiquitin-protein ligase was shown to regulate the degradation of DNA-Polymerase β (DNA-Pol β), in fact, increased levels of DNA-Pol β can be detected following HUWE1 inhibition [82][83]. It is conceivable that the increased HUWE1 with the progression of the disease will lead MM cell to a reduced activity of DNA-Pol β [82]. On its turn, it has also been shown that reduced DNA-Pol β activity is accompanied by an increased frequency of DNA insertions [78], especially the ones longer than 1bp. DNA-Pol β is part of the base excision repair (BER), and one could speculate that, in a subgroup of patients, there is a weakening of BER during tumor progression, whose footprint could be observed by an increased ins/del ratio on the ccfDNA [83]. Further studies should be undertaken on this subject.

In this study we also used a retrospective collection of paired LBs samples, which allowed us to characterize the CM within a patient in follow-up in relation to the evolution of the disease over time. These analyzes should be considered exploratory considering the low number of individuals who progressed from MGUS to MM during follow-up. There are few persistent mutations identified in the samples of patients who have had progression of the disease, while the new mutations that have appeared with the progression of the disease are very numerous and heterogeneous, and TMB does not appear to track disease progression.

To date, few NGS studies have used follow-up samples obtained from the same individuals who progressed from pre-malignant states to MM [84][85]. Overall, the genetic variants identified in this investigation displayed significant heterogeneity and could not be attributed to a singular or a small number of well-defined biological pathways. If we relate the data to the size of the coding sequence

of the gene, the TMB per gene is quite similar, emphasizing the complex and heterogeneous characteristics of this analysis.

Among the many technologies that allow the detection of tumor-specific genetic and epigenetic aberrations in the ctDNA fraction, we have exploited dPCR to absolutely detect and quantify some genetic events, even in the presence of extremely low mutation copy numbers, on a large cohort of samples and with the only limitation of being able to screen a limited number of already known alterations. Several studies have observed that more than over half of MM patients exhibiting *RAS* activation possess activating mutations in NRAS or KRAS genes, predominantly located within codons 12, 13, or 61 [86][67] correlating with reduced overall and progression-free survival [87], furthermore, the mutations on *KRAS* and *NRAS*, are mutually exclusive in about 90% of cases. Data from TCGA and Catalogue Of Somatic Mutations In Cancer (COSMIC) databases confirms this observation. The study we conducted using dPCR aims to investigate the theoretically more frequent SNV mutations in MM in samples taken at different times and pathological stages of the same individual and to compare the correspondence between the mutations detectable in the BM compared to those obtained from the LB.

The first clear result of this analysis is that the investigated mutations are more difficult to detect in ccfDNA than in the BM of the same individual. This data is in agreement with the NGS analysis carried out in which no SNVs were found in the *KRAS* and *NRAS* genes, and a significant difference in the mutational frequency was detected between the analyzed samples extracted from plasma and those reported in the genomic databases of BM and MM.

The BM is always the tissue with the highest number of copies of mutated DNA per µL, followed by the BC and Plasma. The comparative analyzes between LBs and BM samples from the same individual highlighted a correlation of the mutational burden between tissues only for some of the samples analyzed. The mutational profile detected in LBs does not report a full correspondence with the BMs analyzed, on average DNA extracted from BC compared to DNA extracted from plasma seems to be the best option to exploit the potential prospective detection of mutations in LBs. By analyzing bone marrow and peripheral blood samples from the same subjects, it was seen that in some cases there are mutational events that are not detectable at the same time in the analyzed samples, leading to the assumption that this may be due to a spatial heterogeneity typical of MM [46] [55].

Furthermore, due to the fact that ccfDNA concentrations are extremely low, the analyzed samples could contain only a few ctDNA molecules and one cannot overlook the fact that any ccfDNA used for the analysis of a specific mutation could contain other mutated molecules which would remain excluded from further analysis, thus obtaining false negative results.

We can observe that in 28 patients with BM, only 4 had a ratio between copies of mutated DNA per µL and copies of wt DNA per µL greater than 0.1, therefore we have a proportion of individuals with a significant load of mutations in line with the total frequency expected (18%) of the 3 mutations *KRAS* Q61H, *NRAS* Q61R, *NRAS* Q61K according to TCGA. However, for 4 patients we did not measure any mutations in the BM and for the majority of them (20 patients) we instead measured frequencies in the BM that are much lower than the number of malignant PCs that are typically found in the biopsy at diagnosis (10%). Some studies have observed that *KRAS* mutations have been rarely detected in cases of MGUS [37]; however, it is the most frequently mutated gene in SMM, suggesting its involvement in the progression from SMM to MM [43]. *NRAS* mutations seem to play a crucial role in promoting drug resistance. Indeed, a prevalence of *NRAS* mutations has been observed in relapsed MM [35], consequently, *NRAS* mutations have been associated with reduced sensitivity to treatments in relapsed MM [36]. *RAS* genes activation is reported in about 50% of newly diagnosed MM and about 75% of relapsed/refractory MM (rrMM), leading to increased cell proliferation and survival by activating the *RAS/MEK/ERK* pathway [67]. All this leads us to think that the disease occurs with alternative mechanisms and that they do not involve *RAS* genes but that these begin to mutate as medium/late events.

NGS and dPCR to investigate the mutational landscape in paired samples from the same individual in precancerous conditions and in MM have the advantage of being very sensitive and reliable but limit the potential for investigating other genomic events. Furthermore, only some of the causative molecular variations of MM have been definitively characterized and their clinical relevance is not yet fully understood [23]. The study of these paired samples sheds light on the evolutionary genetic landscape and offers further information on the mutational behavior of mutant clones overtime during progression. Significant efforts are currently being made to establish liquid biopsy as a method for early cancer detection, with ctDNA mutation analysis reported in early-stage tumors [88][89][90]. However, comprehensive large-scale validation studies are required to fully grasp the potential and limitations of this application. [91].

In parallel to NGS sequencing and dPCR studies on patient samples, studies were also carried out on cell lines aimed at exploring the functional effects of *NRAS* p.Q61R overexpression in MM. The *NRAS* Q61R (Gln61Arg) mutation has a frequency of 6.78% (TCGA) in the population of patients with MM, making it the most frequent SNV in MM. This is a hotspot mutation that lies within a GTP-binding domain of the NRas protein (UniProt.org), and leading to the activation of Mapk signaling and cell transformation in culture [92][93].

The results of the experiments on viability and cell cycle would seem to suggest that overexpression of *NRAS*, regardless of the p.Q61R mutation, negatively affects cell proliferation, reducing both ATP-dependent and ATP-independent metabolic activity.

Current studies have demonstrated that expression of *NRAS* p.Q61R in human endothelial cells causes a shift towards abnormal morphology and increased migration [94]. The results obtained in cell migration tests revealed in cells overexpressing *NRAS* a more aggressive phenotypic behavior with greater tendency to aggregation and adhesion, which led through further tests to also detect the increased capacity of colony formation. These data suggest that there may be mechanisms through which NRAS could play a significant role in the progression and aggressiveness of MM. Further studies representing a potential added value to validate this hypothesis.

It was observed through the use of a novel mouse model of MM that activates the expression of endogenous *NRAS* p.Q61R in germinal center B cells, that expression of *NRAS* p.Q61R promoted MM highly malignant and recapitulated most of the biological and clinical features of high-risk advanced human MM[95] . Furthermore, it has also been observed that siRNAs targeting the suppression of oncogenic forms of *NRAS* p.Q61R, in the treatment of melanoma cells, lead to a reduction in migration and invasion [96].

Our results on cellular studies have the limitation of highlighting the effects of an overexpression of *NRAS* on a MM and therefore already tumorous cell line, it would be advantageous to investigate the role of *NRAS* on other cellular and molecular models or on other cell lines.

6. Conclusions and future prospects

In MM, the application of LBs represents an emerging field that meets the clinical needs of minimally invasive investigations and preventive and personalized medicine, offering the opportunity to implement precision medicine strategies allowing the profiling of individual patients and the selection of potential therapies targeted. The clinical parameters currently used for risk assessment serve as valuable instruments but demonstrate limitations in accurately predicting individual progression of myeloma precursors. Furthermore, a consensus regarding the optimal clinical parameters and subsequent management strategies remains elusive. [19] [97] [98].

Our objective was to evaluate the potential of liquid biopsies in identifying possible mutations in ccfDNA in patients with MM or earlier stages. We have highlighted the utility of an investigative approach using NGS and dPCR to detect relevant mutations in LBs samples from myeloma precursor conditions. Our findings, relating to the NGS and PCR analyzes conducted, raise novel inquiries concerning the contribution of mutations to disease pathogenesis. The differences in the profile of indels in the progression to MM leads us to hypothesize an involvement of these mutations in important roles of the pathology. Further studies would help to better understand the prognostic value of such approaches in predicting progression and risk stratification of these precursor patients.

Preliminary results obtained from the overexpression of *NRAS* in the MM cell line show an increased aggregation capacity and a reduced metabolic activity. Further information will be obtained through future targets, which include experiments on other cell lines and new tests, also an effort will be dedicated to the manipulation of the *NRAS* gene sequence using siRNA and genome editing in order to thoroughly investigate its role in MM using in vitro and in vivo models.

This study opens new view to understand MM and its presymptomatic phases, highlighting the potential and limitations of LBs, while also seeking to gain a comprehensive understanding of the underlying mechanisms involved in various disease states. This approach could also facilitate the identification of potential drug targets.

7. References

[1] S. K. Kumar *et al.*, "Multiple myeloma," *Nat. Rev. Dis. Prim.*, vol. 3, pp. 1–20, 2017, doi: 10.1038/nrdp.2017.46.

[2] A. Jurczyszyn and A. Suska, "Multiple Myeloma," *Encycl. Biomed. Gerontol. Vol. 1-3*, vol. 2, no. June, pp. V2-461-V2-478, 2019, doi: 10.1016/B978-0-12-801238-3.11412-6.

[3] G. D. Roodman, "Pathogenesis of myeloma bone disease," *Leukemia*, vol. 23, no. 3, pp. 435–441, 2009, doi: 10.1038/leu.2008.336.

[4] T. C. Michels, K. E. Petersen, M. Army, and F. Medicine, "Multiple Myeloma: Diagnosis and Treatment," 2017.

[5] B. G. Barwick, V. A. Gupta, P. M. Vertino, and L. H. Boise, "Cell of origin and genetic alterations in the pathogenesis of multiple myeloma," *Front. Immunol.*, vol. 10, no. MAY, 2019, doi: 10.3389/fimmu.2019.01121.

[6] R. L. Siegel, K. D. Miller, and A. Jemal, "Cancer statistics, 2016," *CA. Cancer J. Clin.*, vol. 66, no. 1, pp. 7–30, 2016, doi: 10.3322/caac.21332.

[7] W. H. International Agency for Research on Cancer. Organization, "Global Multiple Myeloma Statistics," *Globocan 2022*, pp. 1–2, 2020, [Online]. Available: https://gco.iarc.fr/today%0Ahttps://gco.iarc.fr/today/data/factsheets/cancers/35-Multiple-myeloma-fact-sheet.pdf.

[8] O. Landgren and B. M. Weiss, "Patterns of monoclonal gammopathy of undetermined significance and multiple myeloma in various ethnic/racial groups: Support for genetic factors in pathogenesis," *Leukemia*, vol. 23, no. 10, pp. 1691–1697, 2009, doi: 10.1038/leu.2009.134.

[9] R. A. Kyle *et al.*, "Review of 1027 patients with newly diagnosed multiple myeloma," *Mayo Clin. Proc.*, vol. 78, no. 1, pp. 21–33, 2003, doi: 10.4065/78.1.21.

[10] A. J. Cowan *et al.*, "Global burden of multiple myeloma: A systematic analysis for the global burden of disease study 2016," *JAMA Oncol.*, vol. 4, no. 9, pp. 1221–1227, 2018, doi: 10.1001/jamaoncol.2018.2128.

[11] S. V. Rajkumar, "Multiple myeloma: 2020 update on diagnosis, risk-stratification and management," *Am. J. Hematol.*, vol. 95, no. 5, pp. 548–567, 2020, doi: 10.1002/ajh.25791.

[12] Justin I. Odegaard and A. Chawla, "B-cell anergy: from transgenic models to naturally occurring anergic B cells?," *Bone*, vol. 23, no. 1, pp. 1–7, 2008, doi: 10.1038/nri2133.B-cell.

[13] G. J. Morgan, B. A. Walker, and F. E. Davies, "The genetic architecture of multiple myeloma," *Nat. Rev. Cancer*, vol. 12, no. 5, pp. 335–348, 2012, doi: 10.1038/nrc3257.

[14] N. W. C. J. van de Donk, C. Pawlyn, and K. L. Yong, "Multiple myeloma," *Lancet*, vol. 397, no. 10272, pp. 410–427, 2021, doi: 10.1016/S0140-6736(21)00135-5.

[15] E. L. Jenner, J. A. R. Evans, and S. J. Harding, "Serum Free Light Chain (FLC) Analysis: A Guiding Light in Monoclonal Gammopathy Management," *J. Appl. Lab. Med.*, vol. 2, no. 1, pp. 98–106, 2017, doi: 10.1373/jalm.2016.021352.

[16] V. Tietsche de Moraes Hungria, S. Allen, P. Kampanis, and E. M. Soares, "Serum free light chain assays not total light chain assays are the standard of care to assess Monoclonal Gammopathies," *Rev. Bras. Hematol. Hemoter.*, vol. 38, no. 1, pp. 37–43, 2016, doi: 10.1016/j.bjhh.2015.11.003.

[17] J. Mikhael, M. Bhutani, and C. E. Cole, “Multiple Myeloma for the Primary Care Provider: A Practical Review to Promote Earlier Diagnosis Among Diverse Populations,” *Am. J. Med.*, vol. 136, no. 1, pp. 33–41, 2023, doi: 10.1016/j.amjmed.2022.08.030.

[18] M.-V. K. and M. M. Friese C, Yang J, “Molecular and biologic markers of progression in monoclonal gammopathy of undetermined significance to multiple myeloma,” *Physiol. Behav.*, vol. 46, no. 2, pp. 248–256, 2019, doi: 10.3109/10428194.2010.525725.Molecular.

[19] N. W. C. J. van de Donk *et al.*, “The clinical relevance and management of monoclonal gammopathy of undetermined significance and related disorders: Recommendations from the European Myeloma Network,” *Haematologica*, vol. 99, no. 6, pp. 984–996, 2014, doi: 10.3324/haematol.2013.100552.

[20] R. Kyle *et al.*, “Clinical Course and Prognosis of Smoldering (Asymptomatic) Waldenstrom’s Macroglobulinemia,” *Blood*, vol. 112, no. 11, pp. 2709–2709, 2008, doi: 10.1182/blood.v112.11.2709.2709.

[21] T. H. Mouhieddine, L. D. Weeks, and I. M. Ghobrial, “Monoclonal gammopathy of undetermined significance,” *Blood*, vol. 133, no. 23, pp. 2484–2494, 2019, doi: 10.1182/blood.2019846782.

[22] P. Daniel Harris, BA, Lynn McNicoll, MD, Gary Epstein-Lubow, MD, and Kali S. Thomas and M. J. S. Benjamin M. Davis, Glen F. Rall, “Impact of Prior Diagnosis of Monoclonal Gammopathy on Outcomes in Newly Diagnosed Multiple Myeloma,” *Physiol. Behav.*, vol. 176, no. 1, pp. 139–148, 2017, doi: 10.1038/s41375-019-0419-7.Impact.

[23] B. Oben *et al.*, “The Dynamics of Nucleotide Variants in the Progression from Low–Intermediate Myeloma Precursor Conditions to Multiple Myeloma: Studying Serial Samples with a Targeted Sequencing Approach,” *Cancers (Basel).*, vol. 14, no. 4, 2022, doi: 10.3390/cancers14041035.

[24] A. K. Dutta, D. R. Hewett, J. L. Fink, J. P. Grady, and A. C. W. Zannettino, “Cutting edge genomics reveal new insights into tumour development, disease progression and therapeutic impacts in multiple myeloma,” *Br. J. Haematol.*, vol. 178, no. 2, pp. 196–208, 2017, doi: 10.1111/bjh.14649.

[25] R. A. K. Possomato-Vieira, José S. and Khalil and O. 2. 0. E. S. E. and S. Modeling, “Moving From Cancer Burden to Cancer Genomics for Smoldering Myeloma: A Review,” *Physiol. Behav.*, vol. 176, no. 12, pp. 139–148, 2017, doi: 10.1001/jamaoncol.2019.4659.Moving.

[26] C. Cosemans *et al.*, “Prognostic Biomarkers in the Progression From MGUS to Multiple Myeloma: A Systematic Review,” *Clin. Lymphoma, Myeloma Leuk.*, vol. 18, no. 4, pp. 235–248, 2018, doi: 10.1016/j.clml.2018.02.011.

[27] U. Pathogenesis, N. History, and S. V. Rajkumar, “MGUS and Smoldering Multiple Myeloma: Update on Pathogenesis, Natural History, and Management,” *Hematol. Am Soc Hematol Educ Program.*, vol. 340–5, 2005, doi: 10.1182/asheducation-2005.1.340.

[28] N. Korde, S. Y. Kristinsson, and O. Landgren, “Monoclonal gammopathy of undetermined significance (MGUS) and smoldering multiple myeloma (SMM): Novel biological insights and development of early treatment strategies,” *Blood*, vol. 117, no. 21, pp. 5573–5581, 2011, doi: 10.1182/blood-2011-01-270140.

[29] M. Mateos *et al.*, “International Myeloma Working Group risk strati fi cation model for smoldering multiple myeloma (SMM),” *Blood Cancer J.*, 2020, doi: 10.1038/s41408-020-00366-3.

[30] R. Georgakopoulou *et al.*, “Occupational exposure and multiple myeloma risk: An updated review of meta-analyses,” *J. Clin. Med.*, vol. 10, no. 18, 2021, doi: 10.3390/jcm10184179.

[31] S. Cheah *et al.*, “Alcohol and tobacco use and risk of multiple myeloma: A case-control study,” *eJHaem*, vol. 3, no. 1, pp. 109–120, 2022, doi: 10.1002/jha2.337.

[32] R. Parikh, S. M. Tariq, C. R. Marinac, and U. A. Shah, “A comprehensive review of the impact of obesity on plasma cell disorders,” *Leukemia*, vol. 36, no. 2, pp. 301–314, 2022, doi: 10.1038/s41375-021-01443-7.

[33] C. Frank *et al.*, “Search for familial clustering of multiple myeloma with any cancer,” *Leukemia*, vol. 30, no. 3, pp. 627–632, 2016, doi: 10.1038/leu.2015.279.

[34] S. Y. Kristinsson *et al.*, “Patterns of hematologic malignancies and solid tumors among 37,838 first-degree relatives of 13,896 patients with multiple myeloma in Sweden,” *Int. J. Cancer*, vol. 125, no. 9, pp. 2147–2150, 2009, doi: 10.1002/ijc.24514.

[35] M. Pertesi, M. Went, M. Hansson, K. Hemminki, R. S. Houlston, and B. Nilsson, “Genetic predisposition for multiple myeloma,” *Leukemia*, vol. 34, no. 3, pp. 697–708, 2020, doi: 10.1038/s41375-019-0703-6.

[36] S. Manier, Y. Kawano, G. Bianchi, A. M. Roccaro, and I. M. Ghobrial, “Cell autonomous and microenvironmental regulation of tumor progression in precursor states of multiple myeloma,” *Curr. Opin. Hematol.*, vol. 23, no. 4, pp. 426–433, 2016, doi: 10.1097/MOH.0000000000000259.

[37] N. van Nieuwenhuijzen, I. Spaan, R. Raymakers, and V. Peperzak, “From MGUS to multiple myeloma, a paradigm for clonal evolution of premalignant cells,” *Cancer Res.*, vol. 78, no. 10, pp. 2449–2456, 2018, doi: 10.1158/0008-5472.CAN-17-3115.

[38] N. Bolli *et al.*, “Heterogeneity of genomic evolution and mutational profiles in multiple myeloma,” *Nat. Commun.*, vol. 5, 2014, doi: 10.1038/ncomms3997.

[39] S. Pasca *et al.*, “Kras/nras/braf mutations as potential targets in multiple myeloma,” *Front. Oncol.*, vol. 9, no. OCT, pp. 1–5, 2019, doi: 10.3389/fonc.2019.01137.

[40] S. Bezieau *et al.*, “High incidence of N and K-Ras activating mutations in multiple myeloma and primary plasma cell leukemia at diagnosis,” *Hum. Mutat.*, vol. 18, no. 3, pp. 212–224, 2001, doi: 10.1002/humu.1177.

[41] B. A. Walker *et al.*, “Mutational spectrum, copy number changes, and outcome: Results of a sequencing study of patients with newly diagnosed myeloma,” *J. Clin. Oncol.*, vol. 33, no. 33, pp. 3911–3920, 2015, doi: 10.1200/JCO.2014.59.1503.

[42] B. A. Walker *et al.*, “Identification of novel mutational drivers reveals oncogene dependencies in multiple myeloma,” *Blood*, vol. 132, no. 6, pp. 587–597, 2018, doi: 10.1182/blood-2018-03-840132.

[43] E. M. Boyle *et al.*, “The molecular make up of smoldering myeloma highlights the evolutionary pathways leading to multiple myeloma,” *Nat. Commun.*, vol. 12, no. 1, 2021, doi: 10.1038/s41467-020-20524-2.

[44] J. Xu *et al.*, “Molecular signaling in multiple myeloma: Association of RAS/RAF mutations and MEK/ERK pathway activation,” *Oncogenesis*, vol. 6, no. 5, 2017, doi: 10.1038/oncsis.2017.36.

[45] G. Mulligan *et al.*, “Mutation of NRAS but not KRAS significantly reduces myeloma sensitivity to single-agent bortezomib therapy,” *Blood*, vol. 123, no. 5, pp. 632–639, 2014, doi: 10.1182/blood-2013-05-504340.

[46] B. Ferreira *et al.*, “Liquid biopsies for multiple myeloma in a time of precision medicine,” *J. Mol. Med.*, vol. 98, no. 4, pp. 513–525, 2020, doi: 10.1007/s00109-020-01897-9.

[47] S. Volik, M. Alcaide, R. D. Morin, and C. Collins, “Cell-free DNA (cfDNA): Clinical significance and utility in cancer shaped by emerging technologies,” *Mol. Cancer Res.*, vol. 14, no. 10, pp. 898–908, 2016, doi: 10.1158/1541-7786.MCR-16-0044.

[48] C. Alix-Panabières and K. Pantel, “Liquid biopsy: From discovery to clinical application,” *Cancer Discov.*, vol. 11, no. 4, pp. 858–873, 2021, doi: 10.1158/2159-8290.CD-20-1311.

[49] M. Fleischhacker and B. Schmidt, “Circulating nucleic acids (CNAs) and cancer-A survey,” *Biochim. Biophys. Acta - Rev. Cancer*, vol. 1775, no. 1, pp. 181–232, 2007, doi: 10.1016/j.bbcan.2006.10.001.

[50] D. Vrabel, A. Souckova, L. Sedlarikova, and S. Sevcikova, “Liquid Biopsies in Multiple Myeloma,” *Liq. Biopsy*, 2019, doi: 10.5772/intechopen.78630.

[51] C. C. Huang, M. Du, and L. Wang, “Bioinformatics analysis for circulating cell-free DNA in cancer,” *Cancers (Basel).*, vol. 11, no. 6, pp. 1–15, 2019, doi: 10.3390/cancers11060805.

[52] J. C. M. Wan *et al.*, “Liquid biopsies come of age: Towards implementation of circulating tumour DNA,” *Nat. Rev. Cancer*, vol. 17, no. 4, pp. 223–238, 2017, doi: 10.1038/nrc.2017.7.

[53] F. Diehl *et al.*, “Circulating mutant DNA to assess tumor dynamics,” *Nat. Med.*, vol. 14, no. 9, pp. 985–990, 2008, doi: 10.1038/nm.1789.

[54] L. A. Diaz and A. Bardelli, “Liquid biopsies: Genotyping circulating tumor DNA,” *J. Clin. Oncol.*, vol. 32, no. 6, pp. 579–586, 2014, doi: 10.1200/JCO.2012.45.2011.

[55] M.-V. K. and M. M. Friese C, Yang J, “Tracking myeloma tumor DNA in peripheral blood Johannes,” *Physiol. Behav.*, vol. 46, no. 2, pp. 248–256, 2019, doi: 10.1016/j.beha.2020.101146.Tracking.

[56] G. De Rubis, S. Rajeev Krishnan, and M. Bebawy, “Liquid Biopsies in Cancer Diagnosis, Monitoring, and Prognosis,” *Trends Pharmacol. Sci.*, vol. 40, no. 3, pp. 172–186, 2019, doi: 10.1016/j.tips.2019.01.006.

[57] H. Sata *et al.*, “Quantitative polymerase chain reaction analysis with allele-specific oligonucleotide primers for individual IgH VDJ regions to evaluate tumor burden in myeloma patients,” *Exp. Hematol.*, vol. 43, no. 5, pp. 374-381.e2, 2015, doi: 10.1016/j.exphem.2015.01.002.

[58] A. Oberle *et al.*, “Monitoring multiple myeloma by next-generation sequencing of V (D) J rearrangements from circulating myeloma cells and cell-free Correspondence :,” vol. 102, no. D, pp. 1105–1111, 2017, doi: 10.3324/haematol.2016.161414.

[59] O. Kis *et al.*, “Circulating tumour DNA sequence analysis as an alternative to multiple myeloma bone marrow aspirates,” *Nat. Commun.*, vol. 8, no. May, pp. 1–11, 2017, doi: 10.1038/ncomms15086.

[60] S. Mithraprabhu *et al.*, “Circulating tumour DNA analysis demonstrates spatial mutational heterogeneity that coincides with disease relapse in myeloma,” *Leukemia*, vol. 31, no. 8, pp. 1695–1705, 2017, doi: 10.1038/leu.2016.366.

[61] C. Wood-Bouwens, B. T. Lau, C. M. Handy, H. J. Lee, and H. P. Ji, “Single-Color Digital PCR Provides High-Performance Detection of Cancer Mutations from Circulating DNA,” *J. Mol. Diagnostics*, vol. 19, no. 5, pp. 697–710, 2017, doi: 10.1016/j.jmoldx.2017.05.003.

[62] J. Rutering *et al.*, “Mutational Landscape of Metastatic Cancer Revealed from Prospective Clinical Sequencing of 10,000 Patients,” *Nat. Med.*, vol. 5, no. 6, pp. 1–8, 2016, doi: 10.1038/nm.4333.Mutational.

[63] S. Saghafinia, M. Mina, N. Riggi, D. Hanahan, and G. Ciriello, “Pan-Cancer Landscape of

Aberrant DNA Methylation across Human Tumors," *Cell Rep.*, vol. 25, no. 4, pp. 1066-1080.e8, 2018, doi: 10.1016/j.celrep.2018.09.082.

[64] A. Streubel *et al.*, "Comparison of different semi-automated cfDNA extraction methods in combination with UMI-based targeted sequencing," *Oncotarget*, vol. 10, no. 55, pp. 5690–5702, 2019, doi: 10.18632/oncotarget.27183.

[65] Q. Peng, C. Xu, D. Kim, M. Lewis, J. DiCarlo, and Y. Wang, "Targeted Single Primer Enrichment Sequencing with Single End Duplex-UMI," *Sci. Rep.*, vol. 9, no. 1, pp. 1–10, 2019, doi: 10.1038/s41598-019-41215-z.

[66] J. Liu *et al.*, "Biological background of the genomic variations of cf-DNA in healthy individuals," *Ann. Oncol.*, vol. 30, no. 3, pp. 464–470, 2019, doi: 10.1093/annonc/mdy513.

[67] K. Y. Wong, Q. Yao, L. Q. Yuan, Z. Li, E. S. K. Ma, and C. S. Chim, "Frequent functional activation of RAS signalling not explained by RAS/RAF mutations in relapsed/refractory multiple myeloma," *Sci. Rep.*, vol. 8, no. 1, pp. 1–7, 2018, doi: 10.1038/s41598-018-31820-9.

[68] B. Oben *et al.*, "Whole-genome sequencing reveals progressive versus stable myeloma precursor conditions as two distinct entities," *Nat. Commun.*, vol. 12, no. 1, pp. 1–11, 2021, doi: 10.1038/s41467-021-22140-0.

[69] A. Manuscript and H. Malignancies, "Detection of Circulating Tumor DNA in Early- and Late-Stage Human Malignancies," *Natl. Institutes Heal.*, vol. 6, no. 224, pp. 69–122, 2014, doi: 10.1126/scitranslmed.3007094.Detection.

[70] A. Mikulasova *et al.*, "The spectrum of somatic mutations in monoclonal gammopathy of undetermined significance indicates a less complex genomic landscape than that in multiple myeloma," *Haematologica*, vol. 102, no. 9, pp. 1617–1625, 2017, doi: 10.3324/haematol.2017.163766.

[71] L. Zhang *et al.*, "Identification of clinical implications and potential prognostic models of chromatin regulator mutations in multiple myeloma," *Clin. Epigenetics*, vol. 14, no. 1, pp. 1–12, 2022, doi: 10.1186/s13148-022-01314-7.

[72] C. Lin *et al.*, "Recent advances in the ARID family: Focusing on roles in human cancer," *Onco. Targets. Ther.*, vol. 7, pp. 315–324, 2014, doi: 10.2147/OTT.S57023.

[73] N. Bolli *et al.*, "Analysis of the genomic landscape of multiple myeloma highlights novel prognostic markers and disease subgroups," *Leukemia*, vol. 32, no. 12, pp. 2604–2616, 2018, doi: 10.1038/s41375-018-0037-9.

[74] B. Tessoulin *et al.*, "Whole-exon sequencing of human myeloma cell lines shows mutations related to myeloma patients at relapse with major hits in the DNA regulation and repair pathways," *J. Hematol. Oncol.*, vol. 11, no. 1, pp. 1–13, 2018, doi: 10.1186/s13045-018-0679-0.

[75] C. Xie *et al.*, "Identification of mutation gene prognostic biomarker in multiple myeloma through gene panel exome sequencing and transcriptome analysis in Chinese population," *Comput. Biol. Med.*, vol. 163, no. June, p. 107224, 2023, doi: 10.1016/j.compbiomed.2023.107224.

[76] A. Niavarani, A. S. Farahani, M. Sharafkhah, and M. Rassoulzadegan, "Pancancer analysis identifies prognostic high-APOBEC1 expression level implicated in cancer in-frame insertions and deletions," vol. 39, no. 3, pp. 327–335, 2018, doi: 10.1093/carcin/bgy005.

[77] A. Niavarani, A. S. Farahani, M. Sharafkhah, and M. Rassoulzadegan, "Pancancer analysis identifies prognostic high-APOBEC1 expression level implicated in cancer in-frame

insertions and deletions," *Carcinogenesis*, vol. 39, no. 3, pp. 327–335, 2018, doi: 10.1093/carcin/bgy005.

[78] Q. Hao *et al.*, "DNA repair mechanisms that promote insertion-deletion events during immunoglobulin gene diversification," *Sci. Immunol.*, vol. 8, no. 81, pp. 1–37, 2023, doi: 10.1126/sciimmunol.ade1167.

[79] R. Casellas *et al.*, "Mutations, kataegis, and translocations in B lymphocytes: towards a mechanistic understanding of AID promiscuous activity," vol. 16, no. 3, pp. 164–176, 2016, doi: 10.1038/nri.2016.2.Mutations.

[80] N. Bolli *et al.*, "Genomic patterns of progression in smoldering multiple myeloma," pp. 1–10, 2018, doi: 10.1038/s41467-018-05058-y.

[81] E. H. Rustad *et al.*, "Timing the initiation of multiple myeloma," *Nat. Commun.*, 2020, doi: 10.1038/s41467-020-15740-9.

[82] V. Kunz *et al.*, "Targeting of the E3 ubiquitin-protein ligase HUWE1 impairs DNA repair capacity and tumor growth in preclinical multiple myeloma models," *Sci. Rep.*, vol. 10, no. 1, pp. 1–11, 2020, doi: 10.1038/s41598-020-75499-3.

[83] J. L. Parsons *et al.*, "Ubiquitin ligase ARF-BP1/Mule modulates base excision repair," *EMBO J.*, vol. 28, no. 20, pp. 3207–3215, 2009, doi: 10.1038/emboj.2009.243.

[84] N. Van Nieuwenhuijzen, I. Spaan, R. Raymakers, and V. Peperzak, "From MGUS to Multiple Myeloma , a Paradigm for Clonal Evolution of Premalignant Cells," pp. 2449–2456, 2018, doi: 10.1158/0008-5472.CAN-17-3115.

[85] M. Bustoros, R. Sklavenitis-pisto, J. Park, R. Redd, and B. Zhitomirsky, "Genomic Profiling of Smoldering Multiple Myeloma Identi fi es Patients at a High Risk of Disease Progression," vol. 38, no. 21, pp. 2380–2390, doi: 10.1200/JCO.20.00437.

[86] L. A. Johnson *et al.*, "Dendritic cells enter lymph vessels by hyaluronan-mediated docking to the endothelial receptor LYVE-1," *Nat. Immunol.*, vol. 18, no. 7, pp. 762–770, 2017, doi: 10.1038/ni.3750.

[87] L. M. Mustachio, A. Chelariu-Raicu, L. Szekvolgyi, and J. Roszik, "Targeting KRAS in cancer: Promising therapeutic strategies," *Cancers (Basel).*, vol. 13, no. 6, pp. 1–14, 2021, doi: 10.3390/cancers13061204.

[88] C. Abbosh *et al.*, "Phylogenetic ctDNA analysis depicts early-stage lung cancer evolution," *Nature*, vol. 545, no. 7655, pp. 446–451, 2017, doi: 10.1038/nature22364.

[89] J. D. Cohen *et al.*, "Detection and localization of surgically resectable cancers with a multi-analyte blood test," *Science (80-.).*, vol. 359, no. 6378, pp. 926–930, 2018, doi: 10.1126/science.aar3247.

[90] J. Phallen *et al.*, "Direct detection of early-stage cancers using circulating tumor DNA," *Sci. Transl. Med.*, vol. 9, no. 403, 2017, doi: 10.1126/scitranslmed.aan2415.

[91] I. A. Cree *et al.*, "The evidence base for circulating tumour DNA blood-based biomarkers for the early detection of cancer: A systematic mapping review," *BMC Cancer*, vol. 17, no. 1, pp. 1–17, 2017, doi: 10.1186/s12885-017-3693-7.

[92] C. Petti, A. Molla, C. Vegetti, S. Ferrone, A. Anichini, and M. Sensi, "Coexpression of NRASQ61R and BRAFV600E in human melanoma cells activates senescence and increases susceptibility to cell-mediated cytotoxicity," *Cancer Res.*, vol. 66, no. 13, pp. 6503–6511, 2006, doi: 10.1158/0008-5472.CAN-05-4671.

[93] J. M. Loree *et al.*, "Clinical and functional characterization of atypical KRAS/NRAS

mutations in metastatic colorectal cancer," *Clin. Cancer Res.*, vol. 27, no. 16, pp. 4587–4598, 2021, doi: 10.1158/1078-0432.CCR-21-0180.

[94] E. Boscolo *et al.*, "NRASQ61R mutation in human endothelial cells causes vascular malformations," *Angiogenesis*, vol. 25, no. 3, pp. 331–342, 2022, doi: 10.1007/s10456-022-09836-7.

[95] Z. Wen *et al.*, "Expression of NrasQ61R and MYC transgene in germinal center B cells induces a highly malignant multiple myeloma in mice," *Blood*, vol. 137, no. 1, pp. 61–74, 2021, doi: 10.1182/blood.2020007156.

[96] M. Eskandarpour, F. Huang, K. A. Reeves, E. Clark, and J. Hansson, "Oncogenic NRAS has multiple effects on the malignant phenotype of human melanoma cells cultured in vitro," *Int. J. Cancer*, vol. 124, no. 1, pp. 16–26, 2009, doi: 10.1002/ijc.23876.

[97] J. Prochaska and N. Benowitz, "Monoclonal gammopathy of undetermined significance (MGUS) and smoldering (asymptomatic) multiple myeloma: IMWG consensus perspectives risk factors for progression and guidelines for monitoring and management," *Physiol. Behav.*, vol. 176, no. 1, pp. 100–106, 2016, doi: 10.1038/leu.2010.60.Monoclonal.

[98] S. Rögnvaldsson *et al.*, "Iceland screens, treats, or prevents multiple myeloma (iStopMM): a population-based screening study for monoclonal gammopathy of undetermined significance and randomized controlled trial of follow-up strategies," *Blood Cancer J.*, vol. 11, no. 5, 2021, doi: 10.1038/s41408-021-00480-w.